

Rowan University

Rowan Digital Works

Theses and Dissertations

11-29-2017

Substituted hydroxylamines as nitrogen transfer reagents: direct synthetic pathways to structurally rich heteroatomic scaffolds

Dylan John Quinn
Rowan University

Follow this and additional works at: <https://rdw.rowan.edu/etd>

 Part of the [Medicinal-Pharmaceutical Chemistry Commons](#)

Recommended Citation

Quinn, Dylan John, "Substituted hydroxylamines as nitrogen transfer reagents: direct synthetic pathways to structurally rich heteroatomic scaffolds" (2017). *Theses and Dissertations*. 2482.
<https://rdw.rowan.edu/etd/2482>

This Thesis is brought to you for free and open access by Rowan Digital Works. It has been accepted for inclusion in Theses and Dissertations by an authorized administrator of Rowan Digital Works. For more information, please contact graduateresearch@rowan.edu.

**SUBSTITUTED HYDROXYLAMINES AS NITROGEN TRANSFER
REAGENTS: DIRECT SYNTHETIC PATHWAYS TO STRUCTURALLY RICH
HETEROATOMIC SCAFFOLDS**

by

Dylan John Quinn

A Thesis

Submitted to the
Department of Chemistry and Biochemistry
College of Science and Mathematics
In partial fulfillment of the requirement
For the degree of
Master of Science in Pharmaceutical Sciences
at
Rowan University
August 11, 2017

Thesis Chair: Dr. Gustavo Moura-Letts

Dedications

To my brothers, from whom all my strength is derived, I will never stop fighting because I have you by my side.

Acknowledgments

I am sincerely grateful for the faculty and staff at Rowan University's Department of Chemistry and Biochemistry who have created an environment that facilitates both creative and scientific advancement. I am thankful for my parents who have provided me with support and stability throughout my studies.

I would like to thank Joe Lizza for his help with NMR Spectroscopy, Ian Bakanas and Will Neuhaus for their help with troubleshooting and interpreting reaction outcomes, Erica Moscarello for her help with synthesis, and everyone in the GML group, who have become like a family to me.

Finally, I would like to recognize Dr. Gustavo Moura-Letts who has guided me through a very critical point in my scientific career. He has been a role model to me during my time at Rowan University and I am truly grateful to have worked under his supervision.

Abstract

Dylan J. Quinn
SUBSTITUTED HYDROXYLAMINES AS NITROGEN TRANSFER REAGENTS:
DIRECT SYNTHETIC PATHWAYS TO STRUCTURALLY RICH
HETEROATOMIC SCAFFOLDS
2016-2017
Dr. Gustavo Moura-Letts
Master of Science in Pharmaceutical Sciences

Nitrogen is found in virtually all valuable chemical compounds. The abundance of atmospheric nitrogen however, is rendered inaccessible because of the strong N-N triple bond, ultimately preventing its practical utilization in synthetic organic synthesis. The development of powerful nitrogen transfer reagents, such as substituted hydroxylamine derivatives, have played an important role in the introduction of nitrogen into valuable chemical scaffolding.

Herein is reported the methodological development of synthetic nitrogen placement into a range of valuable heteroatomic compounds. This work shows that O-Substituted Hydroxylamine can be used to furnish small heteroatomic compounds, particularly nitriles. Whereas, N-Substituted Hydroxylamine can be employed to access both 3- and 5- membered heterocycles. These works highlight the value of substituted hydroxylamines for their nitrogen transfer capability but also for their ability to afford rapid structural complexity.

Table of Contents

Abstract.....	v
List of Figures	viii
List of Tables.....	ix
Chapter 1: Nitriles.....	1
1.1 Nitrile Discovery	1
1.2 Results and Discussion.....	3
1.3 Conclusion	8
1.4 Experimental.....	8
1.4.1. General Method for the Synthesis of Nitriles.	9
1.4.2. Synthesis of Nitriles From Table 2.....	9
1.4.3. Synthesis of Nitriles From Table 3.....	12
1.4.4. ¹ H NMR and ¹³ C NMR of Nitriles	17
Chapter 2: Nitrones.....	29
2.1 Free Radical Spin Trapping	30
2.2 Pharmaceutical Relevance	31
2.3 Synthesis of Nitrones.....	32
2.4 Results and Discussion.....	35
2.5 Conclusion	45
2.6 Experimental.....	45
2.6.1. General Method for the Synthesis of Nitrones.	46
2.6.2. Synthesis of Nitrones From Table 2.	46
2.6.3. Synthesis of Nitrones From Table 3.	48
2.6.4. Synthesis of Nitrones From Table 4.	51

Table of Contents (Continued)

2.6.5. ^1H NMR and ^{13}C NMR of Nitrones.....	53
Chapter 3: Nitrene Dipolar Cycloaddition.....	62
3.1 Challenges.....	62
3.2 Access to Antibacterial Agents	65
3.3 Results and Discussion.....	66
3.4 Conclusion	73
3.5 Experimental.....	73
3.5.1. General Method for the Synthesis of Vinyl Isoxazolidines.....	74
3.5.2. Synthesis of Vinyl Isoxazolidines From Table 10 and 11.	74
3.5.3. Synthesis of Vinyl Isoxazolidines From Table 12.....	79
3.5.4. ^1H NMR and ^{13}C NMR of Vinyl Isoxazolidines.	82
Chapter 4: Nitrene Photoisomerization.....	92
4.1 A Method Overlooked	92
4.2 Heteroatom Transfer	93
4.3 Results and Discussion.....	94
4.4 Conclusion	100
4.5 Experimental.....	100
4.5.1. General Method for the Synthesis of Vinyl Oxaziridines.	101
4.5.2. Synthesis of Vinyl Oxaziridines From Table 10.....	102
4.5.3. Synthesis of Vinyl Oxaziridines From Table 11.....	103
4.5.4. ^1H NMR and ^{13}C NMR of Vinyl Oxaziridines.	106
References	112

List of Figures

Figure	Page
Figure 1. Discovery of Competing Nitrile Pathway	1
Figure 2. Exploiting Heterogeneous Composition to Control Reaction	2
Figure 3. Heteroatomic Difference: Diaziridine (left) and Oxaziridine (right)....	29
Figure 4. General Structure of the Nitrono Moiety	30
Figure 5. Free Radical, R, Forms a Stable Product with Nitrono	30
Figure 6. Aromatic CH Activation of Nitrono by Iridium Catalyst.....	32
Figure 7. Thermal Oxaziridine Rearrangement to Nitrono	33
Figure 8. Lewis Acid Catalyzed Oxaziridine Rearrangement by Yoon.....	33
Figure 9. Tertiary Hydroxylamine Oxidation to Nitrono.....	34
Figure 10. Carbonyl Condensation with N-Benzyl Hydroxylamine.....	34
Figure 11. Increasing Carbonyl Carbon Partial Positive Stabilization.....	42
Figure 12. Effects of Hydroxylamine N-Substitution on Nucleophilicity	44
Figure 13. Regiomeric-Excess Created by Dipolarophile	62
Figure 14. Dipolar Cycloaddition of Nitrono and Enal	63
Figure 15. Bidentate Dipolarophile Outcompetes Nitrono for Lewis Acid	64
Figure 16. The Design of an Organometallic to Direct Stereoselectivity	64
Figure 17. Enantioselective Synthesis of Beta Lactams	65
Figure 18. Reductive Cleavage of N-O Bond to Afford Negamycin	66
Figure 19. Nitrono Photoisomerization to Oxaziridine	92
Figure 20. Hydroxylation at C2 in the Holton-Taxol Synthesis	93
Figure 21. A Mild Aryl Metal Oxidation by N-Alkyl Oxaziridine	94

List of Tables

Table	Page
Table 1. Nitrile Synthesis Optimization Studies.....	4
Table 2. Nitrile Synthesis Scope.....	6
Table 3. Aromatic Nitrile Synthesis Scope.....	7
Table 4. Nitron Condensation Optimization.....	36
Table 5. Aldonitron Scope.....	37
Table 6. Alpha-Beta Unsaturated Aldonitron Scope.....	40
Table 7. Ketonitron Scope.....	41
Table 8. N-Protecting Group Scope.....	43
Table 9. 3-Vinyl-4-Carbonyl-Isoxazolidine Reaction Optimization.....	68
Table 10. Dipolarphile Scope: Aldehydes and Ketones.....	70
Table 11. Dipolarphile Scope: Nitriles and Esters.....	71
Table 12. Dipole Scope.....	72
Table 13. Photorearrangement Optimization.....	95
Table 14. Oxaziridine Scope.....	97
Table 15. Alpha-Beta Unsaturated Oxaziridine Scope.....	99

Chapter 1

Nitriles

1.1 Nitrile Discovery

Early works in the GML Research Group highlighted the diastereoselective synthesis of diaziridines from ketones and aldehydes using Hydroxylamine O-Sulfonic Acid (HOSA) as the nitrogen source (Beebe, Dohmeier, & Moura-Letts, 2015). During the optimization for this reaction the researchers discovered a competing pathway that led to nitrile formation. After thorough manipulation and reaction optimization, this alternative pathway was exploited to obtain nitriles in good to excellent yields with high chemoselectivity (Quinn, Haun, & Moura-Letts, 2016).

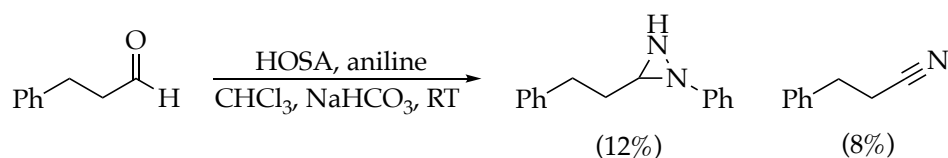


Figure 1. Discovery of Competing Nitrile Pathway

The competition between these pathways is derived from the initial condensation step which allows for a mixture of products (Figure 1). To arrive at the heterocyclic diaziridine, an initial aldehyde-aniline condensation is required. Whereas nitrile formation will require an initial aldehyde-HOSA condensation.

After optimizing for both reaction pathways, it becomes clear that the reaction media is responsible for propagating the desired chemoselectivity for each respective target (Figure 2).

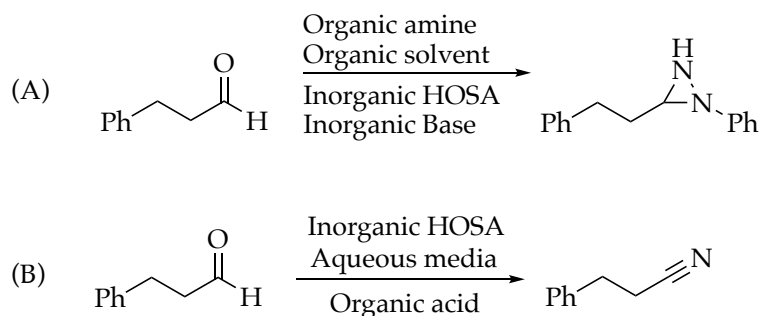


Figure 2. Exploiting Heterogeneous Composition to Control Reaction

By utilizing a polar organic solvent (Figure 2A), diaziridine is obtained in good to excellent yields. This media promotes the aldehyde-aniline condensation by means of a heterogeneous reaction mixture. The inorganic HOSA is slowly introduced into the organic phase by vigorous stirring. The slow addition of HOSA allows for the necessary aldehyde-aniline condensation, prompting diaziridine formation. This also prevents the Aldehyde-HOSA condensation which alternatively leads to nitrile formation. Interestingly, by utilizing an aqueous media, the inverse pathway and concurrent nitrile formation is selectively obtained (Figure 2B).

1.2 Results and Discussion

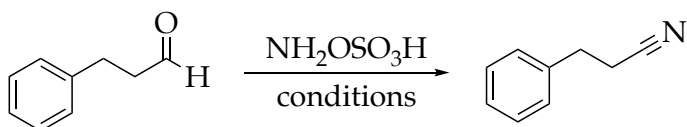
Optimization studies investigated a broad range of organic solvents, additives and temperature to determine whether an aqueous media was required for this reaction to proceed accordingly. Interestingly, the reaction yield is increased dramatically by increasing the stoichiometric ratio of hydroxylamine to aldehyde. By increasing the molar ratio to 2:1 hydroxylamine to aldehyde, a modest yield of 45% is obtained (Table 1, Entry 1). Further testing determined that the molar equivalence of hydroxylamine could be lowered, without compromising the percent yield by employing thermal conditions (Table 1, Entry 6).

Despite the broad range of organic solvents that were investigated including several ionic liquids (Table 1, Entry 14-17), the greatest results were obtained in an aqueous environment with water as the solvent (Table 1, Entry 18-22). Mild heating and an exogenous acid (1 molar equivalent, acetic acid) were required to achieve the nitrile in excellent yields (Table 1, Entry 19). With optimal reaction conditions in hand we next sought to explore the scope for this reaction by exploring functional group tolerance of the aldehyde.

Aliphatic aldehydes were converted to the corresponding nitrile in good to excellent yields under the proposed reactions conditions (Table 2, Entry 1-6).

Table 1

Nitrile Synthesis Optimization Studies



Entry	Stoichiometry ^a	Solvent	Additive ^b	Temperature	Yield ^c
1	1:2	CHCl ₃	none	rt	45%
2	1:1.5	CHCl ₃	none	rt	44%
3	1:1.5	H ₂ O	none	rt	38%
4	1:1.5	ACN	none	rt	25%
5	1:1.5	CHCl ₃	none	40 °C	48%
6	1:1.5	CHCl ₃	none	50 °C	64%
7	1:1.5	CICH ₂ CH ₂ Cl	none	60 °C	58%
8	1:1.5	CICH ₂ CH ₂ Cl	none	80 °C	60%
9	1:1.5	H ₂ O	none	50 °C	58%
10	1:1.5	ACN	none	50 °C	60%
11	1:1.5	DMSO	none	50 °C	40%
12	1:1.5	CICH ₂ CH ₂ Cl	PTSA	50 °C	75%
13	1:1.5	CICH ₂ CH ₂ Cl	TFA	50 °C	79%
14	1:1.5	[TMG][LA]	none	50 °C	53%
15	1:1.5	[TMG][LA]	TFA	50 °C	84%
16	1:1.5	[TMGPS][TFA]	none	50 °C	80%
17	1:1.5	[TMGPS][TFA]	H ₂ O	50 °C	82%
18	1:1.5	H ₂ O	TFA	50 °C	91%
19	1:1.5	H ₂ O	acetic acid	50 °C	95%
20	1:1.5	Vinegar	none	50 °C	94%
21	1:1.25	H ₂ O	acetic acid	50 °C	93%
22	1:1.1	H ₂ O	acetic acid	50 °C	94%

a. Aldehyde:NH₂OSO₃H. b. 1 equiv. of additive. c. Isolated yields.

Alpha-beta unsaturated aldehydes also afforded the respective nitrile in good to excellent yields, however in some cases, traces of unidentified and undesirable side products were detected in the crude proton NMR

and therefore, required purification by standard silica gel column to isolate the main product (Table 2, Entry 9). Despite this occurrence, both aliphatic and aromatic alpha-beta unsaturated aldehydes provided good to excellent yields of the respective nitrile (Table 2, Entry 7,8,10).

Reactivity of aromatic aldehydes showed similar conversion respective to the simple aldehydes in Table 2. Functionalization from electron withdrawing groups to electron donating groups were tolerated at various locations along the aromatic ring and afforded good to excellent results (Table 3). A small decrease in percent yield was observed with electron withdrawing substituents however, continuous stirring over a period of 16 hrs. compared to the standard 6 hrs. increased the yields for these substrates (Table 3 Entries 14 and 15). Like the aliphatic and alpha-beta unsaturated nitriles, the aromatic nitriles were obtained with high purity and required no purification except for only one substrate (Table 3 Entry 14).

Table 2

Nitrile Synthesis Scope

$$\text{R-C}_6\text{H}_4\text{-CHO} \xrightarrow[\text{H}_2\text{O, Acetic acid, 50 }^\circ\text{C}]{\text{NH}_2\text{OSO}_3\text{H}} \text{R-C}_6\text{H}_4\text{-CN}$$

Entry ^a	Aldehyde	Nitrile	Yield ^b	Entry ^a	Aldehyde	Nitrile	Yield ^b
-			-	T3J			97%
T3A	X=Br	X=Br	92%	T3K			85%
T3B	X=Me	X=Me	97%				
T3C	X=OMe	X=OMe	93%				
T3D	X=H	X=H	95%				
T3E	X=Cl	X=Cl	94%	T3L			98%
T3F			91%				
T3G			89%	T3M			91%
T3H			89%	T3N			86% ^d
T3I			93%	T3O			82% ^{c,d}
				T3P			91%

a. Reaction conditions: Aldehyde (1 mmol), Acetic acid (1 mmol), 1 mL of H₂O and NH₂OSO₃H (1.1 mmol) were mixed and heated to 50 °C for 6h. b. Isolated yields. c. Reaction crude was purified by standard silica gel chromatography. d. Reaction achieved 100% conversion after 16h.

Table 3

Aromatic Nitrile Synthesis Scope

Entry ^a	Aldehyde	Nitrile	Yield ^b	Entry ^a	Aldehyde	Nitrile	Yield ^b
-			-	T3J			97%
T3A	X=Br	X=Br	92%	T3K			85%
T3B	X=Me	X=Me	97%				
T3C	X=OMe	X=OMe	93%				
T3D	X=H	X=H	95%				
T3E	X=Cl	X=Cl	94%	T3L			98%
T3F			91%				
T3G			89%	T3M			91%
T3H			89%	T3N			86% ^d
T3I			93%	T3O			82% ^{c,d}
				T3P			91%

a. Reaction conditions: Aldehyde (1 mmol), Acetic acid (1 mmol), 1 mL of H₂O and NH₂OSO₃H (1.1 mmol) were mixed and heated to 50 °C for 6h. b. Isolated yields. c. Reaction crude was purified by standard silica gel chromatography. d. Reaction achieved 100% conversion after 16h.

1.3 Conclusion

This method provides a robust scope and grants access to the nitrile functional group in good to excellent yields. A convenient route to the nitrile functionality with no need for purification makes this an attractive pathway for synthetic and industrial chemists alike. Classical approaches to the nitrile group including the Sandmeyer reaction use copious amounts of nitrogen by employing cyanide salts and amine starting reagents, losing nitrogen gas in the process. This is undesirable because of the previously mentioned energetic barrier of nitrogen gas resulting from the nitrogen-nitrogen triple bond. This method can strategically incorporate one nitrogen atom into the aldehyde functional group allowing for a direct synthesis of Nitriles.

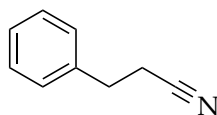
1.4 Experimental

Reagents were obtained from Aldrich Chemical, Acros Organics or Alfa Aesar and used without further purification. Solvents were obtained from EMD Miliphore DrySol and degassed with nitrogen. Reactions were performed in 4-mL glass vials with magnetic stirring. TLC was performed on 0.25 mm E. Merck silica gel 60 F254 plates and visualized under UV light (254 nm) or by staining with potassium permanganate (KMnO₄). Silica flash chromatography was performed on E. Merck 230–400 mesh silica gel 60. Automated chromatography was performed on an ISOLERA Prime instrument with 10 g. SNAP silica gel normal phase cartridges using a flow rate of 12.0 mL/min and a gradient of 0–30% EtOAc in Heptanes over 12 column volumes with UV detection at 254 nm. NMR spectra were recorded on Varian Mercury II 400 MHz Spectrometer at

24 °C in CDCl₃ unless otherwise indicated. Chemical shifts are expressed in ppm relative to solvent signals: CDCl₃ (¹H, 7.23 ppm; ¹³C, 77.0 ppm; coupling constants are expressed in Hz.

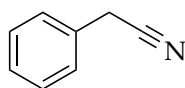
1.4.1. General method for the synthesis of nitriles. In a 4-mL reaction vial, aldehyde (1.0 mmol, 1.0 equiv) and HOSA (1.1 mmol, 1.1 equiv.) were dissolved in 3 mL of de-ionized H₂O with (1 mmol, 1 equiv) acetic acid. The solution was stirred at 50 °C for 6 h or until complete conversion, determined by TLC. The reaction was quenched with aqueous 10% NaHCO₃ (1 mL) and the resulting mixture was extracted with EtOAc (3 x 10 mL), dried (Na₂SO₄), filtered, and concentrated by rotary evaporation to afford the crude product. The product was directly characterized unless traces of impurities required purification by automated silica gel flash chromatography (few examples).

1.4.2. Synthesis of nitriles from Table 2.



(T2A) DJQ-167-4

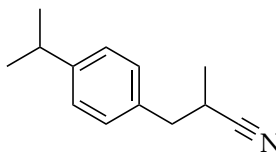
3-Phenylpropanenitrile (T2A): Aldehyde (100mg, 0.75mMol) produced nitrile **2a** (93mg, 95%) as a clear oil. **TLC:** R_f 0.47 (3:1 Heptanes/EtOAc). **IR** (thin film) 2250 cm⁻¹. **¹H-NMR** (400 MHz, CDCl₃): 7.38-7.29 (m, 5H), 2.99 (t, J = 7.3 Hz, 2H), 2.64 (t, J = 7.3Hz, 2H). **¹³C-NMR** (100MHz, CDCl₃): 138.0, 128.8, 128.2, 127.1, 119.1, 31.4, 19.2 ppm. **ESI-MS** m/z (re lint): (pos) 132.1 ([M+H]⁺, 100); (neg) 130.1 ([M-H]⁻, 100).



(T2B) DJQ-173-2

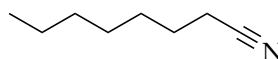
2-Phenylacetonitrile (T2B): Aldehyde (100mg, 0.83mMol) produced nitrile **2b** (89mg, 92%) as a clear oil. **TLC:** R_f 0.48 (3:1 Heptanes/EtOAc). **IR** (thin film) 2255 cm⁻¹. **¹H-NMR** (400 MHz, CDCl₃): 7.43-7.38 (m, 5H), 3.76 (s, 2H). **¹³C-NMR**

(100MHz, CDCl₃) 129.8, 128.9, 127.8, 127.8, 117.8, 23.4 ppm. **ESI-MS** m/z (re lint): (pos) 118.1 ([M+H]⁺, 100); (neg) 116.1 ([M-H]⁻,100).



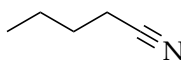
(T2C) DJQ-129-6

3-(4-Isopropylphenyl)-2-methylpropanenitrile (T2C): Aldehyde (100mg, 0.53 mMol) produced nitrile **2c** (93mg, 94%) as a clear oil. **TLC:** R_f 0.68 (3:1 Heptanes/EtOAc). **IR** (thin film) 2290 cm⁻¹. **¹H-NMR** (400 MHz, CDCl₃): 7.23 (q, J = 6.8 Hz, 4H), 2.91-2.73 (m, 4H), 1.31 (d, J = 6.8 Hz, 3H), 1.23 (d, J = 6.8 Hz, 6H). **¹³C-NMR** (100MHz, CDCl₃) 147.8, 134.1, 128.9, 126.7, 122.7, 39.6, 33.7, 27.6, 23.9, 17.6 ppm. **ESI-MS** m/z (re lint): (pos) 188.1 ([M+H]⁺, 100); (neg) 186.1 ([M-H]⁻,100).



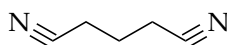
(T2D) DJQ-166-3

Octanenitrile (T2D): Aldehyde (100mg, 0.78 mMol) produced nitrile **2d** (88mg, 90%) as a light-yellow oil. **TLC:** R_f 0.58 (3:1 Heptanes/EtOAc). **IR** (thin film) 2260 cm⁻¹. **¹H-NMR** (400 MHz, CDCl₃): 2.33 (t, J = 6.6 Hz, 2H), 1.61 (tt, J = 6.8, 6.6 Hz, 2H), 1.45-1.43 (m, 2H), 1.23-1.27 (m, 6H), 0.78 (t, J = 7.3 Hz, 3H). **¹³C-NMR** (100MHz, CDCl₃) 119.8, 31.4, 28.6, 28.4, 25.3, 17.1, 14.0 ppm. **ESI-MS** m/z (re lint): (pos) 126.1 ([M+H]⁺, 100); (neg) 124.1 ([M-H]⁻,100).



(T2E)

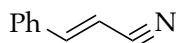
Pentanenitrile (T2E): Aldehyde (100mg, 1.16 mMol) produced nitrile **2e** (85 mg, 88%) as a light-yellow oil. **TLC:** R_f 0.58 (3:1 Heptanes/EtOAc). **IR** (thin film) 2240 cm⁻¹. **¹H-NMR** (400 MHz, CDCl₃): 2.28 (t, J = 7.1 Hz, 2H), 1.65 (quintet, J = 6.9 Hz, 2H), 1.47 (sextet, J = 6.9 Hz, 2H), 0.88 (t, J = 6.9 Hz, 3H). **¹³C-NMR** (100MHz, CDCl₃) 119.7, 26.6, 22.0, 16.7, 13.1 ppm. **ESI-MS** m/z (re lint): (pos) 84.1 ([M+H]⁺, 100); (neg) 82.1 ([M-H]⁻,100).



(T2F) DJQ-172-2

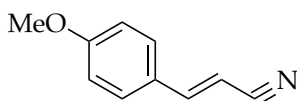
Glutaronitrile (T2F): Aldehyde (100mg, 1.03 mMol) produced nitrile **2f** (83 mg, 86%) as a clear oil. **TLC:** R_f 0.71 (3:1 Heptanes/EtOAc). **IR** (thin film) 2250 cm⁻¹. **¹H-NMR** (400 MHz, CDCl₃): 2.51 (t, J = 7.3 Hz, 4H), 3.74 (quintet, J = 7.3 Hz, 2H).

¹³C-NMR (100MHz, CDCl₃) 117.7, 21.6, 16.2 ppm. ESI-MS m/z (re lint): (pos) 95.1 ([M+H]⁺, 100); (neg) 93.1 ([M-H]⁻,100).



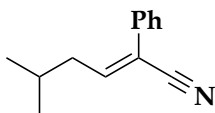
(T2G) DJQ-164-1

Cinnamonnitrile (T2G): Aldehyde (100mg, 0.76 mMol) produced nitrile **2g** (83 mg, 89%) as a light-yellow oil. TLC: R_f 0.75 (3:1 Heptanes/EtOAc). IR (thin film) 2210 cm⁻¹. ¹H-NMR (400 MHz, CDCl₃): 7.41-7.32 (m, 6H), 5.78 (d, J = 16.1 Hz, 1H). ¹³C-NMR (100MHz, CDCl₃) 150.4, 133.3, 131.0, 128.9, 127.2, 118.0, 96.1 ppm. ESI-MS m/z (re lint): (pos) 130.1 ([M+H]⁺, 100); (neg) 128.1 ([M-H]⁻,100).



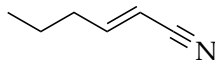
(T2H) DJQ-144-12

(E)-3-(4-Methoxyphenyl)-acrylonitrile (T2H): Aldehyde (100mg, 0.62 mMol) produced nitrile **2h** (86 mg, 87%) as a white solid. TLC: R_f 0.42 (3:1 Heptanes/EtOAc). IR (thin film) 2215 cm⁻¹. ¹H-NMR (400 MHz, CDCl₃): 7.29 (d, J = 6.6 Hz, 2H), 7.25 (d, J = 16.5 Hz, 1H), 6.93 (d, J = 6.6 Hz, 2H), 5.83 (d, J = 16.3 Hz, 1H), 3.89 (s, 3H). ¹³C-NMR (100MHz, CDCl₃) 162.0, 150.0, 129.0, 126.3, 118.7, 114.5, 93.3, 55.4 ppm. ESI-MS m/z (re lint): (pos) 160.1 ([M+H]⁺, 100); (neg) 158.1 ([M-H]⁻,100).



(T2I) DJQ-

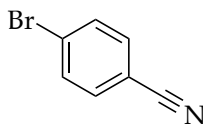
(E)-5-Methyl-2-phenylhex-2-enitrile (T2I): Aldehyde (100mg, 0.53 mMol) produced nitrile **2i** (84 mg, 86%) as a clear oil. TLC: R_f 0.69 (3:1 Heptanes/EtOAc). IR (thin film) 2205 cm⁻¹. ¹H-NMR (400 MHz, CDCl₃): 7.49-7.43 (m, 5H), 6.71 (t, J = 6.8 Hz, 1H), 2.25 (dd, J = 7.5, 6.8 Hz, 2H), 1.79-1.75 (m, 1H), (d, J = 7.1 Hz, 6H). ¹³C-NMR (100MHz, CDCl₃) 148.9, 136.4, 129.4, 128.8, 125.5, 116.2, 107.5, 37.5, 28.8, 22.4 ppm. ESI-MS m/z (re lint): (pos) 186.1 ([M+H]⁺, 100); (neg) 184.1 ([M-H]⁻,100).



(T2J) DJQ-172-1

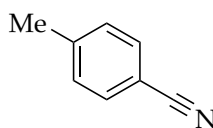
(E)-Hex-2-enitrile (T2J): Aldehyde (100mg, 1.02 mMol) produced nitrile **2j** (89 mg, 92%) as a clear oil. TLC: R_f 0.66 (3:1 Heptanes/EtOAc). IR (thin film) 2210 cm⁻¹. ¹H-NMR (400 MHz, CDCl₃): 6.91 (dt, J = 16.1, 7.1 Hz, 1H), 5.27 (d, J = 16.1 Hz, 1H), 2.24 (dt, J = 7.3, 7.1 Hz, 2H), 1.47 (sextet, J = 7.3 Hz, 2H), 0.82 (t, J = 6.9 Hz, 3H). ¹³C-NMR (100MHz, CDCl₃) 155.8, 117.4, 99.6, 35.1, 20.8, 13.3 ppm. ESI-MS m/z (re lint): (pos) 96.1 ([M+H]⁺, 100); (neg) 94.1 ([M-H]⁻,100).

1.4.3. Synthesis of nitriles from Table 3.



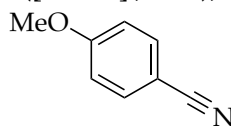
(T3A) DJQ-132

4-Bromobenzonitrile (T3A): Aldehyde (100mg, 0.54 mMol) produced nitrile **3a** (90mg, 92%) as a white solid. **TLC:** *R_f* 0.70 (3:1 Heptanes/EtOAc). **IR** (thin film) 2215 cm⁻¹. **¹H-NMR** (400 MHz, CDCl₃): 7.62 (d, *J* = 7.1 Hz, 2H), 7.49 (d, *J* = 7.1 Hz, 2H). **¹³C-NMR** (100MHz, CDCl₃) 133.4, 132.6, 128.0, 118.0, 111.2 ppm. **ESI-MS** *m/z* (re lint): (pos) 182.0 ([M+H]⁺, 100); (neg) 180.0 ([M-H]⁻,100).



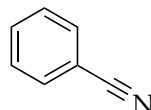
(T3B) DJQ-147

4-Methylbenzonitrile (T3B): Aldehyde (100mg, 0.83 mMol) produced nitrile **3b** (94mg, 97%) as a clear oil. **TLC:** *R_f* 0.66 (3:1 Heptanes/EtOAc). **IR** (thin film) 2210 cm⁻¹. **¹H-NMR** (400 MHz, CDCl₃): 7.54 (d, *J* = 7.0 Hz, 2H), 7.27 (d, *J* = 7.1Hz, 2H), 2.44 (s, 3H). **¹³C-NMR** (100MHz, CDCl₃) 143.6, 132.0, 129.8, 119.1, 109.2, 21.8 ppm. **ESI-MS** *m/z* (re lint): (pos) 118.1 ([M+H]⁺, 100); (neg) 116.1 ([M-H]⁻,100).



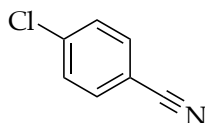
(T3C) DJQ-143-5

4-Methoxybenzonitrile (T3C): Aldehyde (100mg, 0.74mMol) produced nitrile **3c** (94mg, 93%) as a white solid. **TLC:** *R_f* 0.44 (3:1 Heptanes/EtOAc). **IR** (thin film) 2210 cm⁻¹. **¹H-NMR** (400 MHz, CDCl₃): 7.52 (d, *J* = 7.3 Hz, 2H), 6.91 (d, *J* = 7.3 Hz, 2H), 3.78 (s, 3H). **¹³C-NMR** (100MHz, CDCl₃) 162.8, 133.9, 119.2, 114.7, 103.9, 55.5 ppm. **ESI-MS** *m/z* (re lint): (pos) 134.1 ([M+H]⁺, 100); (neg) 132.1 ([M-H]⁻,100).



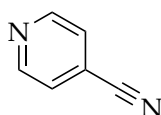
(T3D) DJQ-173

Benzonitrile (T3D): Aldehyde (100mg, 0.94 mMol) produced nitrile **3d** (92mg, 95%) as a clear liquid. **TLC:** *R_f* 0.68 (3:1 Heptanes/EtOAc). **IR** (thin film) 2220 cm⁻¹. **¹H-NMR** (400 MHz, CDCl₃): 7.52-7.32 (m, 5H). **¹³C-NMR** (100MHz, CDCl₃) 132.3, 131.5, 128.6, 118.3, 111.7 ppm. **ESI-MS** *m/z* (re lint): (pos) 104.1 ([M+H]⁺, 100); (neg) 102.1 ([M-H]⁻,100).



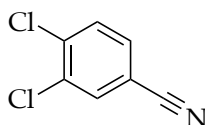
(T3E) DJQ-143-11

4-Chlorobenzonitrile (T3E): Aldehyde (100mg, 0.71 mMol) produced nitrile **3e** (91mg, 94%) as a white solid. **TLC:** R_f 0.75 (3:1 Heptanes/EtOAc). **IR** (thin film) 2220 cm⁻¹. **¹H-NMR** (400 MHz, CDCl₃): 7.58 (d, J = 7.1 Hz, 2H), 7.47 (d, J = 7.1 Hz, 2H). **¹³C-NMR** (100MHz, CDCl₃) 139.5, 133.4, 129.7, 118.0, 110.7 ppm. **ESI-MS** m/z (re lint): (pos) 138.0 ([M+H]⁺, 100); (neg) 136.0 ([M-H]⁻,100).



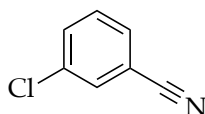
(T3F) DJQ-133A

Isonicotinonitrile (T3F): Aldehyde (100mg, 0.93 mMol) produced nitrile **3f** (88mg, 91%) as a white solid. **TLC:** R_f 0.14 (3:1 Heptanes/EtOAc). **IR** (thin film) 2225 cm⁻¹. **¹H-NMR** (400 MHz, CDCl₃): 8.53 (d, J = 6.8 Hz, 2H), 7.52 (d, J = 6.8 Hz, 2H). **¹³C-NMR** (100MHz, CDCl₃) 150.7, 125.2, 120.4, 116.3 ppm. **ESI-MS** m/z (re lint): (pos) 105.1 ([M+H]⁺, 100); (neg) 103.1 ([M-H]⁻,100).



(T3G) DJQ-149

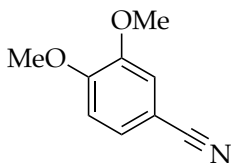
3,4-Dichlorobenzonitrile (T3G): Aldehyde (100mg, 0.57 mMol) produced nitrile **3g** (86mg, 89%) as a white solid. **TLC:** R_f 0.56 (3:1 Heptanes/EtOAc). **IR** (thin film) 2224 cm⁻¹. **¹H-NMR** (400 MHz, CDCl₃): 7.63 (d, J = 6.6 Hz, 1H), 7.50 (s, 1H), 7.29 (d, J = 6.6 Hz, 1H). **¹³C-NMR** (100MHz, CDCl₃) 140.0, 137.7, 134.5, 130.2, 127.8, 115.2, 111.8 ppm. **ESI-MS** m/z (re lint): (pos) 172.0 ([M+H]⁺, 100); (neg) 170.0 ([M-H]⁻,100).



(T3H) DJQ-164-4

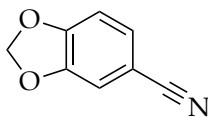
3-Chlorobenzonitrile (T3H): Aldehyde (100mg, 0.71 mMol) produced nitrile **3h** (87 mg, 89%) as a white solid. **TLC:** R_f 0.54 (3:1 Heptanes/EtOAc). **IR** (thin film) 2225 cm⁻¹. **¹H-NMR** (400 MHz, CDCl₃): 7.63 (s, 1H), 7.58-7.51 (m, 2H), 7.41 (t, J = 6.9

Hz, 1H). ¹³C-NMR (100MHz, CDCl₃) 135.1, 133.1, 131.8, 130.4, 130.2, 117.3, 113.8 ppm. ESI-MS m/z (re lint): (pos) 138.0 ([M+H]⁺, 100); (neg) 136.0 ([M-H]⁻,100).



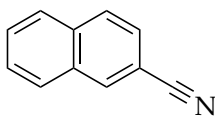
(T3I) DJQ-163-2

3,4-Dimethoxybenzonitrile (T3I): Aldehyde (100mg, 0.60 mMol) produced nitrile **3i** (91 mg, 93%) as a white solid. TLC: R_f 0.29 (3:1 Heptanes/EtOAc). IR (thin film) 2215 cm⁻¹. ¹H-NMR (400 MHz, CDCl₃): 7.25 (d, J = 6.8 Hz, 1H), 7.03 (s, 1H), 6.82 (d, J = 6.8 Hz, 1H), 3.92 (s, 3H), 3.87 (s, 3H). ¹³C-NMR (100MHz, CDCl₃) 152.7, 149.1, 126.4, 119.1, 113.8, 111.1, 103.8, 56.1, 56.0 ppm. ESI-MS m/z (re lint): (pos) 164.1 ([M+H]⁺, 100); (neg) 162.1 ([M-H]⁻,100).



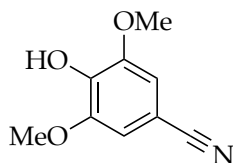
(T3J) DJQ-163-1

Benzo[d][1,3]dioxole-5-carbonitrile (T3J): Aldehyde (100mg, 0.67 mMol) produced nitrile **3j** (96 mg, 97%) as a white solid. TLC: R_f 0.38 (3:1 Heptanes/EtOAc). IR (thin film) 2210 cm⁻¹. ¹H-NMR (400 MHz, CDCl₃): 7.21 (d, J = 6.8 Hz, 1H), 6.99 (s, 1H), 6.77 (d, J = 6.8 Hz, 1H), 6.02 (s, 2H). ¹³C-NMR (100MHz, CDCl₃) 151.5, 147.9, 128.1, 118.8, 111.3, 109.0, 104.8, 102.2 ppm. ESI-MS m/z (re lint): (pos) 148.1 ([M+H]⁺, 100); (neg) 146.1 ([M-H]⁻,100).



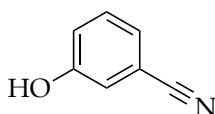
(T3K) DJQ-164-5

4-Naphtonitrile (T3K): Aldehyde (100mg, 0.67 mMol) produced nitrile **3k** (96 mg, 85%) as a tan solid. TLC: R_f 0.77 (3:1 Heptanes/EtOAc). IR (thin film) 2205 cm⁻¹. ¹H-NMR (400 MHz, CDCl₃): 8.19 (d, J = 6.6 Hz, 1H), 8.04 (d, J = 6.6 Hz, 1H), 7.87 (t, J = 6.9 Hz, 2H), 7.65 (d, J = 6.8 Hz, 1H), 7.58 (d, J = 6.8 Hz, 1H), 7.47 (d, J = 6.8 Hz, 1H). ¹³C-NMR (100MHz, CDCl₃) 133.2, 132.8, 132.5, 132.2, 128.6, 128.5, 127.4, 125.0, 124.8, 117.7, 110.0 ppm. ESI-MS m/z (re lint): (pos) 154.1 ([M+H]⁺, 100); (neg) 152.1 ([M-H]⁻,100).



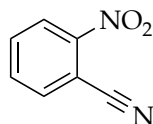
(T3L) DJQ-163-4

4-Hydroxy-3,5-dimethoxybenzonitrile (T3L): Aldehyde (100mg, 0.55 mMol) produced nitrile **3l** (96 mg, 98%) as a white solid. **TLC:** R_f 0.12 (3:1 Heptanes/EtOAc). **IR** (thin film) 3450, 2240 cm^{-1} . **$^1\text{H-NMR}$** (400 MHz, CDCl_3): 6.82 (s, 2H), 3.87 (s, 6H). **$^{13}\text{C-NMR}$** (100MHz, CDCl_3) 147.1, 139.2, 119.3, 109.1, 102.2, 56.5 ppm. **ESI-MS** m/z (re lint): (pos) 180.1 ($[\text{M}+\text{H}]^+$, 100); (neg) 178.1 ($[\text{M}-\text{H}]^-$,100).



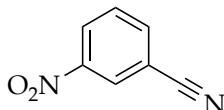
(T3M) DJQ-144-1

3-Hydroxybenzonitrile (T3M): Aldehyde (100mg, 0.82 mMol) produced nitrile **3m** (89mg, 91%) as a yellow solid. **TLC:** R_f 0.27 (3:1 Heptanes/EtOAc). **IR** (thin film) 3380, 2260 cm^{-1} . **$^1\text{H-NMR}$** (400 MHz, CDCl_3): 7.34 (t, $J = 6.9$ Hz, 1H), 7.23 (t, $J = 6.8$ Hz, 1H), 7.14 (s, 1H). 7.12 (d, $J = 6.9$ Hz, 1H). **$^{13}\text{C-NMR}$** (100MHz, CDCl_3) 156.2, 130.6, 124.5, 120.7, 118.7, 112.8 ppm. **ESI-MS** m/z (re lint): (pos) 120.1 ($[\text{M}+\text{H}]^+$, 100); (neg) 118.1 ($[\text{M}-\text{H}]^-$,100).



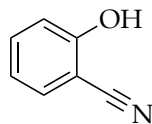
(T3N) DJQ-163-3

2-Nitrobenzonitrile (T3N): Aldehyde (100mg, 0.66mMol) produced nitrile **3n** (84 mg, 86%) as a light yellow solid. **TLC:** R_f 0.53 (3:1 Heptanes/EtOAc). **IR** (thin film) 2240 cm^{-1} . **$^1\text{H-NMR}$** (400 MHz, CDCl_3): 8.33-8.31 (m, 1H), 7.92-7.89 (m, 1H), 7.84-7.82 (m, 2H). **$^{13}\text{C-NMR}$** (100MHz, CDCl_3) 135.5, 134.3, 133.7, 125.5, 114.9, 108.0 ppm. **ESI-MS** m/z (re lint): (pos) 149.1 ($[\text{M}+\text{H}]^+$, 100); (neg) 147.1 ($[\text{M}-\text{H}]^-$,100).



(T3O) DJQ-167-3

3-Nitrobenzonitrile (T3O): Aldehyde (100mg, 0.66 mMol) produced nitrile **3o** (80 mg, 82%) as a light yellow solid. **TLC:** *R_f* 0.55 (3:1 Heptanes/EtOAc). **IR** (thin film) 2235 cm⁻¹. **¹H-NMR** (400 MHz, CDCl₃): 8.51 (s, 1H), 8.44 (d, *J* = 6.6 Hz, 1H), 7.96 (d, *J* = 6.6 Hz, 1H), 7.74 (dt, *J* = 6.6 Hz, 1H). **¹³C-NMR** (100MHz, CDCl₃) 137.6, 130.6, 127.5, 127.4, 127.2, 116.5, 114.1 ppm. **ESI-MS** *m/z* (re lint): (pos) 149.1 ([M+H]⁺, 100); (neg) 147.1 ([M-H]⁻,100).



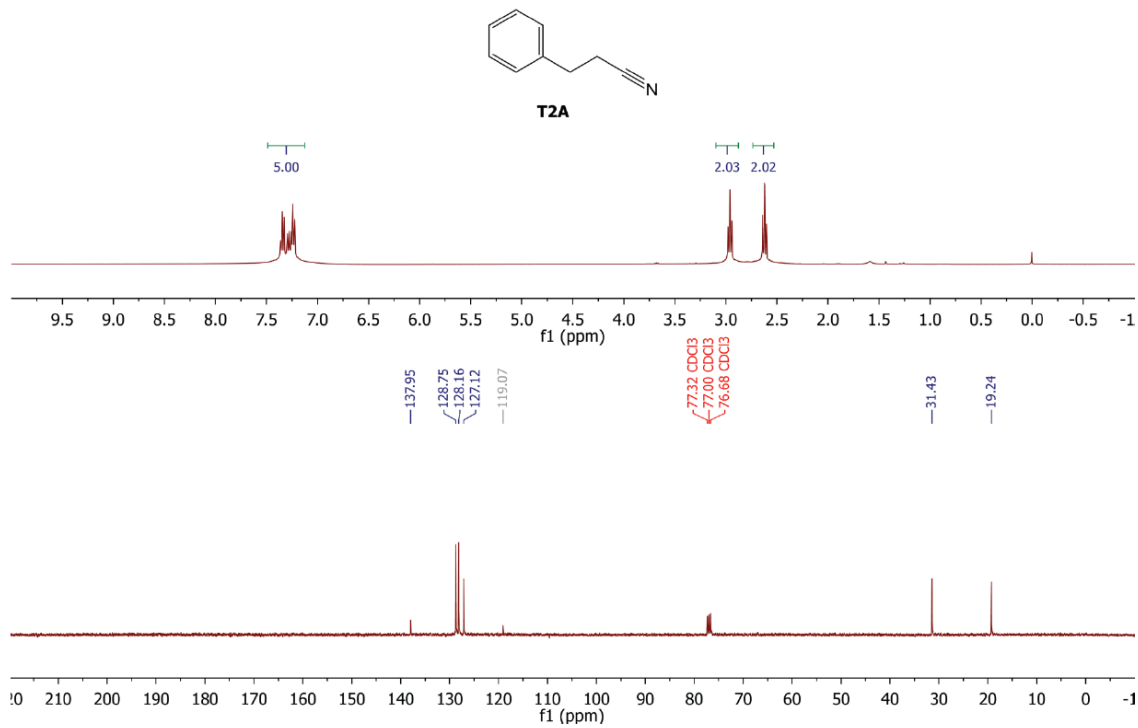
(T3P) DJQ-152

2-Hydroxybenzonitrile (T3P): Aldehyde (100mg, 0.82 mMol) produced nitrile **3p** (93mg, 95%) as a white solid. **TLC:** *R_f* 0.29 (3:1 Heptanes/EtOAc). **IR** (thin film) 3460, 2250 cm⁻¹. **¹H-NMR** (400 MHz, CDCl₃): 7.52-7.44 (m, 2H), 7.39 (bs, 1H), 7.07 (d, *J* = 7.1 Hz, 1H), 6.97 (t, *J* = 7.1 Hz, 1H). **¹³C-NMR** (100MHz, CDCl₃) 159.4, 135.3, 135.2, 133.3, 120.9, 116.9, 99.3 ppm. **ESI-MS** *m/z* (re lint): (pos) 120.1 ([M+H]⁺, 100); (neg) 118.1 ([M-H]⁻,100).

1.4.4. ^1H NMR and ^{13}C NMR of nitriles

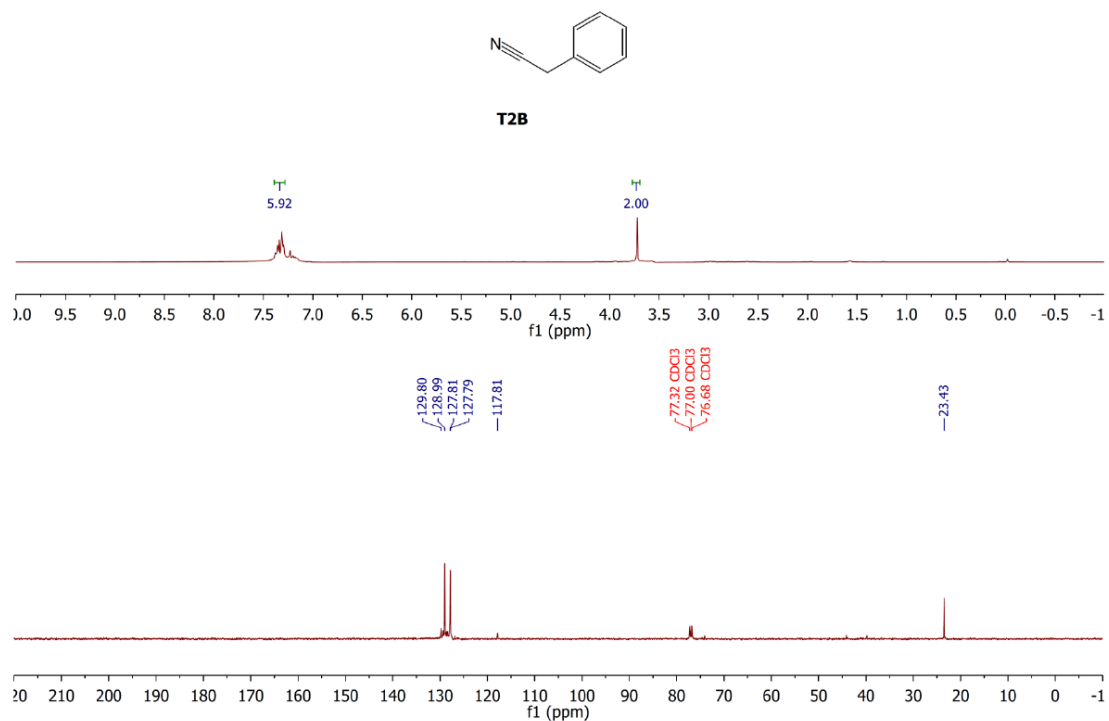
PROTON

DJQ-167-4

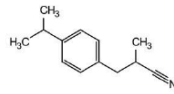


PROTON

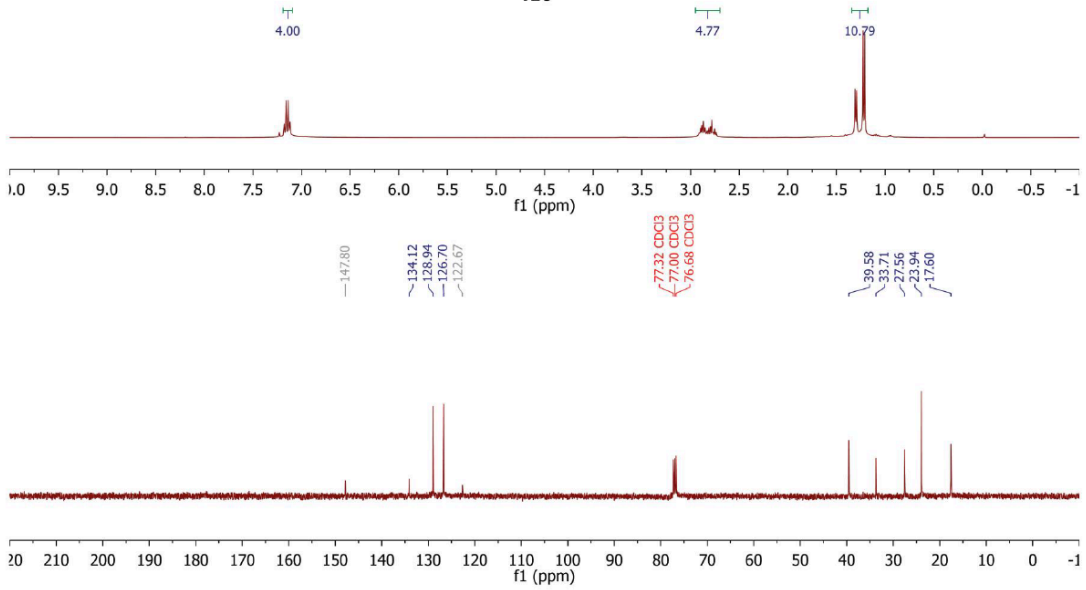
DJQ-173-2



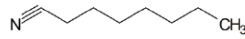
PROTON
DJQ-129F
DJQ-129-6



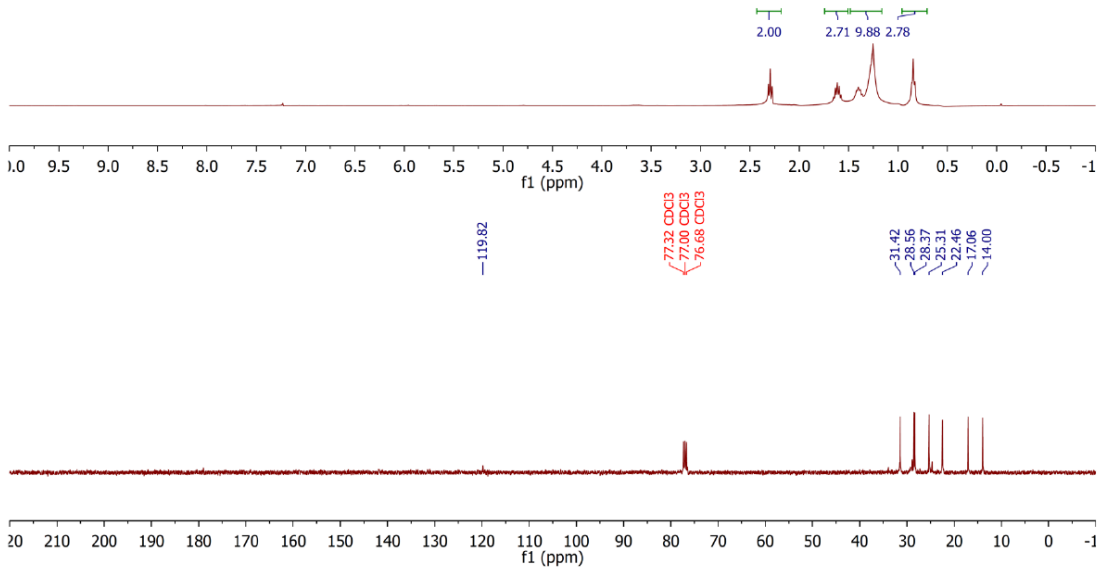
T2C



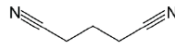
PROTON
DJQ-166-3



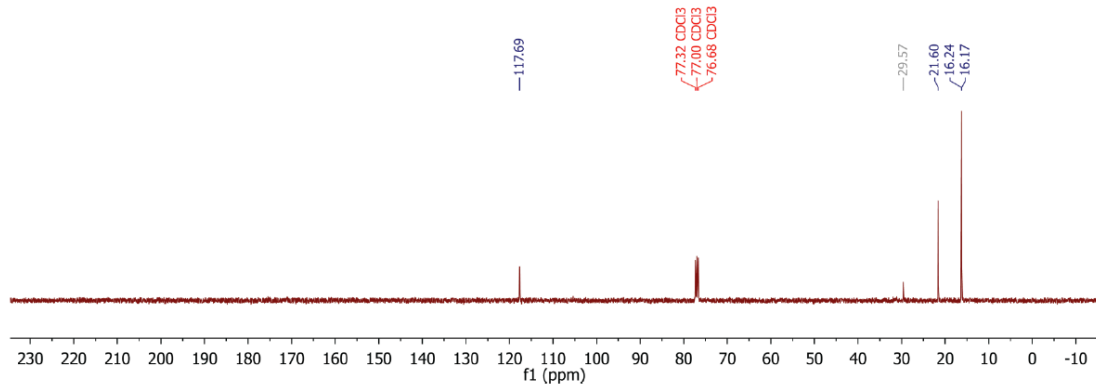
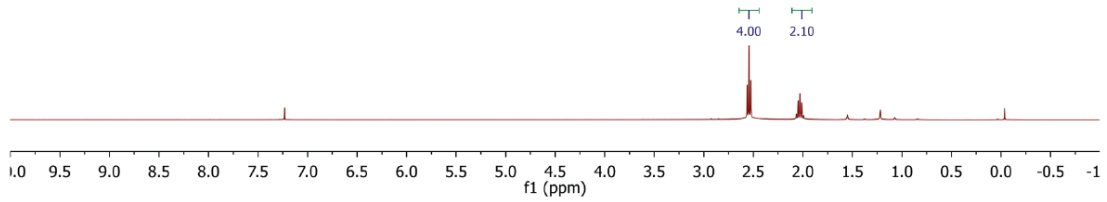
T2D



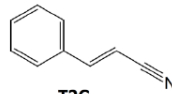
PROTON
DJQ-172-2



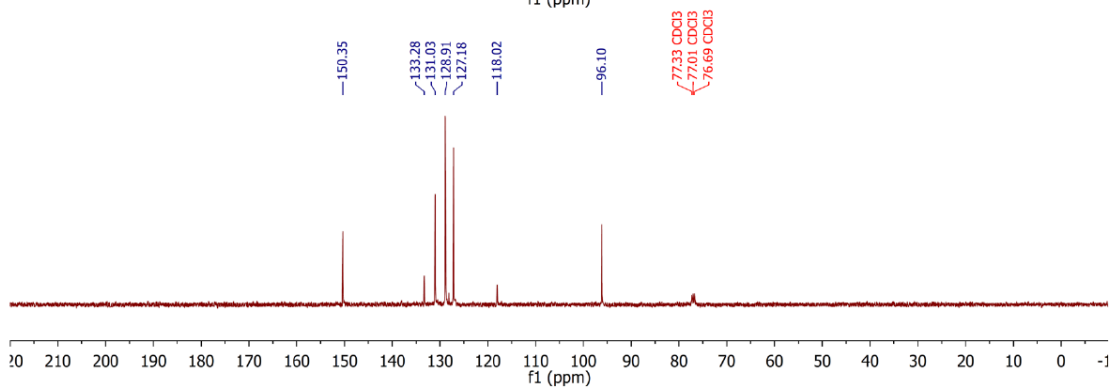
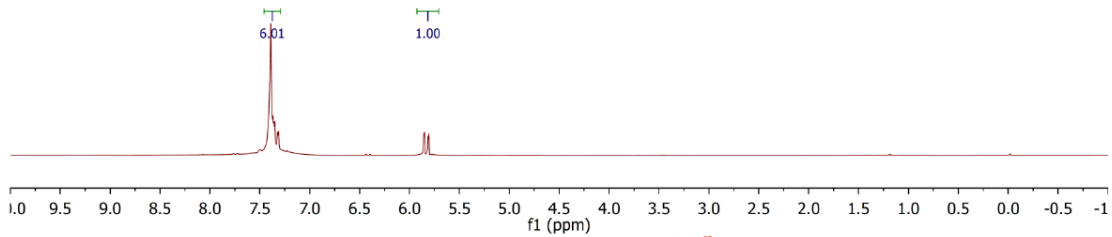
T2F



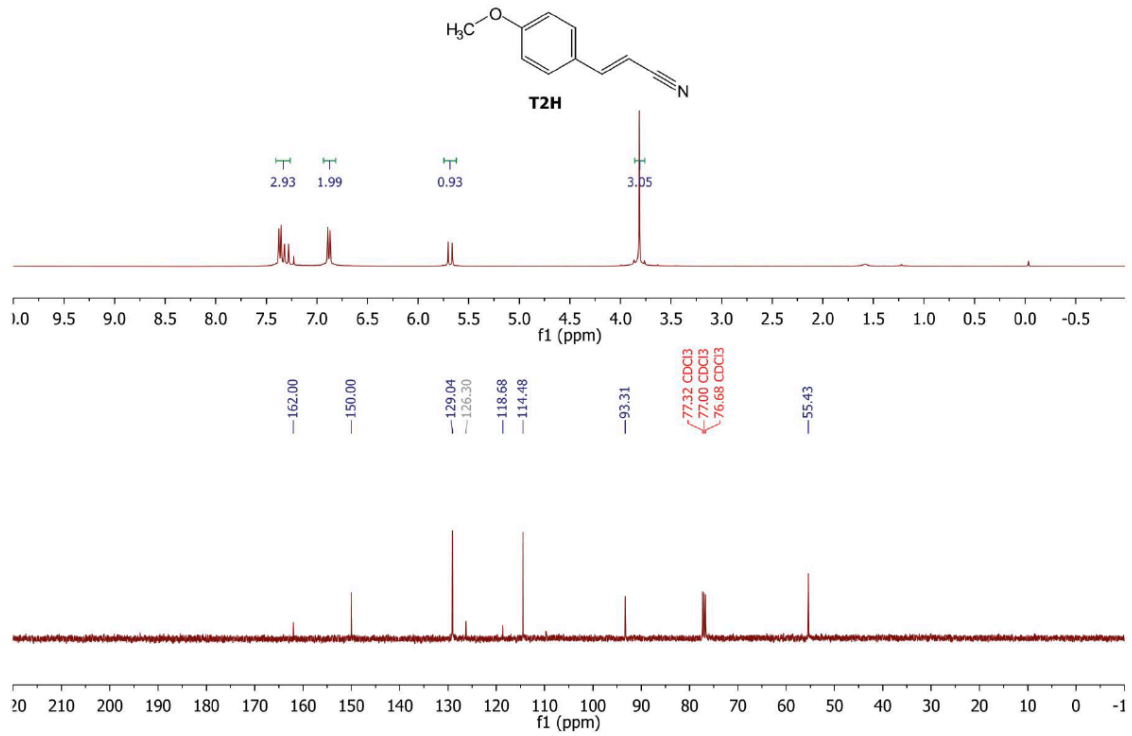
PROTON
DJQ-164-1



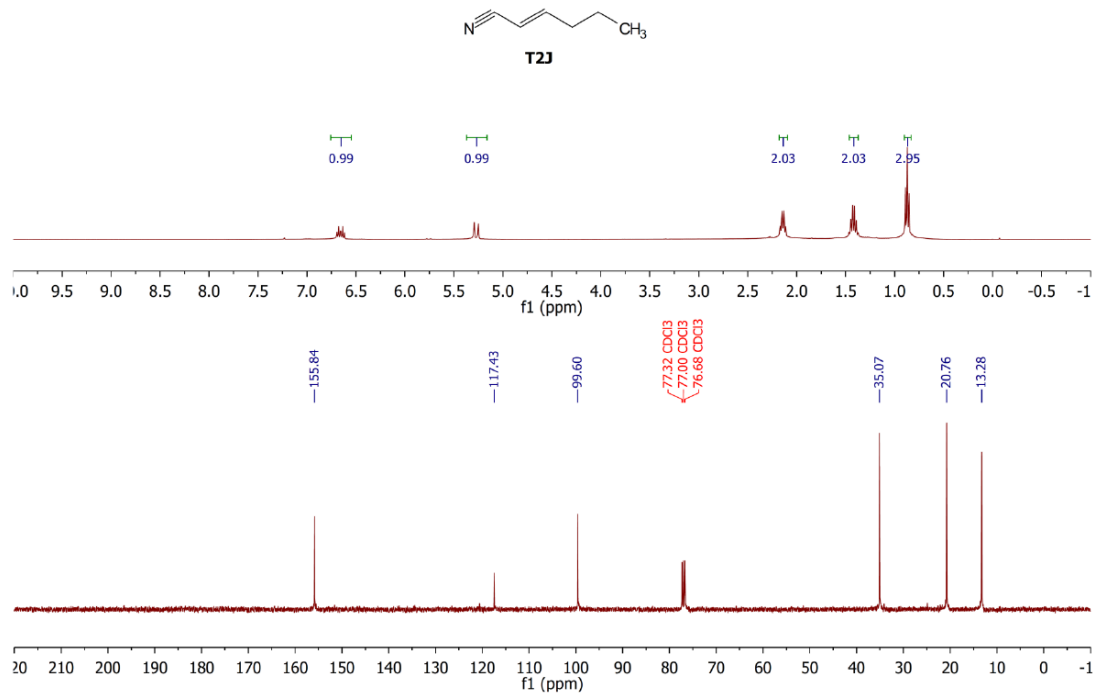
T2G



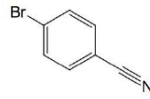
DJQ-144-12



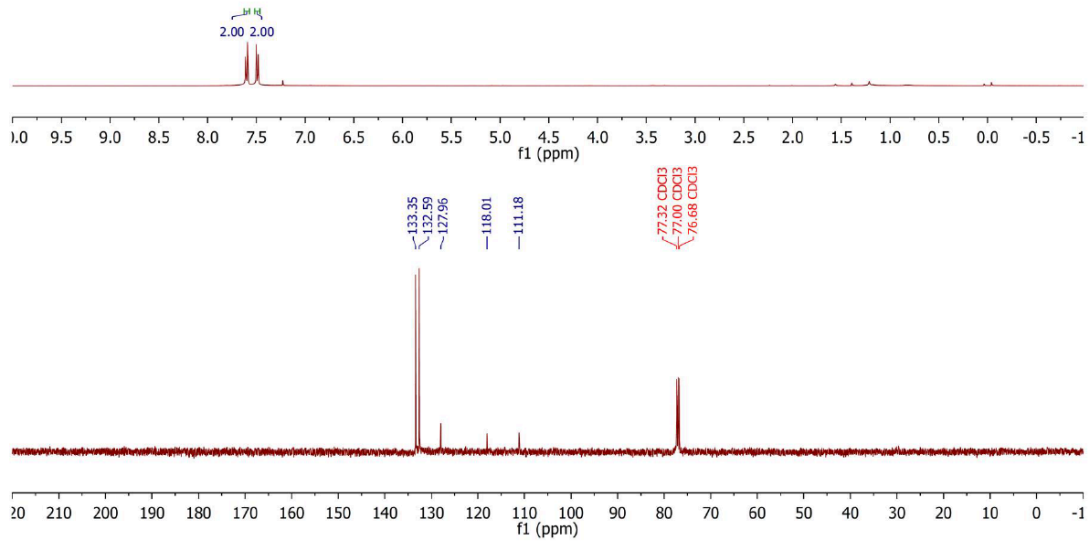
PROTON
DJQ-172-1



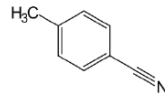
PROTON
DJQ-132-1
DJQ-132



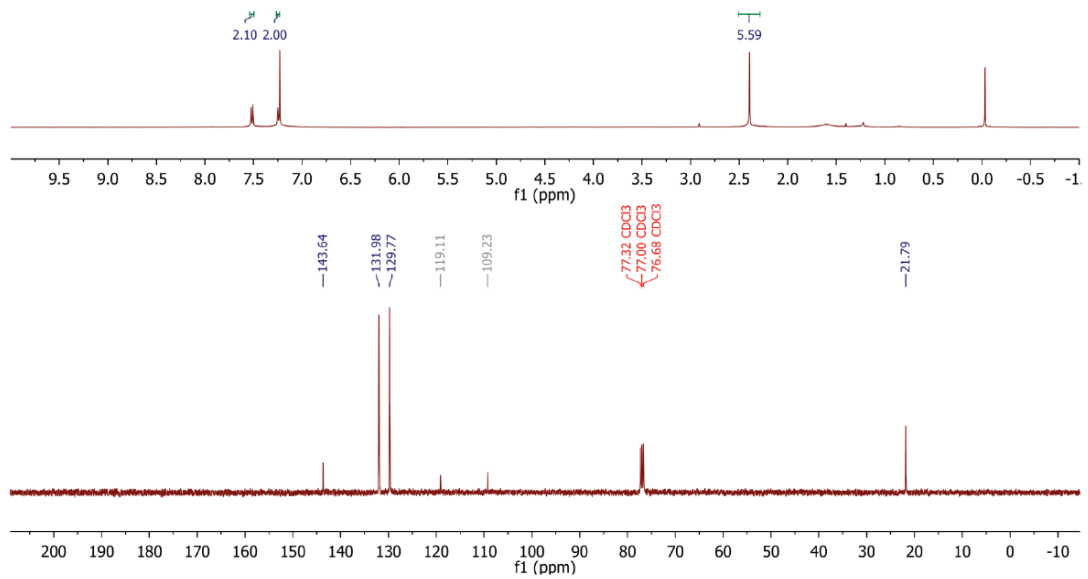
T3A



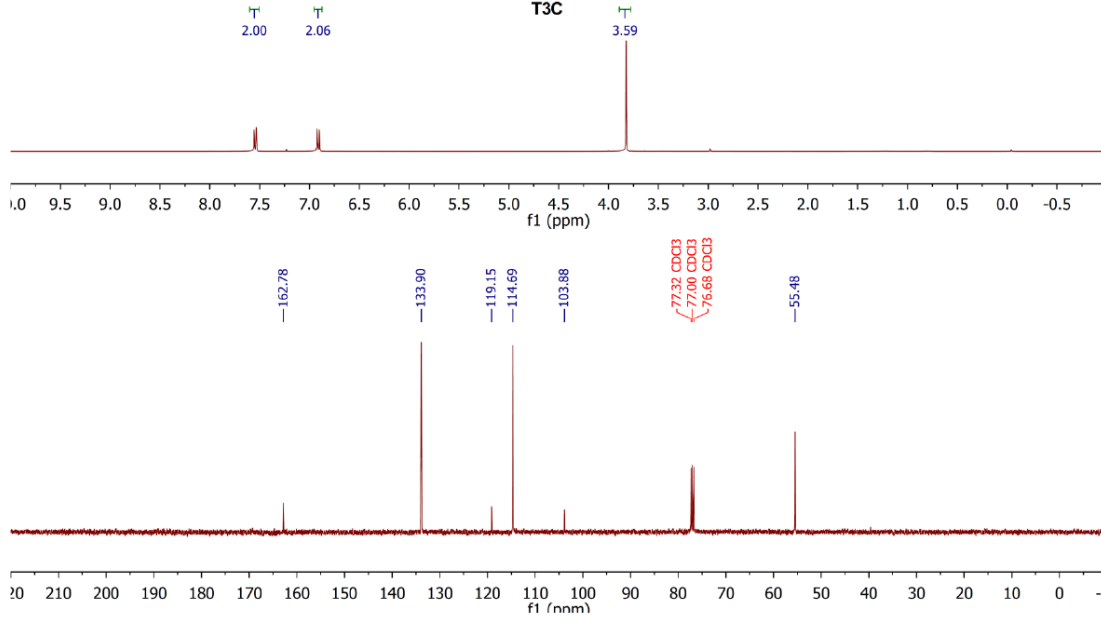
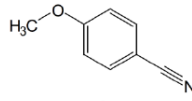
PROTON
DJQ-147



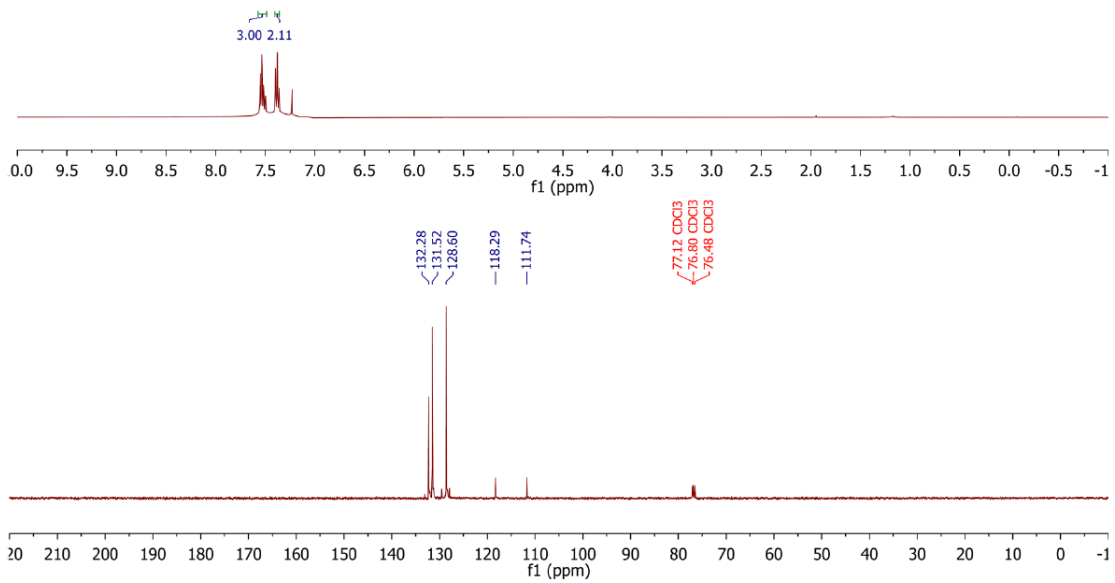
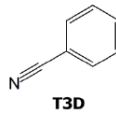
T3B



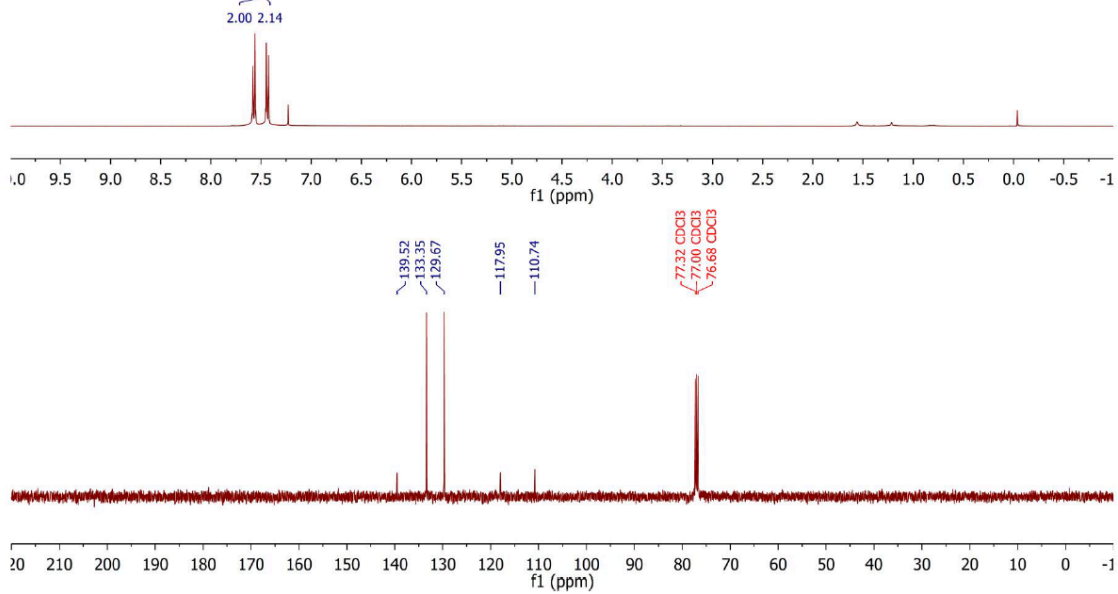
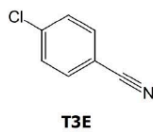
PROTON
DJQ-5
DJQ-143-5



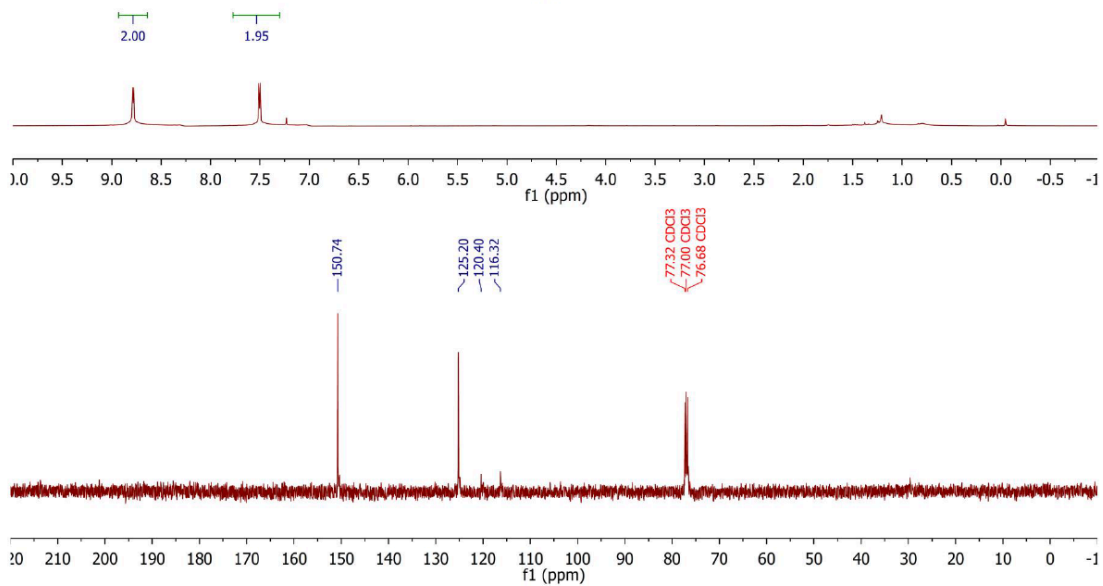
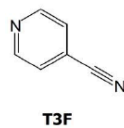
PROTON
DJQ-173-1



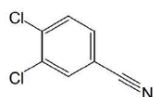
PROTON
DJQ-11
DJQ-143-11



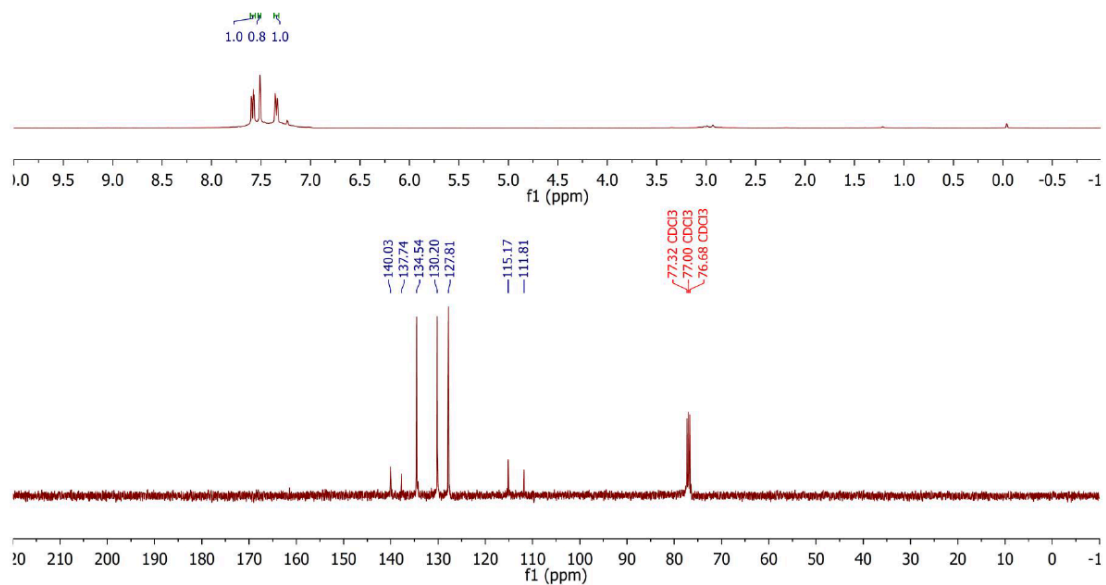
PROTON
DJQ-133A



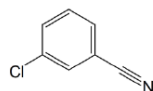
PROTON
149
DJQ-149



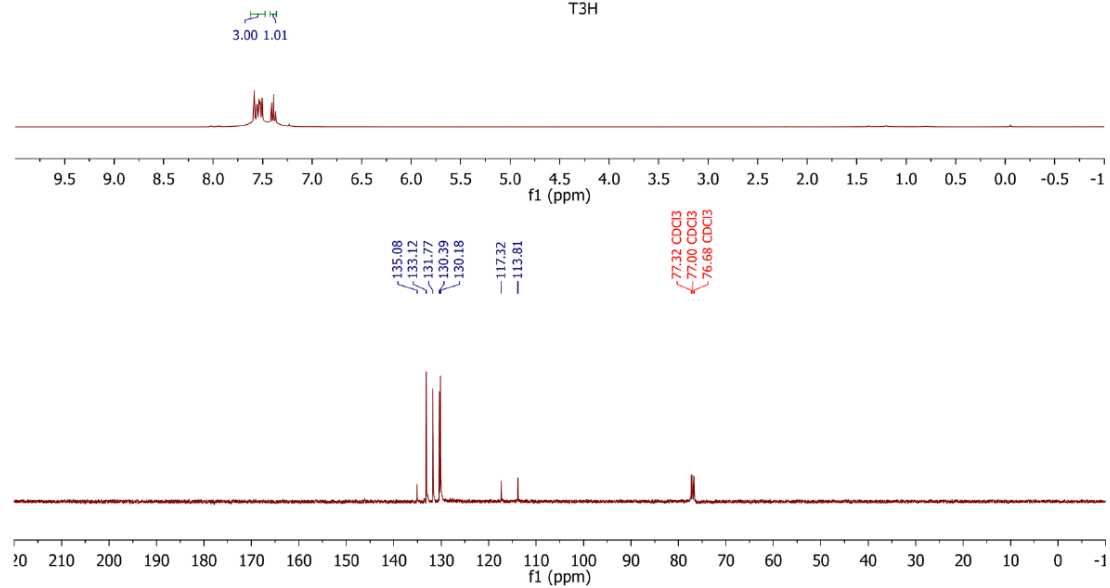
T3G



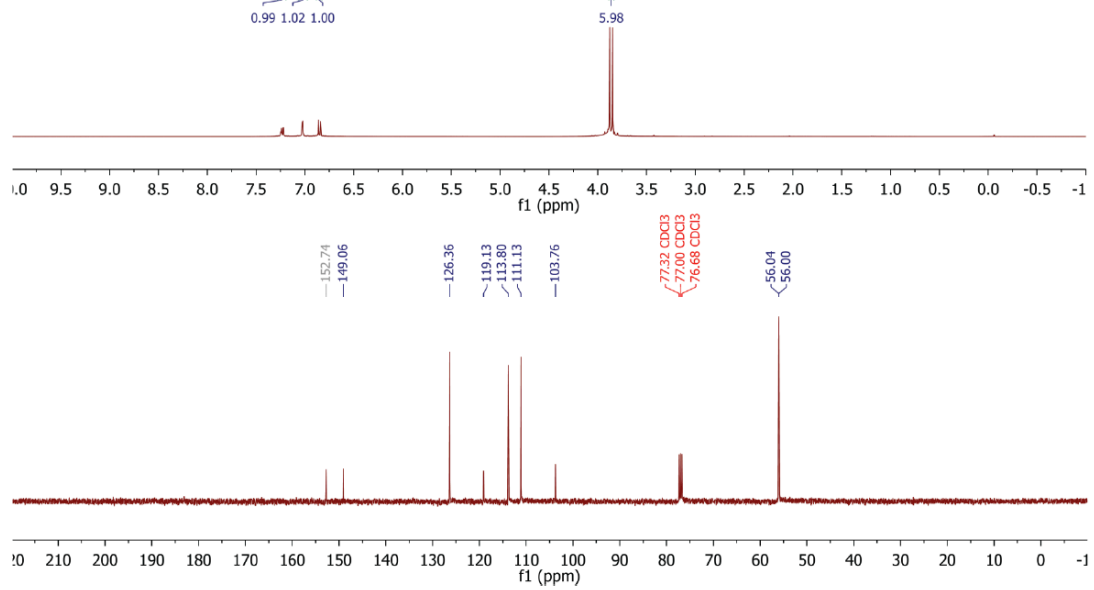
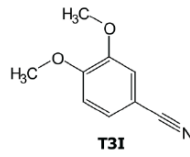
PROTON
DJQ-164-4



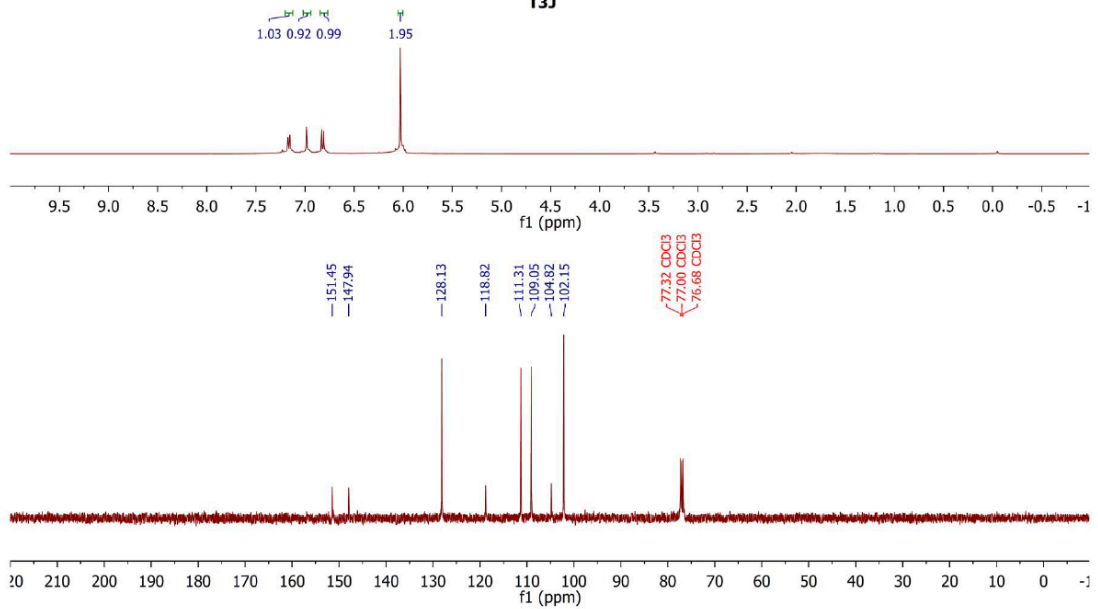
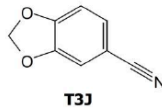
T3H



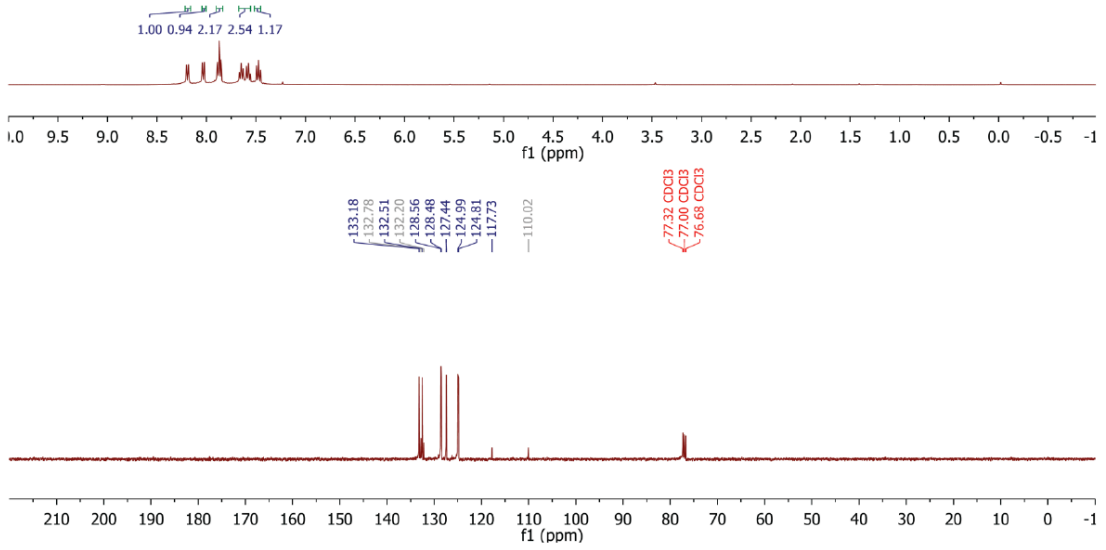
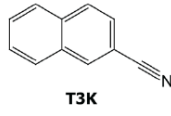
PROTON
DJQ-163-2



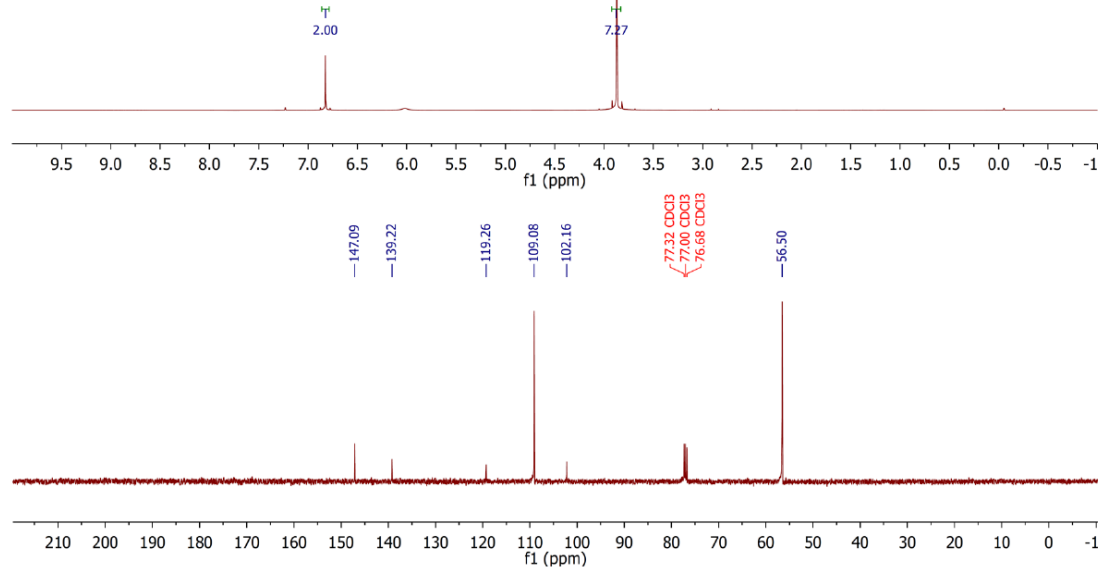
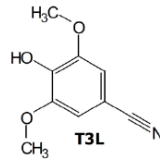
PROTON
DJQ-163-1



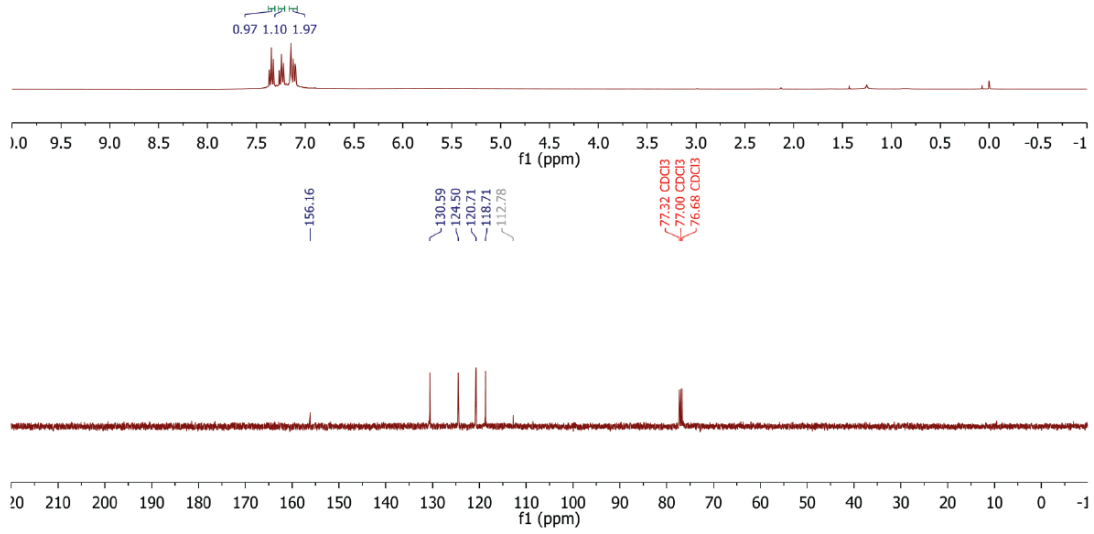
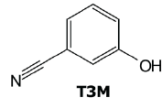
PROTON
DJQ-164-5



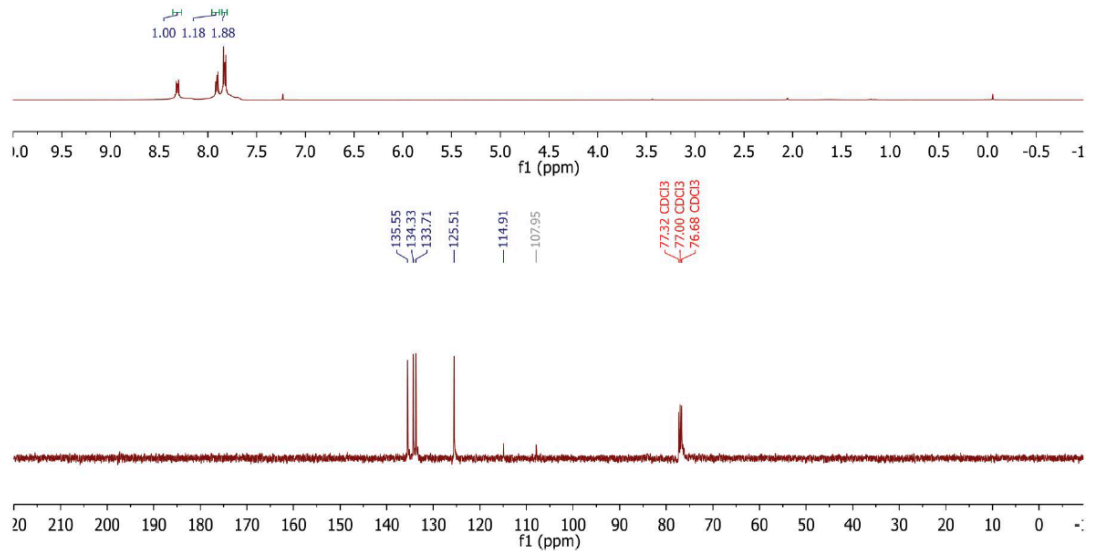
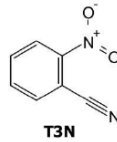
PROTON
DJQ-163-4



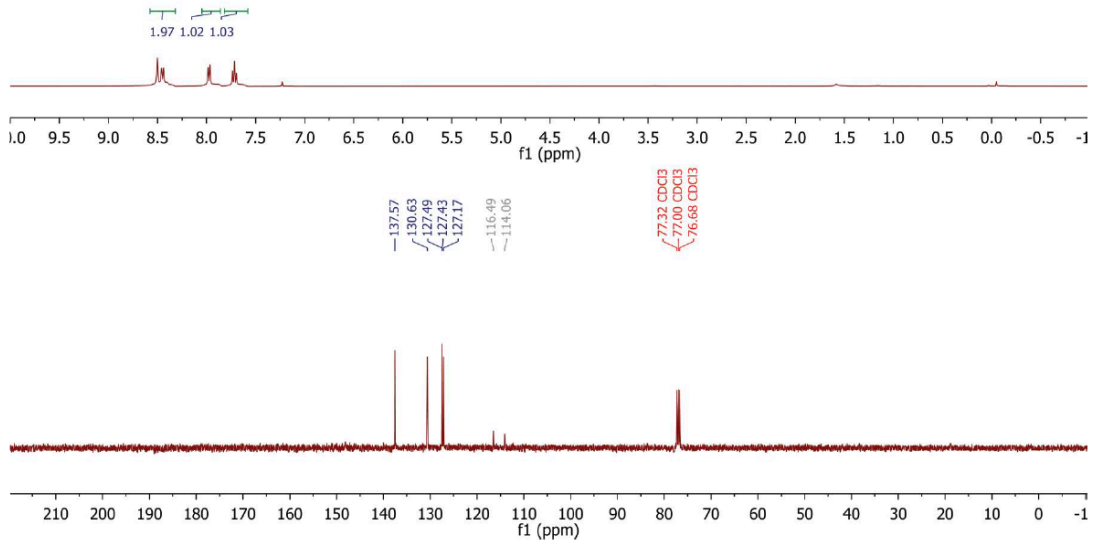
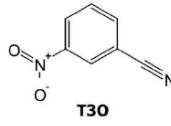
PROTON
DJQ-144-1
DJQ-144-1



PROTON
DJQ-163-3



PROTON
DJQ-167-3



Chapter 2

Nitrones

These early works in the GML Lab formed the foundation for extensive research in hydroxylamine chemistry. Following interests in small heterocyclic frameworks, with a strong expertise in diaziridine chemistry, the GML group sought to perfect a method for the synthesis of Oxaziridines. Similar in structure, the Oxaziridine differs from a Diaziridine by only one heteroatom (Figure 3). Both strained, three-membered heterocycles are important organic reagents for their ability to transfer heteroatoms both enantioselectively and catalytically (Yoon, Williamson, & Michaelis, 2014).



Figure 3. Heteroatomic Difference: Diaziridine (left) and Oxaziridine (right)

Starting with similar reaction conditions from the established diaziridine chemistry, the pursuit of a novel oxaziridine pathway began. N-substituted hydroxylamines were condensed with simple aldehydes in the presence of various additives and media to screen for the formation of Oxaziridine. Unfortunately, no traces of the desired product were observed. Instead however, the major product obtained from these experiments were determined after characterization to be the 1,3-Dipole, Nitron.

The Nitronium moiety consists of nitrogen, making four bonds, with a positive charge, bound to a negatively charged oxygen (Figure 4). The N-O dipole allows for a broad range of chemical transformations (Macaluso & Hamer, 1964) and has been a valuable synthetic intermediate to the organic chemistry community.

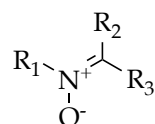


Figure 4. General Structure of the Nitronium Moiety

However, the value of nitroniums has not been limited solely to the field of organic chemistry. The utility of these compounds has been multidisciplinary, finding value in many areas including analytical and pharmaceutical chemistry.

2.1 Free Radical Spin Trapping

Outside the realm of organic chemistry, Nitroniums are commonly employed as free radical scavengers. The addition of a free radical across the double bond of a nitronium yields an adduct that is detectable by EPR spectroscopy (Figure 5). This method has allowed for the detection of previously elusive intermediates (Halpern, et al., 1993).

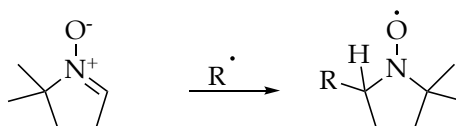


Figure 5. Free Radical, R, Forms a Stable Product with Nitronium

The most commonly used nitrones for this type of spectroscopy are PBN and DMPO. The latter of which has been shown to increase signal to noise ratio for the respective EPR spectra in comparison to previously developed spin traps (Beziere, et al., 2014). Many derivatives of both cyclic and aromatic nitrones are continuously being synthesized to enhance the free-radical spin trapping technique.

Free radicals are a cornerstone of chemistry and have been used to facilitate powerful chemical transformations. Industrial radical polymerization reactions are employed to manufacture valuable polystyrene commodities. A clear mechanistic understanding of free radicals is actively being pursued by means of nitron spin traps to contribute value to these growing markets (Chang, Lau, Parker, & Westmoreland, 1996). These efforts seek to optimize reaction yields at the industrial scale by developing a precise mechanistic understanding of free radical reactivity.

2.2 Pharmaceutical Relevance

The detrimental health effects of oxidative stress, caused by harmful free radicals have been consistently confirmed throughout the literature (Lobo, Phatak, & Chandra, 2010). These studies suggest that the damage caused by free radicals are derived from their sporadic reactivity. Nitrones have been proven to react and effectively neutralize free radicals to form a stable, less reactive adduct. This has prompted research efforts targeting nitrones as potential pharmaceutical agents.

Interestingly, researchers have discovered a nitron-iridium organometallic that demonstrates efficacy comparable to cisplatin for its antitumor properties (Zhao, et al., 2013). The synthesis of this organometallic agent relies on the bidentate coordination of an unactivated aromatic proton and the nitron oxygen to the iridium metallo center.

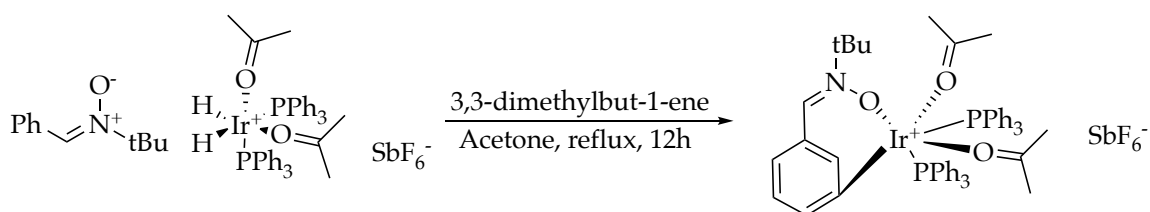


Figure 6. Aromatic CH Activation of Nitron by Iridium Catalyst

Recognizing the vast applications for nitrons in both manufacturing and pharmaceutical industries, the GML group sought to achieve a reaction pathway that could serve as an attractive route to the nitron moiety compared to methods currently being used in industry.

2.3 Synthesis of Nitrons

The following section considers a few of the most practical transformations as well as some synthetically intriguing routes to the nitron moiety. To develop a method that would be most applicable to the industrial community we sought to achieve a broad substrate scope without compromising the simplicity of synthesis.

Nitrones are easily obtained from oxaziridine by simple heating. The strained three membered ring along with a labile nitrogen-oxygen bond make this rearrangement possible. This transformation is greatly accelerated by increasing thermal energy and allows for a direct conversion to the nitronone without any additives or work-up.

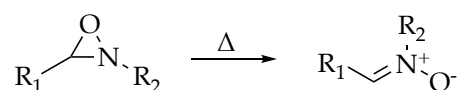


Figure 7. Thermal Oxaziridine Rearrangement to Nitronone

The major drawback to this route however, is the construction of the heterocyclic oxaziridine. The scope of nitronones by this route would be heavily compromised by functional group tolerance of the strained three-membered ring.

The Yoon laboratory demonstrated that an oxaziridine isomerization to nitronone is also possible by employing a Lewis acid catalyst. The additive allows for conversion of functionally stabilized oxaziridines at room temperature and promotes a successive dipolar cycloaddition with the in-situ formed nitronone, serving as the necessary dipole (Partridge, Anzovino, & Yoon, 2008).

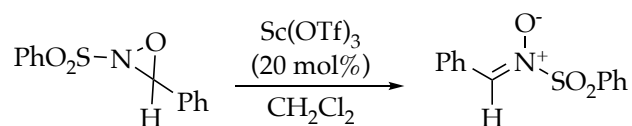


Figure 8. Lewis Acid Catalyzed Oxaziridine Rearrangement by Yoon

Nitrones are also obtained through the oxidation of a tertiary hydroxylamine (Figure 9). This method is subtle and allows for a nitrone functional group to be introduced into a highly structured molecular scaffold with mild oxidation (Colladon, Scarso, & Strukul, 2008).

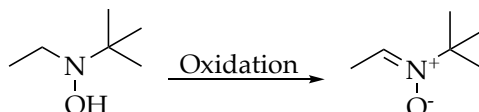


Figure 9. Tertiary Hydroxylamine Oxidation to Nitrone

Though this method may be valuable in many synthetic approaches, it does not generate the type of structural density intended for this work. Previous attempts by the GML group at hydroxylamine synthesis proved tedious and low yielding. To avoid being confined to commercially available hydroxylamine sources we sought a method that would introduce various starting reagents.

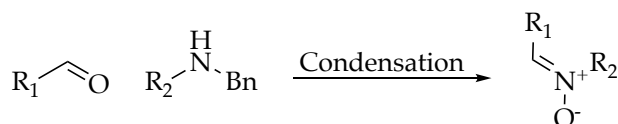


Figure 10. Carbonyl Condensation with N-Benzyl Hydroxylamine

The GML group recognized a hydroxylamine condensation to be the most effective synthetic pathway. R₁ and R₂ may be functionalized by varying both the hydroxylamine and the carbonyl source (Figure 10). In turn, this allows for

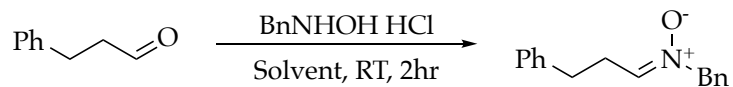
greater functionalization by means of a simple condensation reaction. (Morales, Guijarro, Alonso, Ruano, & Cid, 2016).

2.4 Results and Discussion

With previous experience in hydroxylamine chemistry, the GML group sought to optimize a method for the synthesis of nitrones. In chapter 1, the reaction media played a critical role in HOSA reactivity and therefore a solvent screening was first addressed. After employing an array of solvents, we determined that polar-aprotic solvent allowed for the conversion to the desired product (Table 4). Acetonitrile afforded the best results and was determined to be the most suitable solvent for this reaction.

Next, stoichiometry was explored by manipulating the molar equivalence of the starting reagents. The results of this experiment determined that a stoichiometric excess of inorganic hydroxylamine significantly increased both the rate of the reaction and the desired nitron formation (Table 4 Entry 8-10).

Table 4

Nitron Condensation Optimization

Entry	Solvent	Eq. Hydroxylamine	% Conversion*
1	DCM	1.0	65
2	Chloroform	1.0	59
3	THF	1.0	60
4	Ethyl Ether	1.0	24
5	MeCN	1.0	71
6	Benzene	1.0	15
7	Toluene	1.0	22
8	MeCN	1.5	80
9	MeCN	2.0	92
10	MeCN	3.0	96

*Determined by crude NMR

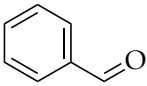
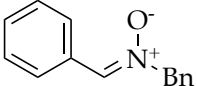
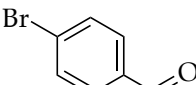
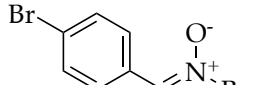
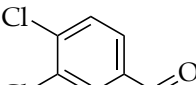
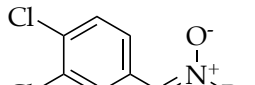
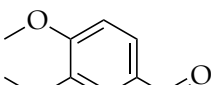
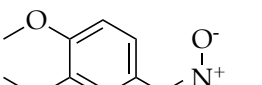
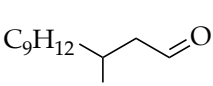
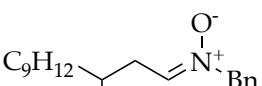
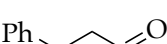

With optimal reaction conditions in hand, the GML Group began to explore the scope of this reaction. The condensation of simple aromatic and aliphatic aldehydes with N-Benzyl Hydroxylamine HCl, afforded the respective nitrones in good to excellent yields. The resulting N-alkyl, aldonitrones boasted a

white crystalline appearance and were easily isolated with a high purity by means of simple aqueous work-up (See experimental at 2.4).

Table 5

Aldonitrone Scope

$$\begin{array}{c}
 \text{R} \\
 \diagup \\
 \text{C}=\text{O} \\
 \diagdown \\
 \text{H}
 \end{array}
 \xrightarrow[\text{MeCN, RT, 2hr}]{\text{BnNHOH HCl}}
 \begin{array}{c}
 \text{O}^- \\
 | \\
 \text{R}-\text{C}=\text{N}^+-\text{Bn} \\
 | \\
 \text{H}
 \end{array}$$

Entry	Aldehyde	Aldonitrone	% Yield
T5A			65
T5B			88
T5C			90
T5D			95
T5E			85
T5F			76

Similarly, enals provided the respective alpha-beta unsaturated nitrones upon condensation with hydroxylamine. However, aliphatic enals showed significantly diminished yields (Table 5). The reoccurrence of this trend across multiple aliphatic substrates prompted a re-optimization of reaction conditions with a focus on aliphatic functional groups.

With a polar organic solvent, such as acetonitrile, the organic carbonyl dissolved adequately as expected, however, the inorganic hydroxylamine salt was only slightly miscible. This system slowly introduces the hydroxylamine into the media upon vigorous stirring. However, stoichiometric analysis determined that the reaction equilibria favored a large excess of hydroxylamine to allow for nitrone formation.

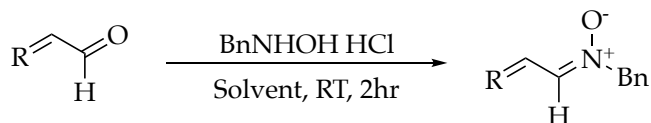
Therefore, we employed an aqueous media for aliphatic carbonyl sources, which previously afforded diminished yields. Running the condensation “on water” would ultimately allow for a reversal in reagent introduction. The organic layer composed of starting aldehyde would slowly be introduced into the aqueous hydroxylamine layer upon vigorous stirring by way of its polar head unit.

Employing an aqueous media for aliphatic enals afforded the respective alpha-beta unsaturated nitrones in good to excellent yield (Table 5), ultimately broadening the scope for this reaction. Simple aliphatic-cyclic Ketonitrones were also obtained in good to excellent yields by condensation “on water” (Table 7 – Entry T7A, T7B). Cyclic enones were also tolerated and showed no traces of addition side products. However, substitution at the carbonyl beta carbon of 3-

methyl cyclohexen-2-one (Table 7 – Entry T7D) resulted in significantly lower yields.

The rates of these reactions were observed to be significantly greater than those previously reported with unsaturated or aromatic enals. The difference in reaction media was hypothesized for this rate acceleration. The Ketonitrones showed full conversion by TLC at 1 hour (Table 7) almost twice as fast as the aldonitrones (Table 6) which required up to 2 hours.

Table 6

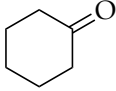
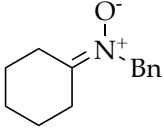
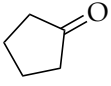
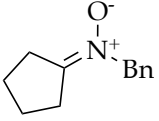
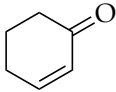
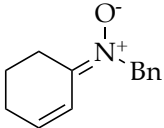
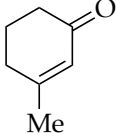
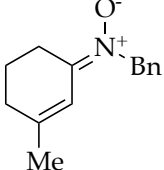
Alpha-Beta Unsaturated Aldonitronone Scope

Entry	Enal	α - β unsaturated aldonitronone	Solvent	% Yield
T6A	Ph-CH=CH-CHO	Ph-CH=CH-CH=N ⁺ (Bn)O ⁻	MeCN	82
T6B	MeOPh-CH=CH-CHO	MeOPh-CH=CH-CH=N ⁺ (Bn)O ⁻	MeCN	95
T6C	Me ₂ NPh-CH=CH-CHO	Me ₂ NPh-CH=CH-CH=N ⁺ (Bn)O ⁻	MeCN	56
T6D	Ph-C(Me)=CH-CHO	Ph-C(Me)=CH-CH=N ⁺ (Bn)O ⁻	MeCN	62
T6E	Me-CH=CH-CHO	Me-CH=CH-CH=N ⁺ (Bn)O ⁻	H ₂ O	68
T6F	Me-CH ₂ -CH ₂ -CH=CH-CHO	Me-CH ₂ -CH ₂ -CH=CH-CH=N ⁺ (Bn)O ⁻	H ₂ O	70
T6G	Me-CH=CH-CH=CH-CHO	Me-CH=CH-CH=CH-CH=N ⁺ (Bn)O ⁻	H ₂ O	85
T6H	C ₅ H ₁₁ -CH=CH-CH=CH-CHO	C ₅ H ₁₁ -CH=CH-CH=CH-CH=N ⁺ (Bn)O ⁻	H ₂ O	90
T6I	Me-C(Me)=CH-CH ₂ -CH ₂ -C(Me)=CH-CHO	Me-C(Me)=CH-CH ₂ -CH ₂ -C(Me)=CH-CH=N ⁺ (Bn)O ⁻	H ₂ O	92

Table 7

Ketonitrone Scope

$$\begin{array}{c}
 \text{R} \\
 \diagdown \\
 \text{C}=\text{O} \\
 \diagup \\
 \text{R}
 \end{array}
 \xrightarrow[\text{H}_2\text{O, RT, 1hr}]{\text{BnNHOH HCl}}
 \begin{array}{c}
 \text{O}^- \\
 | \\
 \text{R}-\text{C}=\text{N}^+-\text{Bn} \\
 \diagup \\
 \text{R}
 \end{array}$$

Entry	Ketone	Ketonitrone	% Yield
T7A			92
T7B			90
T7C			84
T7D			60

These results were particularly exciting because they showed a significant rate enhancement of previously unreactive ketones. We hypothesized that increasing electron density to the carbonyl carbon in stabilized the partial positive charge and diminished conversion (Figure 11). However, by employing

a heterogeneous reaction media, the electron dense, cyclic ketones exhibited excellent reactivity.

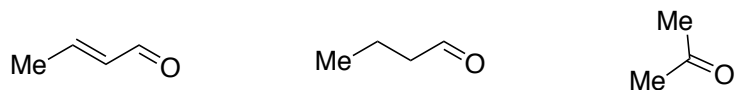


Figure 11. Increasing Carbonyl Carbon Partial Positive Stabilization

To further broaden the scope of this reaction, we next sought to modify the nitrogen protecting group by employing various hydroxylamine sources. N-Benzyl Hydroxylamine afforded the greatest conversion to nitron (Table 8 T8A).

Table 8

N-Protecting Group Scope
$$\text{Ph}-\text{CH}=\text{CH}-\text{CHO} \xrightarrow[\text{Solvent, RT, 2hr}]{\text{RNHOH}} \text{Ph}-\text{CH}=\text{CH}-\text{N}^+(\text{R})=\text{O}^-$$

Entry	Hydroxylamine	Nitrone	Solvent	% Conv. ^a
T8A			MeCN	82
T8B			H ₂ O	88
T8C			H ₂ O	92
T8D			MeCN	80
T8E			MeCN	12
T8F			MeCN	18
T8G			-	-

a. Determined by crude proton NMR, not included in the supporting information.

Whereas *N*-Carbamoyl substituted hydroxylamines exhibited a severe decrease in conversion. More specifically, *N*-Boc substituted hydroxylamine had an observed conversion as low as 18% by crude proton NMR (Table 8 - T8F). We hypothesized that the hydroxylamine electronics ultimately compromised the desired reaction outcome. If the electron density of the hydroxylamine nitrogen

is directed by the electron withdrawing carbamoyl group, nitrogen's lone pair of electrons and respective nucleophilicity would be compromised (Figure 12).

In this case, the hydroxylamine hydroxyl group is theoretically capable of competing as a nucleophile which could potentiate the formation of undesirable side products. The observation of unidentified side products by crude proton NMR and TLC both suggest that these alternative electronics may be preventing the desired formation of nitron.

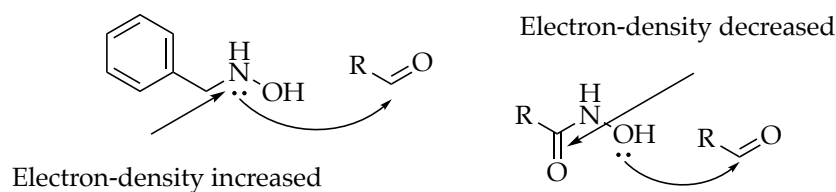


Figure 12. Effects of Hydroxylamine N-Substitution on Nucleophilicity

Though the isolation of N-Carbamoyl Nitrones was initially unsuccessful, there have been reports of their formation “in-situ” during successful dipolar cycloadditions (Ricci, Gioia, Fini, Mazzanti, & Bernardi, 2009). Current research efforts in the GML Lab are focused on exploring new synthetic methods to successfully isolate this elusive class of N-Carbamoyl Nitron.

2.5 Conclusion

Aliphatic and aromatic aldehydes were converted to the respective nitrones while exhibiting promising functional group tolerance. Ketonitrones were also afforded by simple manipulation of the reaction media. This type of chemoselectivity governed by the reaction media can prove beneficial to the industrial community where in some cases, an aqueous environment may be favored over traditional organic solvents.

Again, hydroxylamines have proven to facilitate powerful reactions leading to key synthetic intermediates. However, this method has highlighted a need for further research efforts regarding the nucleophilicity of N-Carbamoyl hydroxylamines. Hydroxylamine chemistry has been well established over the years, but small limitations like these, if overcome, could lead to great scientific advancements.

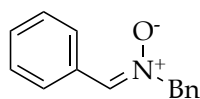
2.6 Experimental

Reagents were obtained from Aldrich Chemical, Acros Organics or Alfa Aesar and used without further purification. Solvents were obtained from EMD Milipore DrySol and degassed with nitrogen. Reactions were performed in 4-ml glass vials with magnetic stirring. TLC was performed on 0.25 mm E. Merck silica gel 60 F254 plates and visualized under UV light (254 nm) or by staining with potassium permanganate (KMnO₄). Silica flash chromatography was performed on E. Merck 230–400 mesh silica gel 60. Automated chromatography was performed on an ISOLERA Prime instrument with 10 g. SNAP silica gel normal phase cartridges using a flow rate of 12.0 mL/min and a gradient of 0–

100% EtOAc in Heptanes over 12 column volumes with UV detection at 254 nm. NMR spectra were recorded on Varian Mercury II 400 MHz Spectrometer at 24 °C in CDCl₃ unless otherwise indicated. Chemical shifts are expressed in ppm relative to solvent signals: CDCl₃ (¹H, 7.23 ppm; ¹³C, 77.0 ppm; coupling constants are expressed in Hz.

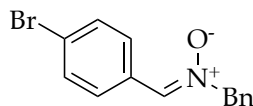
2.6.1. General method for the synthesis of nitrones. In a 4-mL reaction vial, carbonyl (1.0 mmol, 1.0 equivalent) and hydroxylamine (1.1 mmol, 1.1 equivalent) were dissolved in 3 mL of acetonitrile. The reaction was stirred at RT for 2 hours (aldehyde), 1 hour (ketone) or until complete conversion of starting material was confirmed by TLC. The organic was extracted with diethyl ether, 3-50 mL aliquots. The organic layer was washed with 3-10 mL aliquots of aqueous (10%) sodium bicarbonate. The organic layer was dried with 3-10 mL aliquots of saturated aqueous brine solution (NaCl). The organic layer was isolated and dried over anhydrous sodium sulfate, filtered, and concentrated by rotary evaporation to afford the crude product. The product was directly characterized unless traces of impurities required purification by automated silica gel flash chromatography.

2.6.2. Synthesis of nitrones from Table 2.



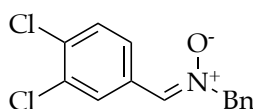
(T2A) DJQ-534

(Z)-N-benzyl-1-phenylmethanimine oxide (T2A) Purification by automated silica gel flash chromatography (10 g cartridge, 14 ml/min. 20:1 Heptanes/EtOAc to 1:4 Heptanes/EtOAc over 12 min) afforded the nitrone **2a** (65% yield) as a white solid. ¹H NMR (400 MHz, Chloroform-*d*) δ 8.31 – 8.11 (m, 2H), 7.53 – 7.44 (m, 2H), 7.43 – 7.33 (m, 7H), 5.04 (s, 2H). ¹³C NMR (101 MHz, Chloroform-*d*) δ 134.27, 130.45, 130.42, 129.21, 128.96, 128.62, 128.45, 71.23.



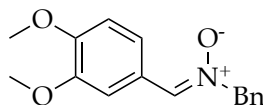
(T2B) DJQ-247

(Z)-N-benzyl-1-(4-bromophenyl) methanimine oxide (T2B) Purification by automated silica gel flash chromatography (10 g cartridge, 14 ml/min. 20:1 Heptanes/EtOAc to 1:4 Heptanes/EtOAc over 12 min) afforded the nitron **2b** (88% yield) as a white solid. $^1\text{H NMR}$ (400 MHz, Chloroform-*d*) δ 8.17 – 8.01 (m, 2H), 7.55 – 7.49 (m, 2H), 7.48 – 7.42 (m, 2H), 7.42 – 7.39 (m, 2H), 7.35 (s, 1H), 5.04 (s, 2H). $^{13}\text{C NMR}$ (101 MHz, Chloroform-*d*) δ 133.16 , 131.66 , 129.90 , 129.27 , 129.10 , 129.02 , 71.37 .



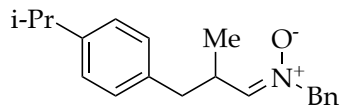
(T2C) DJQ-535

(Z)-N-benzyl-1-(3,4-dichlorophenyl) methanimine oxide (T2C) Purification by automated silica gel flash chromatography (10 g cartridge, 14 ml/min. 20:1 heptanes/EtOAc to 1:4 Heptanes/EtOAc over 12 min) afforded the nitron **2c** (90% yield) as a white solid. $^1\text{H NMR}$ (400 MHz, Chloroform-*d*) δ 9.31 (d, $J = 8.8$ Hz, 1H), 7.86 (s, 1H), 7.51 – 7.44 (m, 2H), 7.45 – 7.34 (m, 4H), 7.29 (dd, $J = 8.8, 2.2$ Hz, 1H), 5.08 (s, 2H). $^{13}\text{C NMR}$ (101 MHz, Chloroform-*d*) δ 132.83 , 129.71 , 129.27 , 129.23 , 129.17 , 129.01 , 127.37 , 126.65 , 72.17 .



(T2D) DJQ-532

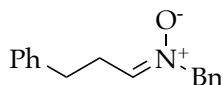
(Z)-N-benzyl-1-(3,4-dimethoxyphenyl) methanimine oxide (T2D) Purification by automated silica gel flash chromatography (10 g cartridge, 14 ml/min. 20:1 heptanes/EtOAc to 1:4 Heptanes/EtOAc over 12 min) afforded the nitron **2d** (95% yield) as a white solid. $^1\text{H NMR}$ (400 MHz, Chloroform-*d*) δ 8.37 (d, $J = 2.0$ Hz, 1H), 7.48 – 7.43 (m, 2H), 7.41 – 7.36 (m, 3H), 7.34 (s, 1H), 6.86 (d, $J = 8.5$ Hz, 1H), 5.01 (s, 2H), 3.90 (d, $J = 2.0$ Hz, 6H). $^{13}\text{C NMR}$ (101 MHz, Chloroform-*d*) δ 150.69 , 134.16 , 129.22 , 128.96 , 128.91 , 123.74 , 123.08 , 110.88 , 110.52 , 70.83 , 55.86 .



(T2E) DJQ-248

(Z)-N-benzyl-3-(4-isopropylphenyl)-2-methylpropan-1-imine oxide (T2E)

Purification by automated silica gel flash chromatography (10 g cartridge, 14 ml/min. 20:1 heptanes/EtOAc to 1:4 Heptanes/EtOAc over 12 min) afforded the nitrone **2e** (85 % yield) as a white solid. $^1\text{H NMR}$ (400 MHz, Chloroform-*d*) δ 7.45 – 7.23 (m, 5H), 7.17 – 7.00 (m, 4H), 6.49 (d, $J = 7.3$ Hz, 1H), 4.82 (s, 2H), 3.39 (hept, $J = 7.0$ Hz, 1H), 2.87 (hept, $J = 6.9$ Hz, 1H), 2.76 (dd, $J = 13.6, 7.0$ Hz, 1H), 2.68 (dd, $J = 13.6, 7.2$ Hz, 1H), 2.07 – 2.00 (m, 1H), 1.24 (dd, $J = 7.2, 2.2$ Hz, 6H), 1.08 (dd, $J = 6.9, 0.8$ Hz, 3H). $^{13}\text{C NMR}$ (101 MHz, Chloroform-*d*) δ 143.57, 129.15, 128.96, 128.84, 128.80, 69.36, 38.80, 33.67, 32.54, 24.04, 16.18.

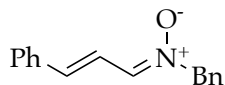


(T2F) DJQ-539

(Z)-N-benzyl-3-phenylpropan-1-imine oxide (T2F)

Purification by automated silica gel flash chromatography (10 g cartridge, 14 ml/min. 20:1 heptanes/EtOAc to 1:4 Heptanes/EtOAc over 12 min) afforded the nitrone **2f** (76% yield) as a white solid. $^1\text{H NMR}$ (400 MHz, Chloroform-*d*) δ 7.40 – 7.30 (m, 5H), 7.26 (tt, $J = 7.8, 1.7$ Hz, 2H), 7.24 – 7.17 (m, 1H), 7.17 – 7.11 (m, 2H), 6.62 (t, $J = 5.4$ Hz, 1H), 4.84 (s, 2H), 2.85 – 2.79 (m, 4H). $^{13}\text{C NMR}$ (101 MHz, Chloroform-*d*) δ 140.41, 138.16, 129.25, 128.87, 128.52, 128.27, 126.26, 69.28, 31.15, 27.94.

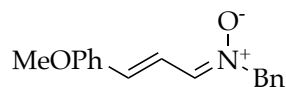
2.6.3. Synthesis of nitrones from Table 3.



(T3A) DJQ-393

(1Z,2E)-N-benzyl-3-phenylprop-2-en-1-imine oxide (T3A)

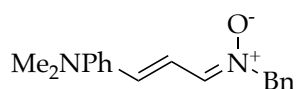
Purification by automated silica gel flash chromatography (10 g cartridge, 14 ml/min. 20:1 heptanes/EtOAc to 1:4 Heptanes/EtOAc over 12 min) afforded the nitrone **3a** (82% yield) as a white solid. $^1\text{H NMR}$ (400 MHz, Chloroform-*d*) δ 7.49 – 7.38 (m, 8H), 7.35 – 7.29 (m, 3H), 7.21 (dd, $J = 9.5, 0.7$ Hz, 1H), 6.94 (d, $J = 16.3$ Hz, 1H), 4.95 (s, 2H). $^{13}\text{C NMR}$ (101 MHz, Chloroform-*d*) δ 138.37, 136.46, 129.25, 129.17, 128.99, 128.97, 128.81, 127.28, 118.40, 69.29.



(T3B) DJQ-394

(1Z,2E)-N-benzyl-3-(4-methoxyphenyl)prop-2-en-1-imine oxide (T3A)

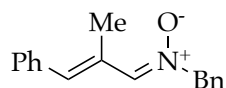
Purification by automated silica gel flash chromatography (10 g cartridge, 14 ml/min. 20:1 heptanes/EtOAc to 1:4 Heptanes/EtOAc over 12 min) afforded the nitrone **3b** (95% yield) as a white solid. $^1\text{H NMR}$ (400 MHz, Chloroform-*d*) δ 7.49 – 7.38 (m, 6H), 7.33 – 7.24 (m, 1H), 7.17 (dd, $J = 9.5, 0.6$ Hz, 1H), 7.00 – 6.77 (m, 3H), 4.93 (s, 2H), 3.80 (s, 3H). $^{13}\text{C NMR}$ (101 MHz, Chloroform-*d*) δ 160.53, 138.20, 136.80, 129.20, 128.95, 128.91, 128.88, 128.80, 116.36, 114.31, 69.06, 55.32.



(T3C) DJQ-416

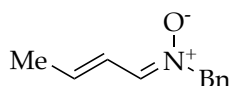
(1Z,2E)-N-benzyl-3-(4-(dimethylamino)phenyl)prop-2-en-1-imine oxide (T3C)

Purification by automated silica gel flash chromatography (10 g cartridge, 14 ml/min. 20:1 heptanes/EtOAc to 1:4 Heptanes/EtOAc over 12 min) afforded the nitrone **3c** (56% yield) as an orange solid. $^1\text{H NMR}$ (400 MHz, Chloroform-*d*) δ 7.44 – 7.36 (m, 6H), 7.29 – 7.22 (m, 1H), 7.14 (d, $J = 9.6$ Hz, 1H), 6.84 (d, $J = 16.0$ Hz, 1H), 6.66 – 6.60 (m, 2H), 4.91 (s, 2H), 2.97 (s, 6H). $^{13}\text{C NMR}$ (101 MHz, Chloroform-*d*) δ 139.33, 137.49, 133.40, 129.16, 128.89, 128.86, 128.73, 113.90, 111.98, 68.72, 40.15.



(T3D) DJQ-500

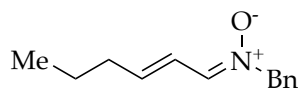
(1Z,2E)-N-benzyl-2-methyl-3-phenylprop-2-en-1-imine oxide (T3D) Purification by automated silica gel flash chromatography (10 g cartridge, 14 ml/min. 20:1 heptanes/EtOAc to 1:4 Heptanes/EtOAc over 12 min) afforded the nitrone **3c** (56% yield) as an orange solid.



(T3E) DJQ-537

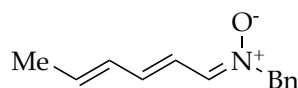
(1Z,2E)-N-benzylbut-2-en-1-imine oxide (T3C) Purification by automated silica gel flash chromatography (10 g cartridge, 14 ml/min. 20:1 heptanes/EtOAc to 1:4 Heptanes/EtOAc over 12 min) afforded the nitrone **3e** (68% yield) as pale oil. $^1\text{H NMR}$ (400 MHz, Chloroform-*d*) δ 7.37 (dtt, $J = 5.2, 3.3, 2.0$ Hz, 5H), 6.98 (d, $J = 9.4$

Hz, 1H), 6.81 – 6.70 (m, 1H), 6.20 (dq, $J = 16.0, 7.0$ Hz, 1H), 4.86 (s, 2H), 1.86 (dd, $J = 6.9, 1.7$ Hz, 3H). ^{13}C NMR (101 MHz, Chloroform- d) δ 138.21 , 136.08 , 129.17 , 128.89 , 128.83 , 122.35 , 68.90 , 19.01 .



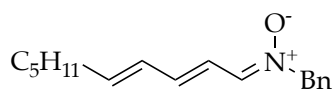
(T3F) DJQ-421

(1Z,2E)-N-benzylhex-2-en-1-imine oxide (T3F) Purification by automated silica gel flash chromatography (10 g cartridge, 14 ml/min. 20:1 heptanes/EtOAc to 1:4 Heptanes/EtOAc over 12 min) afforded the nitronium **3f** (70% yield) as a pale oil. ^1H NMR (400 MHz, Chloroform- d) δ 7.40 (dtd, $J = 5.6, 2.7, 1.3$ Hz, 4H), 6.98 (d, $J = 9.4$ Hz, 1H), 6.76 (ddt, $J = 15.9, 9.5, 1.6$ Hz, 1H), 6.19 (dt, $J = 15.6, 7.1$ Hz, 1H), 4.88 (s, 2H), 2.17 (qd, $J = 7.2, 1.6$ Hz, 2H), 1.49 – 1.41 (m, 2H), 0.90 (t, $J = 7.4$ Hz, 3H). ^{13}C NMR (101 MHz, Chloroform- d) δ 143.37 , 136.29 , 129.25 , 128.91 , 128.86 , 121.13 , 68.93 , 35.34 , 21.81 , 13.67 .



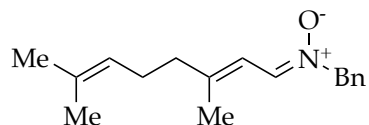
(T3G) DJQ-421

(1Z,2E,4E)-N-benzylhexa-2,4-dien-1-imine oxide (T3G) Purification by automated silica gel flash chromatography (10 g cartridge, 14 ml/min. 20:1 heptanes/EtOAc to 1:4 Heptanes/EtOAc over 12 min) afforded the nitronium **3g** (85% yield) as a white solid.



(T3H) DJQ-586

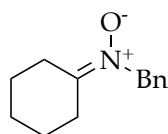
(1Z,2E,4E)-N-benzyldeca-2,4-dien-1-imine oxide (T3H) Purification by automated silica gel flash chromatography (10 g cartridge, 14 ml/min. 20:1 heptanes/EtOAc to 1:4 Heptanes/EtOAc over 12 min) afforded the nitronium **3h** (90% yield) as a white solid.



(T3I) DJQ-498

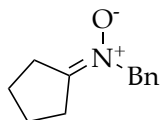
(1Z,2E)-N-benzyl-3,7-dimethylocta-2,6-dien-1-imine oxide (T3I) Purification by automated silica gel flash chromatography (10 g cartridge, 14 ml/min. 20:1 heptanes/EtOAc to 1:4 Heptanes/EtOAc over 12 min) afforded the nitronone **3i** (92% yield) as a yellow oil. ¹H NMR (400 MHz, Chloroform-*d*) δ 7.43 – 7.37 (m, 4H), 7.22 (d, *J* = 10.0 Hz, 1H), 6.60 (dq, *J* = 10.0, 1.3 Hz, 1H), 5.06 (ddtd, *J* = 5.6, 4.3, 2.7, 1.3 Hz, 1H), 4.90 (s, 2H), 2.16 (q, *J* = 5.8, 4.2 Hz, 4H), 1.76 (d, *J* = 1.2 Hz, 3H), 1.68 – 1.65 (m, 3H), 1.58 (d, *J* = 1.3 Hz, 3H). ¹³C NMR (101 MHz, Chloroform-*d*) δ 149.91, 133.81, 133.34, 129.05, 128.85, 128.74, 123.18, 115.87, 69.11, 40.37, 26.28, 25.64, 17.93, 17.68.

2.6.4. Synthesis of nitrones from Table 4.



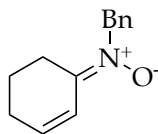
(T4A) DJQ-553

N-benzylcyclohexanimine oxide (T4A) Purification by automated silica gel flash chromatography (10 g cartridge, 14 ml/min. 1:1 Heptanes/EtOAc to 0:1 Heptanes/EtOAc over 12 min) afforded the nitronone **4a** (92% yield) as a pale oil. ¹H NMR (400 MHz, Chloroform-*d*) δ 7.39 – 7.23 (m, 5H), 5.07 (s, 2H), 2.75 (t, *J* = 6.5 Hz, 2H), 2.45 (t, *J* = 6.0 Hz, 2H), 1.68 – 1.61 (m, 2H), 1.53 (dddd, *J* = 10.5, 8.1, 4.6, 2.9 Hz, 4H). ¹³C NMR (101 MHz, Chloroform-*d*) δ 150.01, 134.08, 128.77, 128.02, 127.49, 63.76, 30.09, 26.96, 25.62, 24.60.



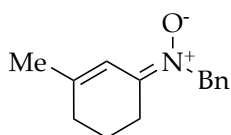
(T4B) DJQ-552

N-benzylcyclopentanimine oxide (T4B) Purification by automated silica gel flash chromatography (10 g cartridge, 14 ml/min. 1:1 Heptanes/EtOAc to 0:1 Heptanes/EtOAc over 12 min) afforded the nitronone **4b** (90% yield) as a pale oil. ¹H NMR (400 MHz, Chloroform-*d*) δ 7.44 – 7.24 (m, 5H), 4.93 (s, 2H), 2.72 – 2.64 (m, 2H), 2.56 – 2.50 (m, 2H), 1.89 – 1.74 (m, 4H). ¹³C NMR (101 MHz, Chloroform-*d*) δ 128.76, 128.25, 128.11, 65.25, 31.17, 31.11, 26.34, 24.53.



(T4C) DJQ-554

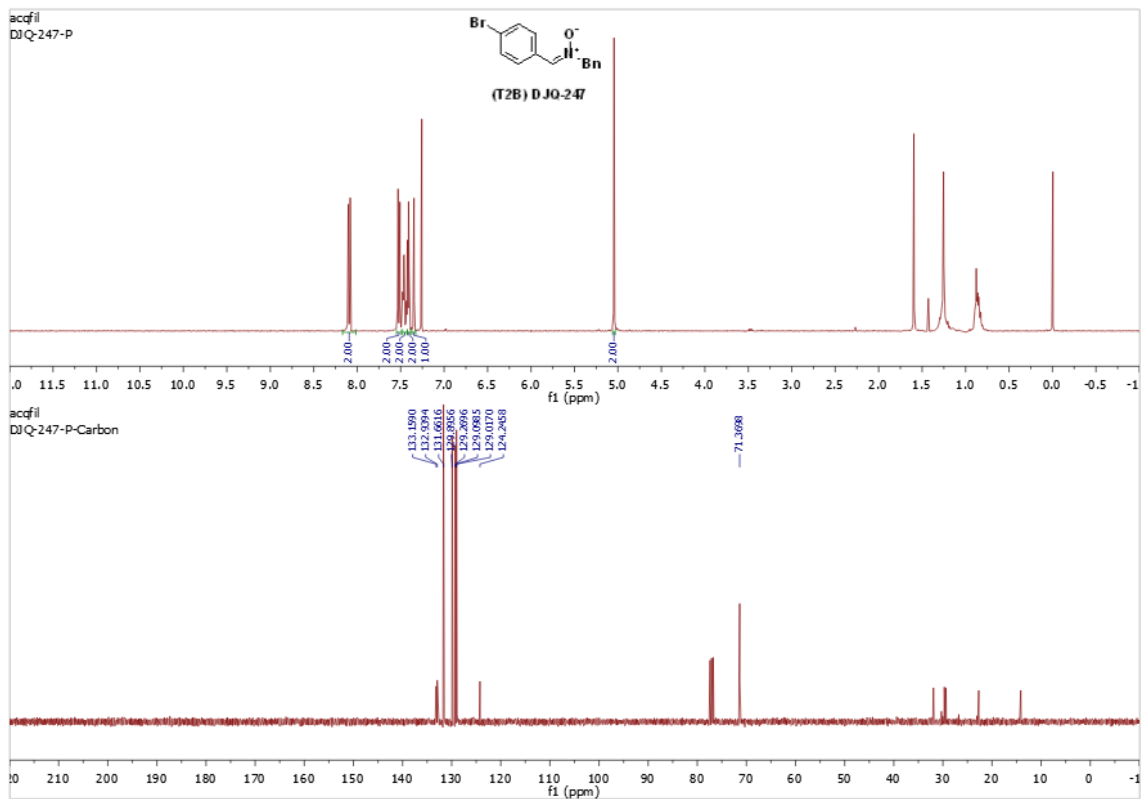
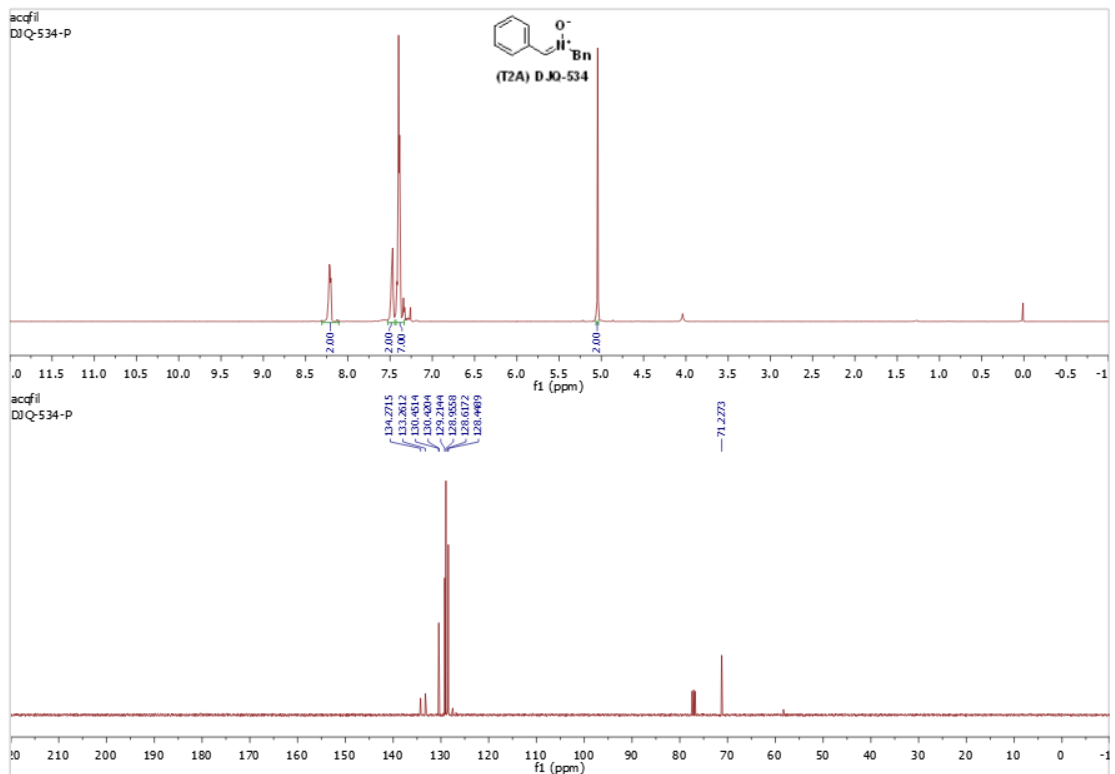
(E)-N-benzylcyclohex-2-en-1-imine oxide (T4C) Purification by automated silica gel flash chromatography (10 g cartridge, 14 ml/min. 1:1 Heptanes/EtOAc to 0:1 Heptanes/EtOAc over 12 min) afforded the nitron **4c** (84% yield) as a pale oil. $^1\text{H NMR}$ (400 MHz, Chloroform-*d*) δ 7.38 – 7.26 (m, 5H), 6.47 (dtd, $J = 10.3, 2.0, 0.8$ Hz, 1H), 6.11 (dt, $J = 10.5, 4.5$ Hz, 1H), 5.11 (s, 2H), 2.80 (t, $J = 6.6$ Hz, 2H), 2.16 (dt, $J = 6.2, 4.3$ Hz, 2H), 1.82 – 1.75 (m, 2H). $^{13}\text{C NMR}$ (101 MHz, Chloroform-*d*) δ 145.35 , 136.23 , 128.75 , 128.11 , 127.67 , 119.46 , 62.91 , 24.89 , 24.80 , 20.68 .

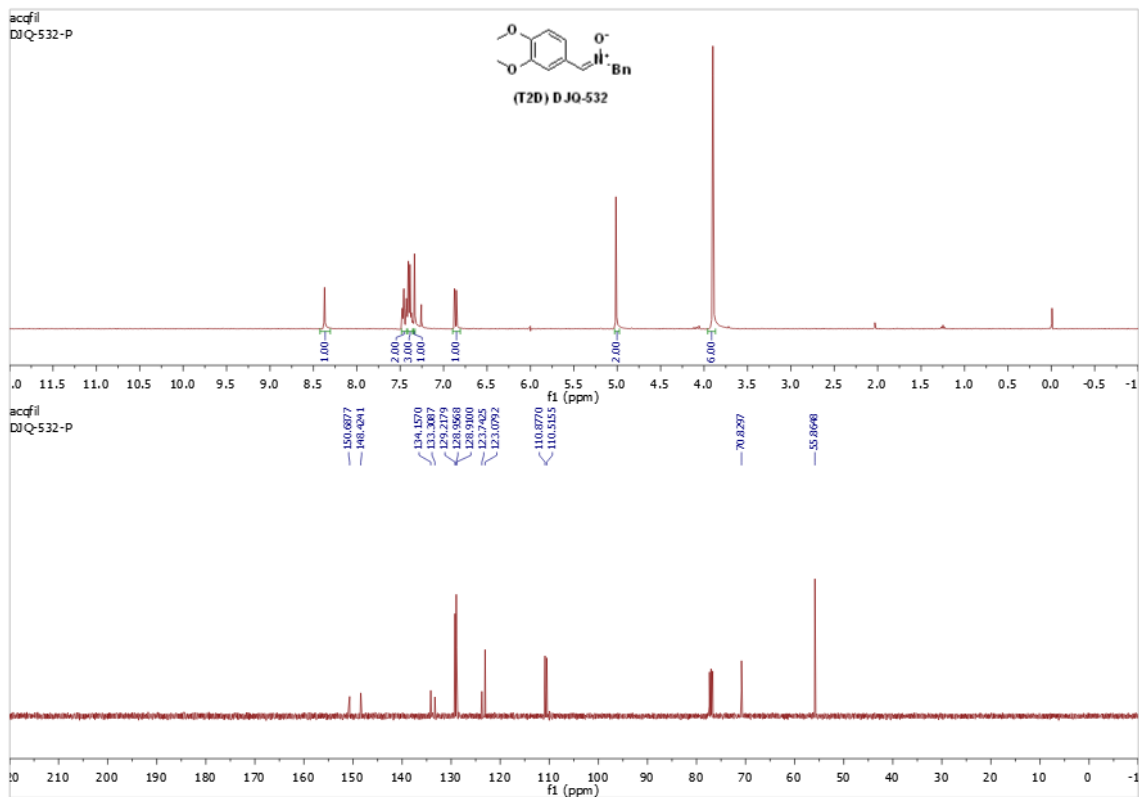
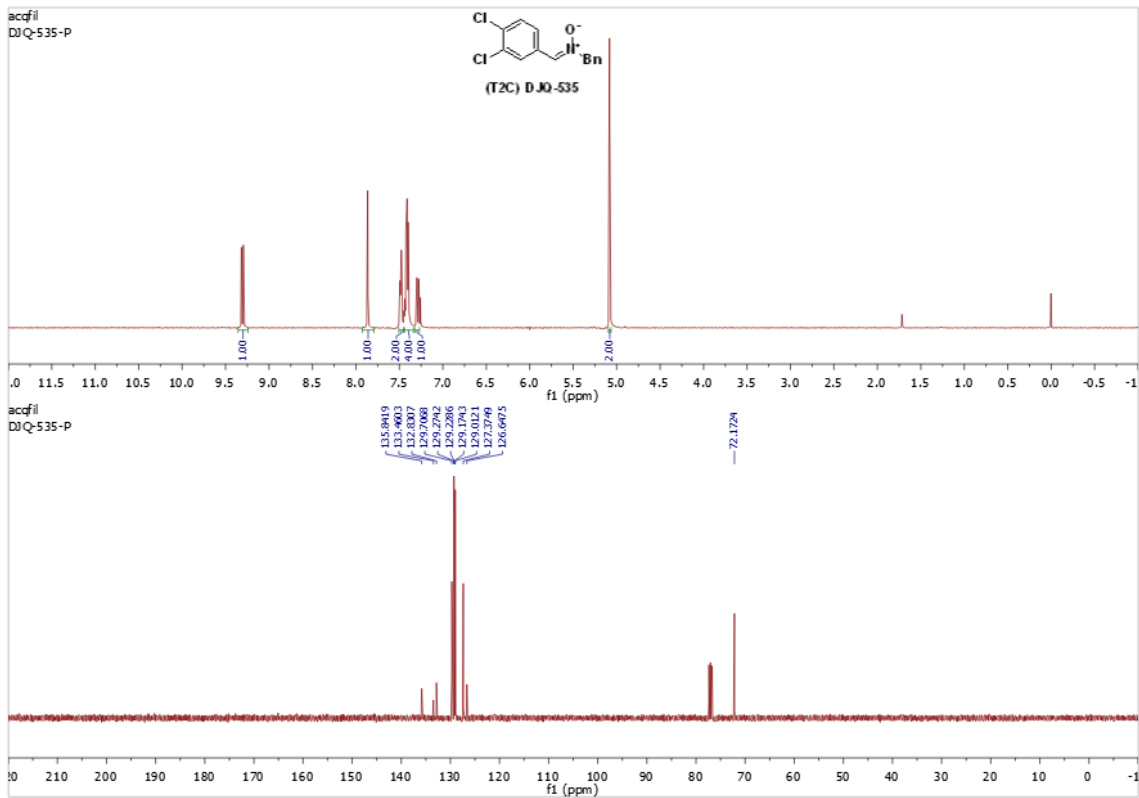


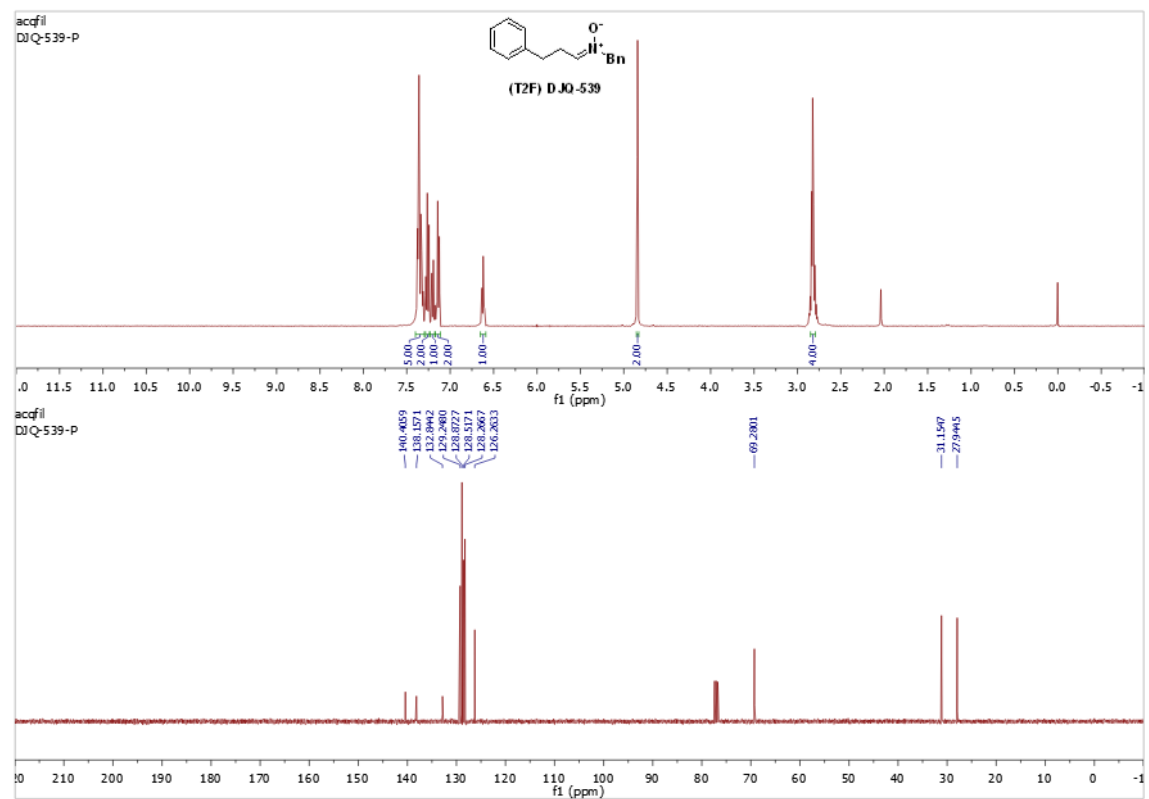
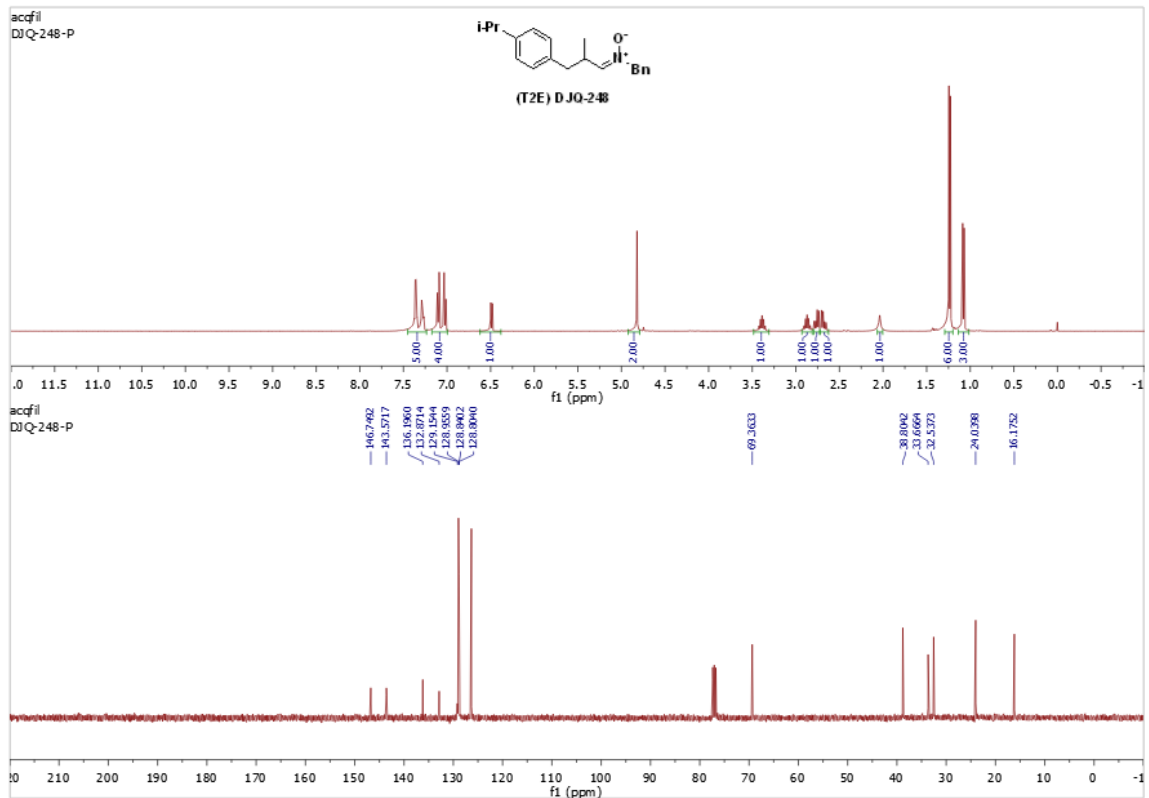
(T4D) DJQ-555

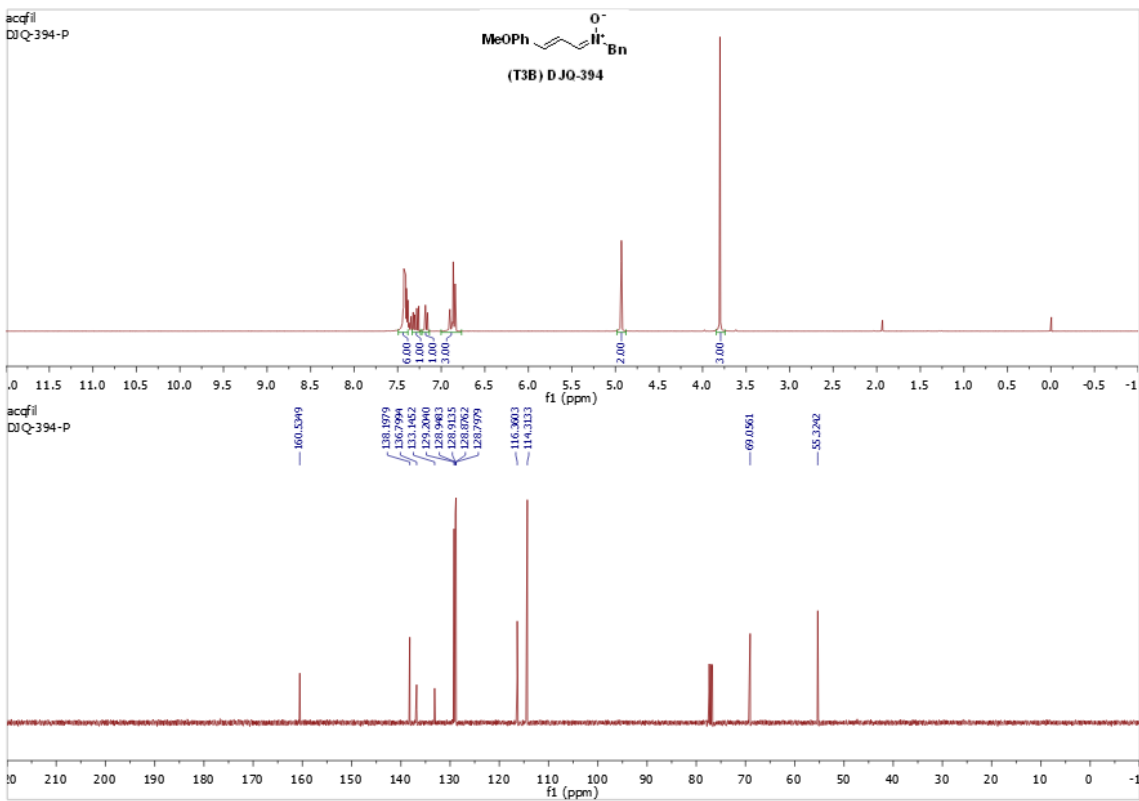
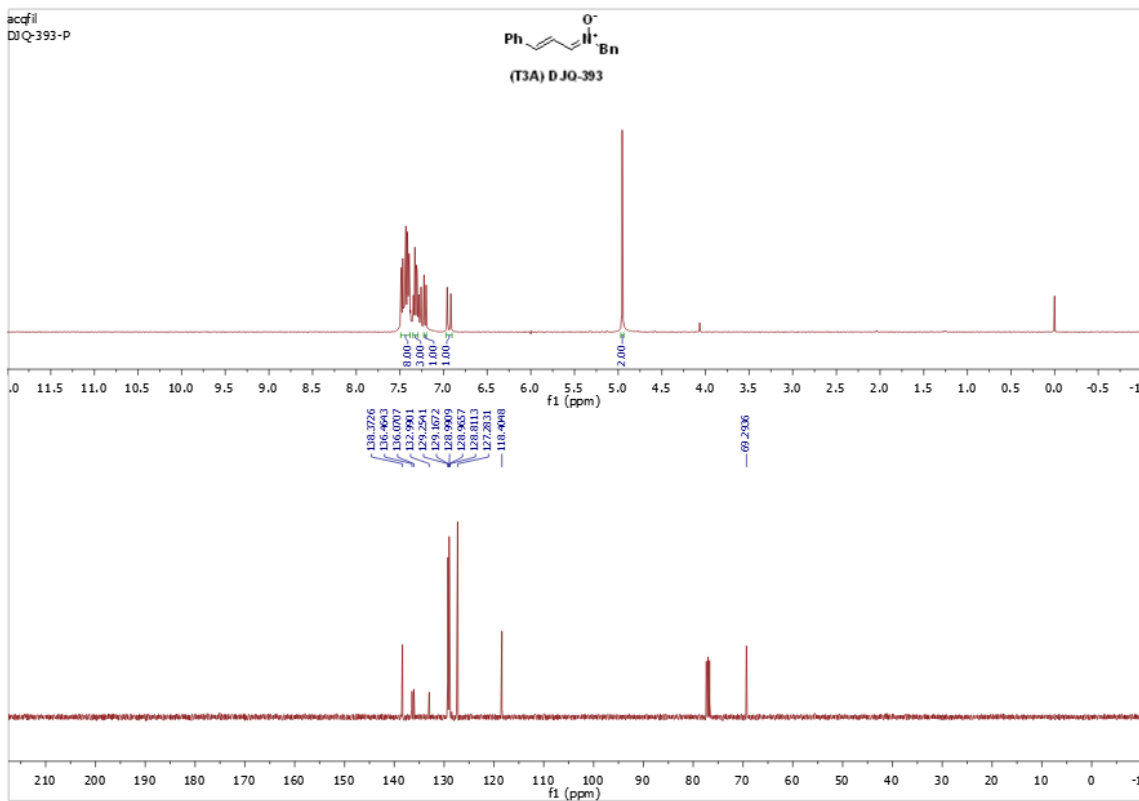
(E)-N-benzyl-3-methylcyclohex-2-en-1-imine oxide (T4D) Purification by automated silica gel flash chromatography (10 g cartridge, 14 ml/min. 1:1 heptanes/EtOAc to 0:1 Heptanes/EtOAc over 12 min) afforded the nitron **4d** (60% yield) as a pale oil. $^1\text{H NMR}$ (400 MHz, Chloroform-*d*) δ 7.39 – 7.26 (m, 7H), 6.22 (h, $J = 1.4$ Hz, 1H), 5.09 (s, 2H), 5.03 (s, 1H), 2.74 (t, $J = 6.6$ Hz, 2H), 2.46 (t, $J = 6.5$ Hz, 1H), 2.08 (t, $J = 6.3$ Hz, 3H), 1.89 (d, $J = 1.4$ Hz, 1H), 1.84 (d, $J = 1.4$ Hz, 3H), 1.76 (q, $J = 6.5$ Hz, 3H). $^{13}\text{C NMR}$ (101 MHz, Chloroform-*d*) δ 147.06 , 146.50 , 134.38 , 128.77 , 128.72 , 127.96 , 127.60 , 127.45 , 116.74 , 115.43 , 63.54 , 62.39 , 26.21 , 24.93 , 24.58 , 24.30 , 21.99 , 20.91 .

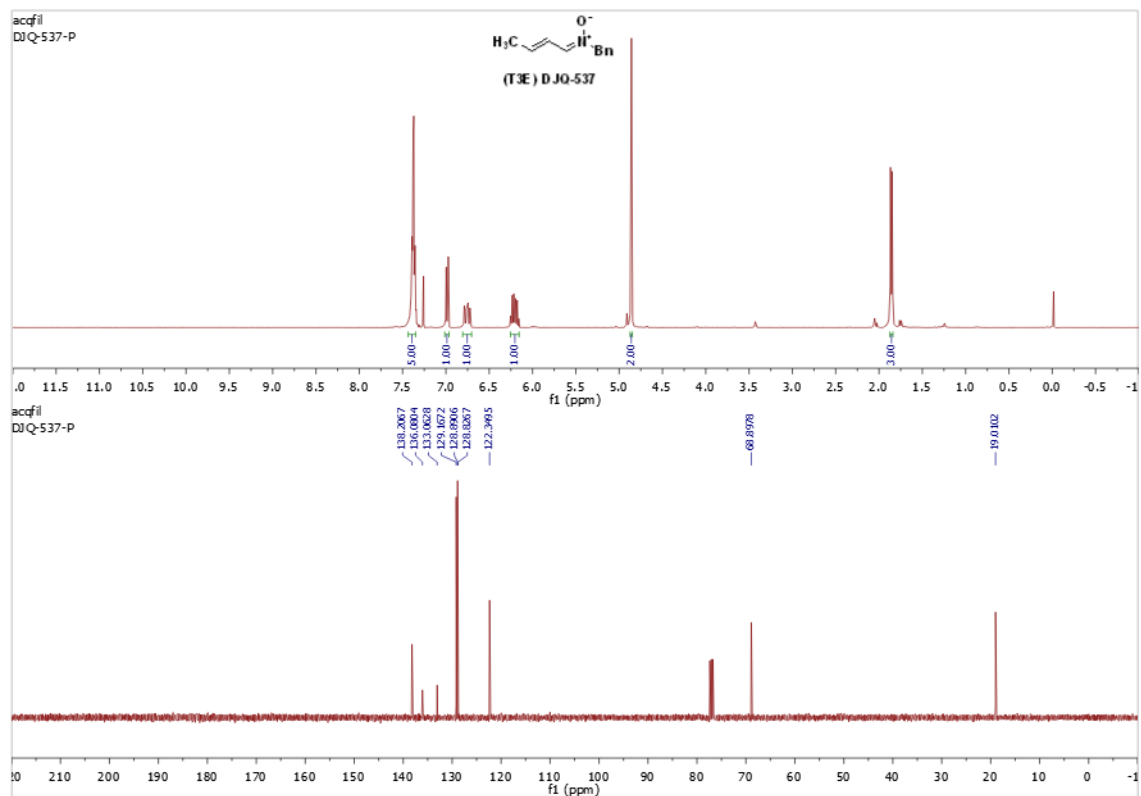
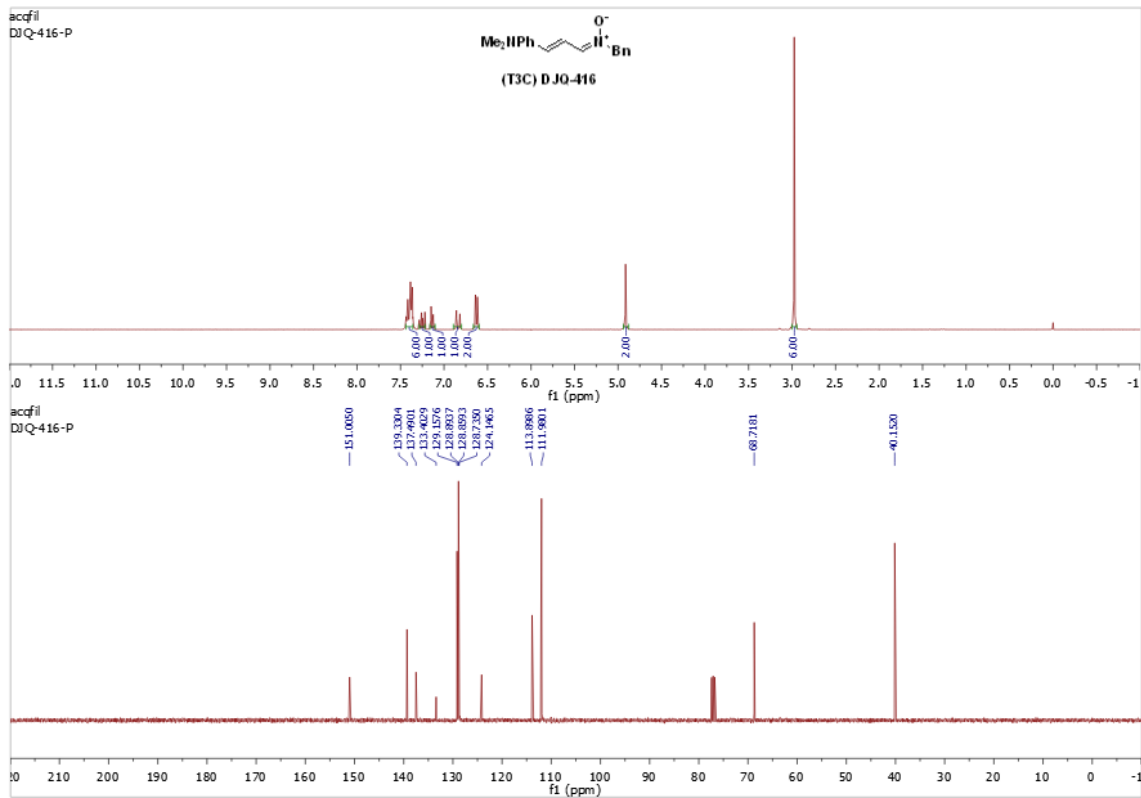
2.6.5. ^1H NMR and ^{13}C NMR of nitrones.

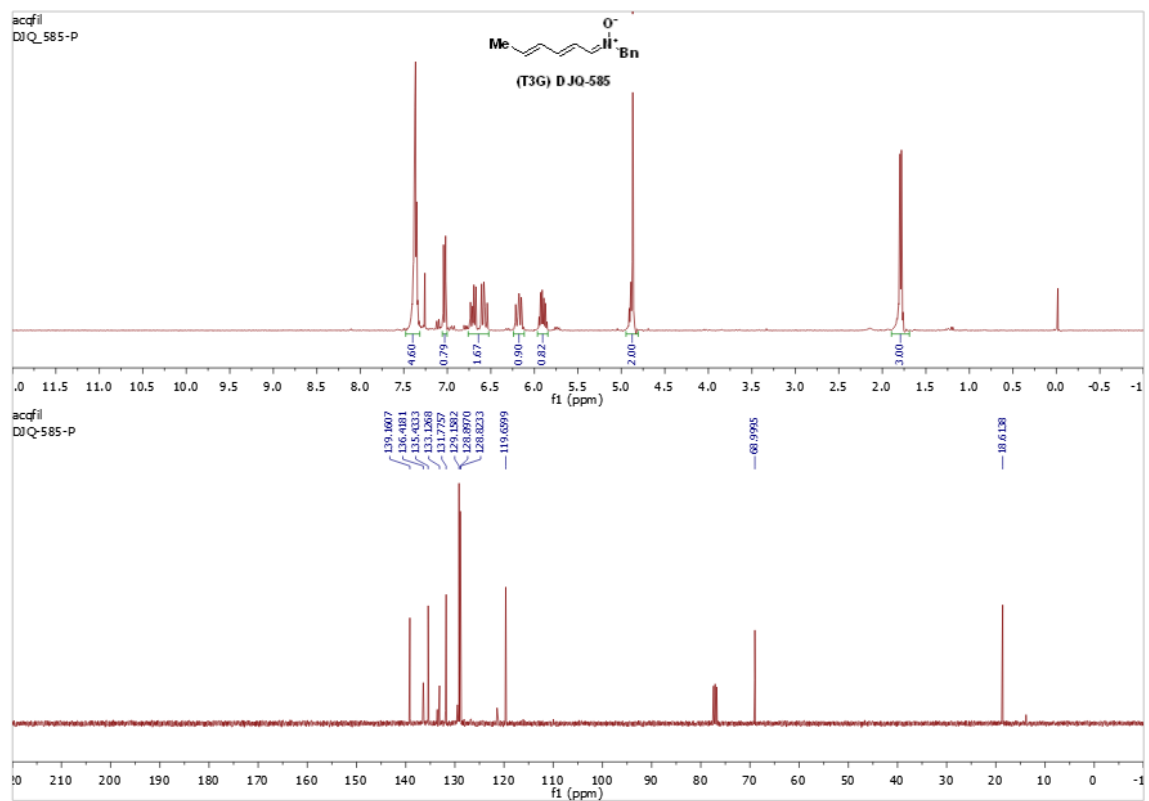
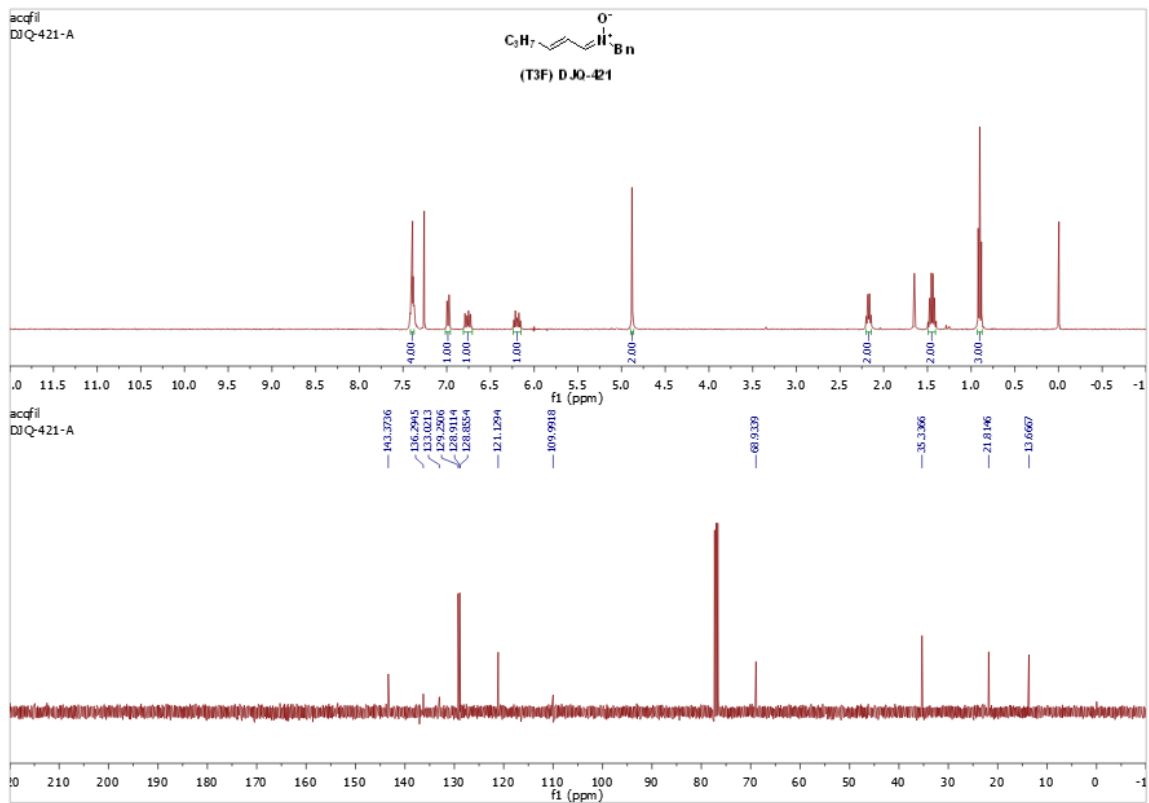


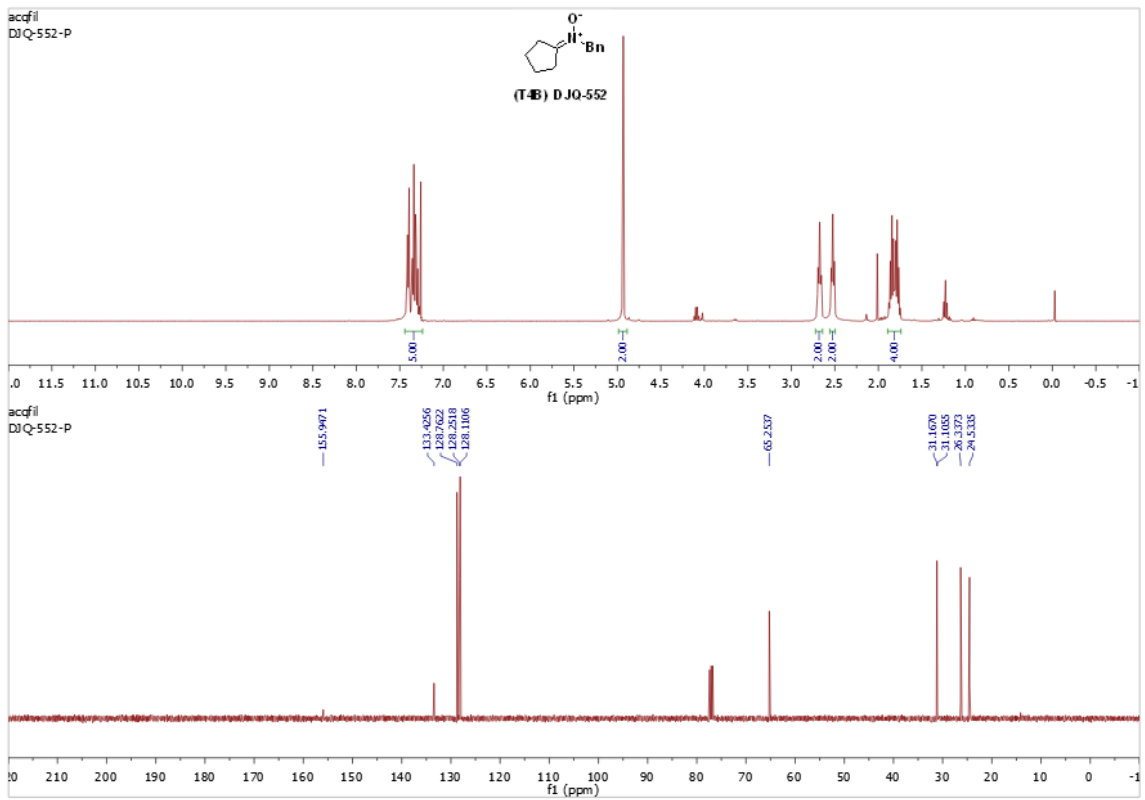
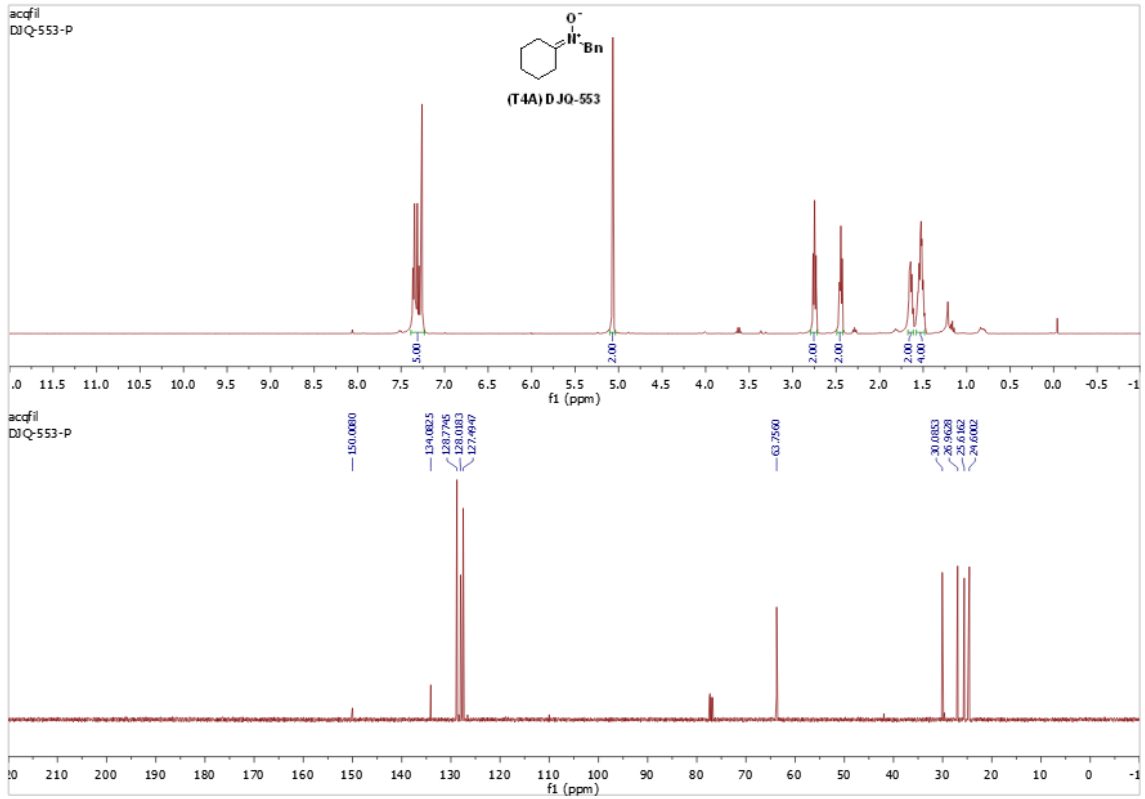


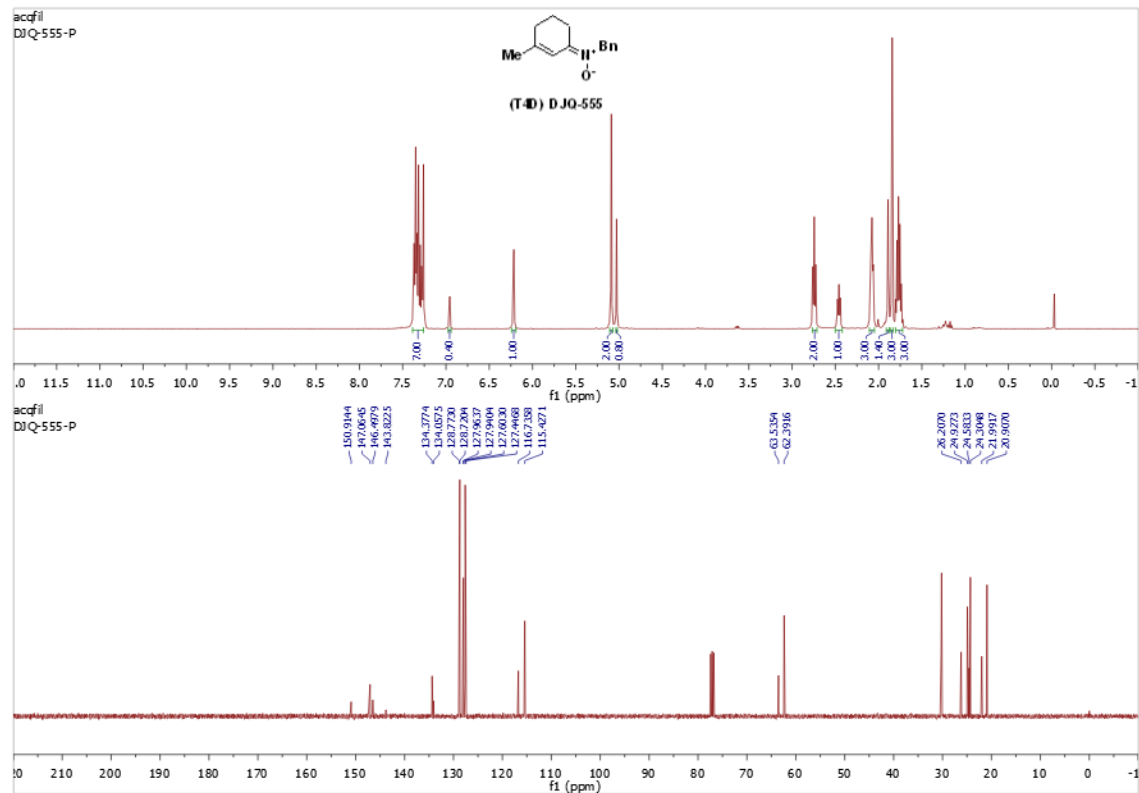
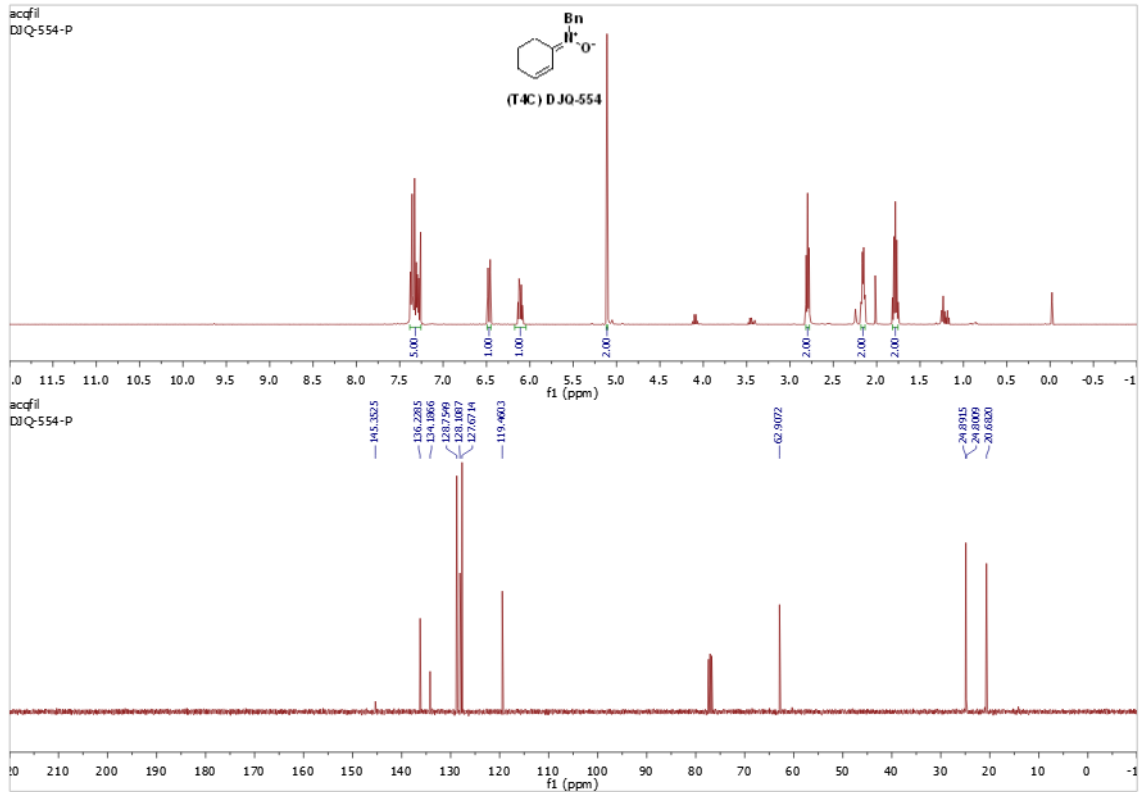












Chapter 3

Nitrone Dipolar Cycloaddition

The dipolar cycloaddition of nitrones with appropriate dipolarphiles is arguably one of the most powerful synthetic transformations for the nitrone moiety (Hashimoto & Maruoka, 2015). In chapter 2, the in-situ formation of carbamoyl nitrones allowed for a successive dipolar cycloaddition to afford the respective N-Carbamoyl Isoxazolidines (Ricci, Gioia, Fini, Mazzanti, & Bernardi, 2009). By recognizing the potential for isoxazolidine cycloadducts to serve as successful therapeutic agents, (Section 3.2) we sought to develop a more general method that would provide novel isoxazolidine scaffolds with key synthetic handles. However, literature reports have highlighted many challenges in the dipolar cycloaddition of nitrones that would first have to be addressed.

3.1 Challenges

First, the electronics of the dipole-dipolarophile pair strongly influence the regioselectivity of the cycloaddition. Asymmetric dipolarphiles with in-proportional electronic guidance allow for a mixture of regioisomeric cycloadducts (Figure 13).

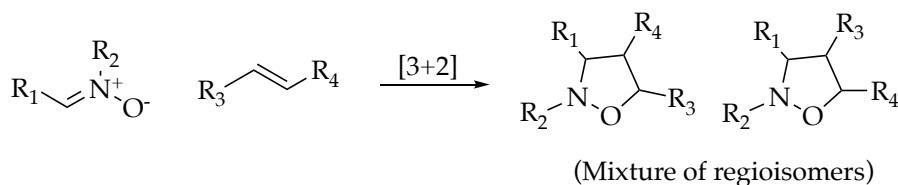


Figure 13. Regiomer-Excess Created by Dipolarphile

This problem of regiomer excess can be controlled by employing an appropriate dipolarophile for the cycloaddition. An electron-deficient dipolarophile, such as an enal, can be paired with a nitron where R is electron rich (Figure 14) to direct regioselectivity of the product.

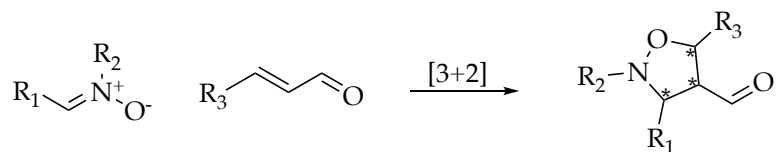


Figure 14. Dipolar Cycloaddition of Nitron and Enal

The use of Lewis acid catalysis for the nitron dipolar cycloaddition has been another challenging endeavor for the synthetic community (Gothelf & Jorgensen, 2000). The negatively charged oxygen of a nitron acts as a strong base and can compete with the dipolarophile for Lewis acid binding. Ultimately, this results in catalyst poisoning and diminished yields.

To address this problem, Jorgenson employed a bi-dentate dipolarophile that outcompetes the nitron for Lewis acid binding (Figure 15). Nitrones lose binding preference in the presence of dipolarphiles capable of making multiple bonds to the metal catalyst (Gothelf & Jorgensen, 2000).

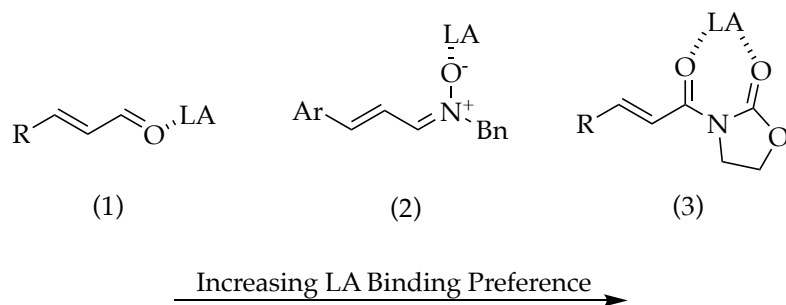


Figure 15. Bidentate Dipolarphile Outcompetes Nitrone for Lewis Acid

The generation of multiple stereocenters (Figure 14) further demonstrates the synthetic utility of this reaction. Stereoselectivity for this dipolar cycloaddition has been an active area of research and has been addressed by some of the leading academic researchers in the field of organic chemistry.

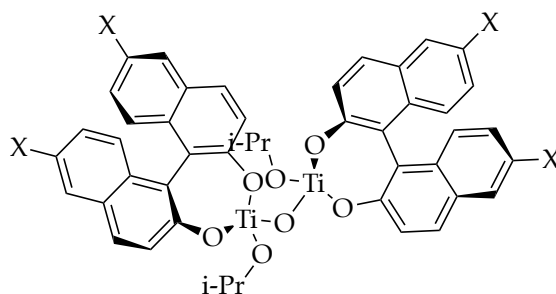


Figure 16. The Design of an Organometallic to Direct Stereoselectivity

The bis-titanium metalorganic compound (Figure 16) designed by Maruoka utilizes both axial chirality and steric repulsions to direct stereoselectivity and preferential binding, respectively. This method prevents nitrones with bulky nitrogen protecting groups from binding to the metal

catalyst. However, as this method relies heavily on steric interactions, the substrate scope can be significantly limited to a unique set of dipolarphiles, such as acrolein. (Kano, Hashimoto, & Maruoka, 2005)

Recognizing these challenges and understanding the techniques chemists have used to overcome them was a key step in developing a successful synthesis of isoxazolidines. Despite these many obstacles, the demand for continued improvement in the nitrono cycloaddition remains due to the pharmaceutical relevance of the isoxazolidine scaffold.

3.2 Access to Antibacterial Agents

The evolution of antibiotic resistant bacterial strains has resulted in the growing demand for efficacious small molecule antibiotics. Beta lactams have historically exhibited powerful antibacterial properties since the advent of penicillin.

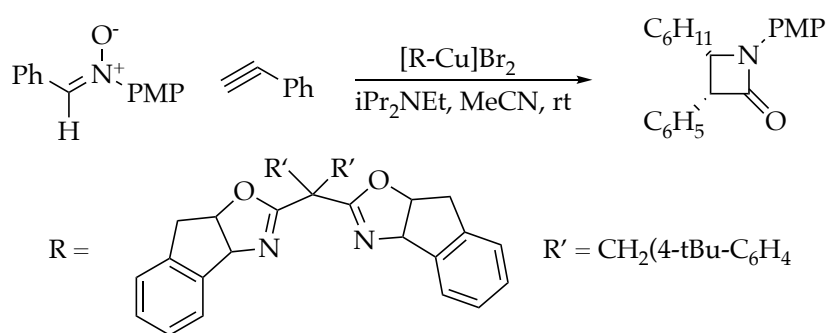


Figure 17. Enantioselective Synthesis of Beta Lactams

An enantioselective synthesis of lactam derivatives utilizing nitrones (Figure 17) has had direct applications to the pharmaceutical industry (Evans, Miller, Lectka, & Matt, 1999). Though lactams have historically served as a cornerstone for bacterial infection treatment, new structural motifs are required to address continued bacterial evolution. One such motif can be accessed directly from the isoxazolidine scaffold.

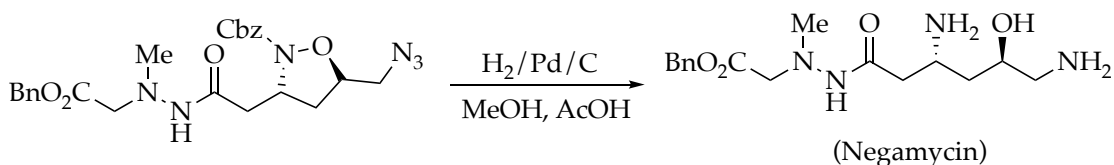


Figure 18. Reductive Cleavage of N-O Bond to Afford Negamycin

The labile nitrogen-oxygen bond of an isoxazolidine may be targeted and easily cleaved under reductive conditions to afford pharmaceutically relevant amino acids (Figure 18). The conformation of the isoxazolidine has been preserved throughout the reaction allowing for a diastereoselective approach to the total synthesis of the natural product, Negamycin (Bates, Khanizeman, Hirao, Tay, & Sae-Lao, 2014). This antibacterial agent boasts several functional groups that can be modified through structure activity relationships to produce novel antibacterial pharmaceuticals.

3.3 Results and Discussion

Acknowledging the pharmaceutical relevance for highly structured isoxazolidines, the GML group sought out to develop a library of 3-Vinyl-4-

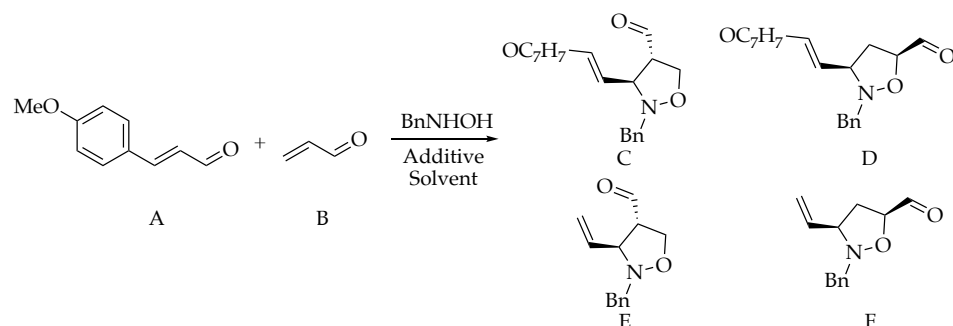
Carbonyl-Isoxazolidines from simple hydroxylamines and conjugated carbonyls. The in-situ formed nitrones had previously been isolated and characterized, serving as a strong reference throughout the development of the method as well as supporting their occurrence as a reaction intermediate.

During initial optimization studies, it was observed that acrolein (Table 9 – B) after condensation with N-Benzylhydroxylamine, underwent a successive dipolar cycloaddition with unreacted acrolein starting material, instead of reacting with the target dipolarophile (Table 9 – A). This led us to hypothesize an optimal enal – dipolarophile pair that would promote a desirable chemoselectivity. The incompatibility of aromatic enals such as cinnamaldehyde to serve as dipolarphiles allowed for a one-pot conversion to the cycloadduct without compromising chemoselectivity.

Next, we addressed the thermal activation of this cycloaddition by screening different temperatures. In doing so we found that increasing the temperature to 80°C afforded the highest percent yield however increasing the temperature past this point began to have a negative effect on the diastereoselectivity of the reaction (Table 9, Entry 7 and 8). Whereas lowering the temperature did not help to improve the diastereoselectivity, however it did drastically diminish conversion to the desired cycloadduct (Table 9, Entry 6).

Table 9

3-Vinyl-4-Carbonyl-Isoxazolidine Reaction Optimization



Entry ^a	Enal	Dipolarophile	Additive ^e	Solvent	Time	Temperature	% Yield of C:D:E:F ^b	d.r. ^c
1	B	B	none	Acetonitrile	48h	rt	0:0:20:2	8:1
2	B ^d	A	none	Acetonitrile	48h	rt	5:1:10:2	8:1
3	B	A	none	Acetonitrile	48h	rt	8:2:6:2	6:1
4	A	B	none	Acetonitrile	48h	rt	40:4:0:0	10:1
5	A	B	none	Acetonitrile	48h	40 °C	53:6:0:0	15:1
6	A	B	none	Acetonitrile	16h	60 °C	64:9:0:0	15:1
7	A	B	none	Acetonitrile	16h	80 °C	88:4:0:0	15:1
8	A	B	none	Acetonitrile	18h	90 °C	80:16:0:0	10:1
9	A	B	none	dioxane	16h	80 °C	80:4:0:0	15:1
10	A	B	none	DCE	16h	80 °C	73:8:0:0	15:1
11	A	B	none	DMF	16h	80 °C	64:12:0:0	15:1
12	A	B	Cu(OTf) ₂	Acetonitrile	6h	rt	64:28:0:0	20:1
13	A	B	Cu(OAc) ₂	Acetonitrile	6h	rt	35:24:0:0	20:1
14	A	B	AgOTf	Acetonitrile	6h	rt	53:22:0:0	20:1
15	A	B	AuOTf	Acetonitrile	6h	rt	48:20:0:0	15:1
16	A	B	Fe(OTf) ₃	Acetonitrile	6h	rt	46:32:0:0	15:1

a. Ratio of enal:dipolarophile:hydroxylamine, 1:2:1. b. Isolated yields. c. Ratio for the major isomer, measured by ¹H-NMR. d. ratio of enal:dipolarophile is 1:1. e. Lewis acid were added in 20 mol%.

To lower the energetic requirement for this reaction, we investigated several Lewis acid metal catalysts. While a noticeable rate enhancement was observed with the addition of 20 molar percent copper triflate, along with a modest increase in diastereoselectivity, the percent yield of the desired cycloadduct was decreased (Table 9 – Entry 12). It was determined that the small

increase in diastereoselectivity obtained with the use of Lewis acid metal catalysts, did not make up for the loss in percent yield and that thermal conditions remained the most practical approach.

With optimal reaction conditions in hand, we next sought to explore the scope for this reaction. Due to the reluctance of cinnamaldehyde to proceed as a dipolarophile we employed para-methoxy cinnamaldehyde as the enal for the cycloaddition. This would prevent the occurrence of previously observed, side cycloadditions. Both simple enals and enones served as suitable dipolarphiles. Straight enal alkyl chains showed traces of regioexcess (Table 10 – Entries A – C). However, enal alkyl chain branching, as observed in methacrolein (Table 10 – Entry D) afforded complete regioselectivity. Both cyclic and acyclic ketones demonstrated similar regioselectivity. This regioselectivity unfortunately came at the cost of a small but noticeable decrease in diastereoselectivity (Table 10 – Entry D-G).

We next sought to expand the scope for this reaction by screening alternative dipolarphiles. Acrylonitrile served as a suitable dipolarophile and afforded complete regioselectivity for the 3-Vinyl-4-Carbonyl Isoxazolidine.

Table 10

Dipolarophile Scope: Aldehydes and Ketones

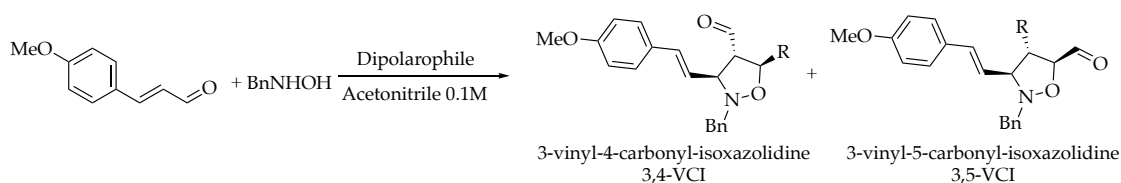
Entry ¹	Dipolarophile	Product	%Yield of 3,4-VCI ²	%Yield of 3,5-VCI ²	d.r. ³
T10A			88	4	15:1
T10B			90	2	16:1
T10C			84	4	15:1
T10D			0	91	12:1
T10E			0	90	12:1
T10F			0	92	12:1
T10G			0	73	12:1

1. Ratio of enal:dipolarophile:hydroxylamine, 1:2:1. 2. Isolated yields. 3. Ratio for the major isomer, measured by ¹H-NMR.

Interestingly, diesters showed preferential for the formation of 3-Vinyl-4-Carbonyl Isoxazolidine (Table 11 – D, E) whereas simple esters showed a reversal in regioselectivity with a preference for 3-Vinyl-5-Carbonyl Isoxazolidine (Table 11 – B, C).

Table 11

Dipolarophile Scope: Nitriles and Esters



Entry ¹	Dipolarophile	Product	% Yield of 3,4-VCI ²	% Yield of 3,5-VCI ²	d.r. ³
T11A			95	0	15:1
T11B			0	91	16:1
T11C			0	84	15:1
T11D			88	0	18:1
T11E			89	0	18:1

1. Ratio of enal:dipolarophile:hydroxylamine, 1:2:1. 2. Isolated yields. 3. Measured by ¹H-NMR.

Table 12

Dipole Scope

Entry ¹	Enal	Product	% of 3,4-VBI ²	% of 3,7-VBI ²	d.r. ³
T12A			0	73	15:1
T12B			0	79	16:1
T12C			0	69	15:1
T12D			0	84	12:1
T12E			0	86	12:1
T12F			0	79	12:1
T12G			0	84	16:1
T12H			0	80	14:1

1. Ratio of enal:dipolarophile:hydroxylamine, 1:2:1. 2. Isolated yields. 3. Measured by ¹H-NMR.

3.4 Conclusion

This method for the synthesis of 3,4 and 3,5 Vinyl Isoxazolidines demonstrated the ability for N-Substituted hydroxylamine to rapidly build molecular complexity. Using simple enones and enals with seemingly similar structure, a regioselective and stereochemically rich heterocycle was achieved. Selective condensation onto the enal rather than the dipolarophile was a challenge encountered early in this project that we tackled by employing suitable starting reagents. Further research efforts could consider the hydroxylamine source as another variable in which to broaden the scope for this reaction.

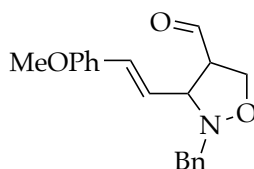
3.5 Experimental

Reagents were obtained from Aldrich Chemical, Acros Organics or Alfa Aesar and used without further purification. Solvents were obtained from EMD Milipore DrySol and degassed with nitrogen. Reactions were performed in 4-mL glass vials with magnetic stirring. TLC was performed on 0.25 mm E. Merck silica gel 60 F254 plates and visualized under UV light (254 nm) or by staining with potassium permanganate (KMnO_4). Silica flash chromatography was performed on E. Merck 230–400 mesh silica gel 60. Automated chromatography was performed on a ISOLERA Prime instrument with 10 g. SNAP silica gel normal phase cartridges using a flow rate of 12.0 mL/min and a gradient of 0–20% EtOAc in Heptanes over 12 column volumes with UV detection at 254 nm. NMR spectra were recorded on Varian Mercury II 400 MHz Spectrometer at 24 °C in CDCl_3 , unless otherwise indicated. Chemical shifts are expressed in ppm

relative to solvent signals: CDCl_3 (^1H , 7.23 ppm; ^{13}C , 77.0 ppm; coupling constants are expressed in Hz).

3.5.1. General method for the synthesis of vinyl isoxazolidines. In a 4-mL glass vial, 1 mMol enal and 1.1 eq. hydroxylamine were dissolved in 1 mL acetonitrile. The mixture was stirred at room temperature for five minutes after which 3 molar equivalents dipolarophile was added. The reaction was stirred vigorously at 80°C for 16 hours. The organic was extracted with 150 mL diethyl ether. The organic layer was washed with 3-25 mL aliquots of (10%) aqueous sodium bicarbonate. The organic layer was dried with 3-25 mL aliquots of saturated aqueous brine solution (NaCl). The organic layer is finally isolated and dried over anhydrous sodium sulfate, filtered, and concentrated by rotary evaporation to afford the crude product. The crude product is filtered through silica gel over a gradient of 4:1 Heptanes/EtOAc over 12 column volumes to obtain the respective isoxazolidine in good to excellent yields.

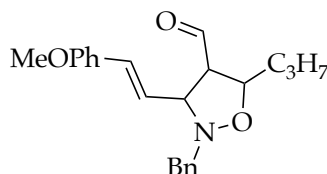
3.5.2. Synthesis of vinyl isoxazolidines from Table 10 and 11.



(T7A) EM-141

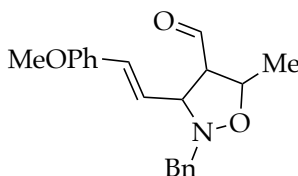
(E)-2-benzyl-3-(4-methoxystyryl)isoxazolidine-4-carbaldehyde (T7A): Purification by automated silica gel flash chromatography (10 g cartridge, 14 ml/min. 20:1 heptanes/EtOAc to 1:4 heptanes/EtOAc over 12 min) yielded the isoxazolidine **7a** (115 mg, 90%) as a yellow oil. **TLC:** R_f 0.20 (3:1 heptanes/EtOAc). **$^1\text{H NMR}$** (400 MHz, CDCl_3) δ 9.76 (dd, J = 2.4, 0.6 Hz, 1H), 7.38 – 7.32 (m, 6H), 7.29 (d, J = 10.0 Hz, 1H), 6.89 – 6.86 (m, 2H), 6.61 (d, J = 15.8 Hz, 1H), 6.09 (dd, J = 15.8, 8.5 Hz, 1H), 4.24 (dd, J = 8.9, 4.0 Hz, 1H), 4.16 – 4.09 (m, 2H), 3.82 (d, J = 0.6 Hz,

3H), 3.78 (d, $J = 14.1$ Hz, 1H), 3.63 (d, $J = 7.4$ Hz, 1H), 3.35 – 3.29 (m, 1H). **¹³C NMR** (101 MHz, CDCl₃) δ 198.86, 134.58, 128.81, 128.29, 127.85, 127.71, 127.33, 114.06, 65.49, 61.65, 55.30, 30.89.



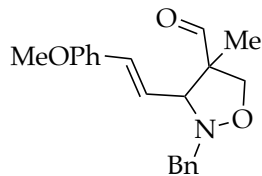
(T7B) DJQ-407

(E)-2-benzyl-3-(4-methoxystyryl)-5-propylisoxazolidine-4-carbaldehyde (T7B): Purification by automated silica gel flash chromatography (10 g cartridge, 14 ml/min. 20:1 heptanes/EtOAc to 1:4 heptanes/EtOAc over 12 min) yielded the isoxazolidine **7b** (100 mg, 70%) as a yellow oil. **TLC:** R_f 0.38 (3:1 heptanes/EtOAc). **¹H NMR** (400 MHz, CDCl₃) δ 9.75 (dd, $J = 2.7, 0.7$ Hz, 1H), 7.52 – 7.24 (m, 7H), 6.96 – 6.84 (m, 2H), 6.54 (d, $J = 15.8$ Hz, 1H), 6.06 (dd, $J = 15.7, 8.5$ Hz, 1H), 4.51 – 4.17 (m, 1H), 4.13 (d, $J = 14.3$ Hz, 1H), 3.81 (d, $J = 0.7$ Hz, 3H), 3.77 – 3.61 (m, 1H), 3.01 (ddd, $J = 7.8, 5.4, 2.7$ Hz, 1H), 1.87 (dddd, $J = 13.4, 9.7, 7.8, 5.6$ Hz, 1H), 1.60 (ddt, $J = 13.5, 9.6, 5.9$ Hz, 1H), 1.47 – 1.30 (m, 2H), 0.93 (td, $J = 7.4, 3.1$ Hz, 3H). **¹³C NMR** (101 MHz, CDCl₃) δ 198.89, 133.85, 128.55, 128.16, 127.81, 127.08, 123.69, 114.03, 76.92, 67.75, 55.30, 37.26, 19.16, 13.87.



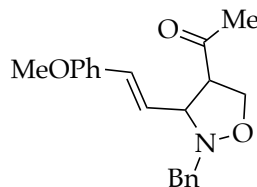
(T7C) DJQ-486

(E)-2-benzyl-3-(4-methoxystyryl)-5-methylisoxazolidine-4-carbaldehyde (T7C): Purification by automated silica gel flash chromatography (10 g cartridge, 14 ml/min. 20:1 heptanes/EtOAc to 1:4 heptanes/EtOAc over 12 min) yielded the isoxazolidine **7c** (85 mg, 70%) as a pale oil. **TLC:** R_f 0.31 (3:1 heptanes/EtOAc). **¹H NMR** (400 MHz, CDCl₃) δ 9.76 (t, $J = 2.0$ Hz, 1H), 7.39 – 7.25 (m, 9H), 6.88 – 6.85 (m, 2H), 6.53 (d, $J = 15.9$ Hz, 1H), 6.13 – 6.05 (m, 1H), 4.52 – 4.47 (m, 1H), 4.13 (d, $J = 14.2$ Hz, 1H), 3.85 (d, $J = 14.3$ Hz, 1H), 3.81 (d, $J = 1.5$ Hz, 3H), 3.75 (d, $J = 6.7$ Hz, 1H), 2.97 (s, 1H), 1.43 (dd, $J = 6.2, 1.5$ Hz, 3H). **¹³C NMR** (101 MHz, CDCl₃) δ 198.76, 133.80, 128.56, 128.23, 127.81, 127.15, 123.75, 114.04, 73.10, 68.94, 59.37, 55.30, 20.72.



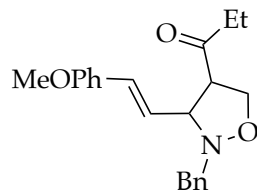
(T7D) DJQ-415

(E)-2-benzyl-3-(4-methoxystyryl)-4-methylisoxazolidine-4-carbaldehyde (T7D): Purification by automated silica gel flash chromatography (10 g cartridge, 14 ml/min. 20:1 heptanes/EtOAc to 1:4 heptanes/EtOAc over 12 min) yielded the isoxazolidine **7d** (165 mg, 90%) as a yellow oil. **TLC:** R_f 0.35 (3:1 heptanes/EtOAc). **¹H NMR** (400 MHz, CDCl₃) δ 9.59 (s, 1H), 7.39 (d, *J* = 7.1 Hz, 2H), 7.35 – 7.29 (m, 4H), 7.25 (tt, *J* = 6.0, 1.6 Hz, 1H), 6.93 – 6.78 (m, 2H), 6.53 (d, *J* = 15.8 Hz, 1H), 5.89 (ddd, *J* = 15.8, 8.8, 0.6 Hz, 1H), 4.19 (d, *J* = 14.8 Hz, 1H), 3.81 (d, *J* = 0.6 Hz, 3H), 3.76 (d, *J* = 14.8 Hz, 1H), 3.43 (q, *J* = 8.3 Hz, 1H), 2.52 (dd, *J* = 12.7, 7.8 Hz, 1H), 2.25 (dd, *J* = 12.7, 8.4 Hz, 1H), 1.30 (s, 3H). **¹³C NMR** (101 MHz, CDCl₃) δ 205.12, 133.59, 128.35, 128.18, 127.72, 127.08, 124.71, 114.02, 69.67, 59.15, 55.30, 44.00, 19.07.



(T7E) DJQ-410

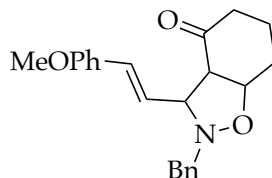
(E)-1-(2-benzyl-3-(4-methoxystyryl)isoxazolidin-4-yl)ethan-1-one (T7E): Purification by automated silica gel flash chromatography (10 g cartridge, 14 ml/min. 20:1 heptanes/EtOAc to 1:4 heptanes/EtOAc over 12 min) yielded the isoxazolidine **7e** (180 mg, 80%) as a yellow oil. **TLC:** R_f 0.45 (3:1 heptanes/EtOAc). **¹H NMR** (400 MHz, CDCl₃) δ 7.39 (d, *J* = 7.1 Hz, 2H), 7.34 (ddd, *J* = 4.3, 2.5, 1.3 Hz, 4H), 7.29 – 7.23 (m, 1H), 6.92 – 6.82 (m, 2H), 6.56 (d, *J* = 15.8 Hz, 1H), 5.92 (dd, *J* = 15.8, 8.6 Hz, 1H), 4.29 (dd, *J* = 9.5, 4.7 Hz, 1H), 4.18 (d, *J* = 14.1 Hz, 1H), 3.81 (d, *J* = 0.8 Hz, 3H), 3.70 (d, *J* = 14.1 Hz, 1H), 3.35 (q, *J* = 8.3 Hz, 1H), 2.72 (ddd, *J* = 12.8, 9.4, 7.8 Hz, 1H), 2.39 (ddd, *J* = 13.0, 8.5, 4.7 Hz, 1H), 2.11 (d, *J* = 0.8 Hz, 3H). **¹³C NMR** (101 MHz, CDCl₃) δ 133.80, 128.91, 128.14, 127.71, 127.21, 124.54, 114.04, 80.49, 69.42, 59.76, 55.30, 39.01, 25.38.



(T7F) DJQ-464

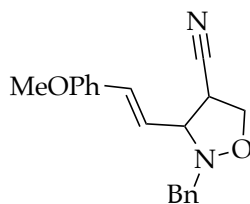
(E)-1-(2-benzyl-3-(4-methoxystyryl)isoxazolidin-4-yl)propan-1-one (T7F): Purification by automated silica gel flash chromatography (10 g cartridge, 14 ml/min. 20:1 heptanes/EtOAc to 1:4 heptanes/EtOAc over 12 min) yielded the

isoxazolidine **7f** (105 mg, 70%) as a pale oil. **TLC**: Rf 0.50 (3:1 heptanes/EtOAc). **¹H NMR** (400 MHz, CDCl₃) δ 7.41 – 7.22 (m, 8H), 6.89 – 6.83 (m, 2H), 6.54 (d, *J* = 15.8 Hz, 1H), 5.91 (dd, *J* = 15.9, 8.5 Hz, 1H), 4.33 (dd, *J* = 9.4, 4.9 Hz, 1H), 4.16 (d, *J* = 14.1 Hz, 1H), 3.81 (d, *J* = 0.7 Hz, 3H), 3.70 (d, *J* = 14.1 Hz, 1H), 3.35 (q, *J* = 8.3 Hz, 1H), 2.76 – 2.68 (m, 1H), 2.65 – 2.56 (m, 1H), 2.47 (ddd, *J* = 11.5, 7.2, 4.4 Hz, 1H), 2.42 – 2.36 (m, 1H), 0.95 (td, *J* = 7.3, 0.6 Hz, 3H). **¹³C NMR** (101 MHz, CDCl₃) δ 159.51, 137.57, 133.73, 128.89, 128.10, 127.69, 127.19, 124.59, 114.01, 69.45, 59.76, 55.30, 39.09, 30.54, 7.13.



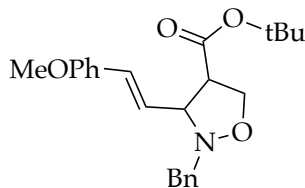
(T7G) DJQ-397

(E)-2-benzyl-3-(4-methoxystyryl)hexahydrobenzo[d]isoxazol-4(2H)-one (T7G): Purification by automated silica gel flash chromatography (10 g cartridge, 14 ml/min. 20:1 heptanes/EtOAc to 1:4 heptanes/EtOAc over 12 min) yielded the isoxazolidine **7g** (110 mg, 65%) as a yellow oil. **TLC**: Rf 0.15 (3:1 heptanes/EtOAc). **¹H NMR** (400 MHz, CDCl₃) δ 7.41 – 7.35 (m, 2H), 7.35 – 7.27 (m, 4H), 7.25 – 7.21 (m, 1H), 6.88 – 6.82 (m, 2H), 6.59 (d, *J* = 15.8 Hz, 1H), 6.10 – 6.01 (m, 1H), 4.57 (dt, *J* = 7.7, 4.3 Hz, 1H), 4.10 (d, *J* = 14.1 Hz, 1H), 3.88 – 3.79 (m, 5H), 3.00 (t, *J* = 6.7 Hz, 1H), 2.51 (dt, *J* = 17.0, 5.1 Hz, 1H), 2.34 (ddd, *J* = 16.6, 10.2, 6.1 Hz, 1H), 2.07 – 1.97 (m, 1H), 1.96 – 1.88 (m, 2H), 1.87 – 1.79 (m, 1H). **¹³C NMR** (101 MHz, CDCl₃) δ 137.48, 133.11, 128.95, 128.20, 127.74, 127.19, 125.05, 113.94, 70.51, 60.81, 55.28, 39.92, 26.47, 19.05.



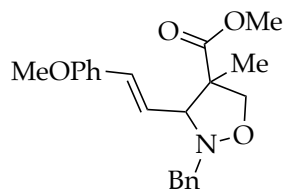
(T7H) DJQ-462

(E)-2-benzyl-3-(4-methoxystyryl)isoxazolidine-4-carbonitrile (T7H): Purification by automated silica gel flash chromatography (10 g cartridge, 14 ml/min. 20:1 heptanes/EtOAc to 1:4 heptanes/EtOAc over 12 min) yielded the isoxazolidine **7h** (80 mg, 90%) as a pale oil. **TLC**: Rf 0.20 (3:1 heptanes/EtOAc). **¹H NMR** (400 MHz, CDCl₃) δ 7.42 – 7.38 (m, 2H), 7.36 – 7.24 (m, 5H), 6.95 – 6.83 (m, 2H), 6.68 (d, *J* = 15.8 Hz, 1H), 6.20 (dd, *J* = 15.8, 8.9 Hz, 1H), 4.30 (t, *J* = 8.6 Hz, 1H), 4.18 (d, *J* = 14.3 Hz, 1H), 4.08 (dd, *J* = 8.4, 6.7 Hz, 1H), 3.82 (d, *J* = 0.5 Hz, 3H), 3.71 (d, *J* = 14.3 Hz, 1H), 3.61 (td, *J* = 8.5, 6.7 Hz, 1H), 3.51 (t, *J* = 8.2 Hz, 1H). **¹³C NMR** (101 MHz, CDCl₃) δ 136.95, 136.61, 128.74, 128.44, 128.30, 128.22, 127.46, 119.86, 114.09, 69.99, 68.68, 55.33, 38.48.



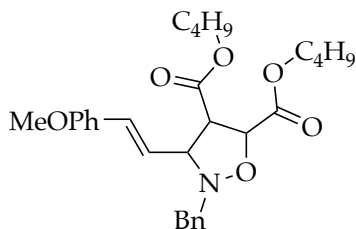
(T7I) DJQ-463

Tert-butyl(E)-2-benzyl-3-(4-methoxystyryl)isoxazolidine-4-carboxylate (T7I): Purification by automated silica gel flash chromatography (10 g cartridge, 14 ml/min. 20:1 heptanes/EtOAc to 1:4 heptanes/EtOAc over 12 min) yielded the isoxazolidine **7i** (90 mg, 90%) as a pale oil. **TLC:** Rf 0.56 (3:1 heptanes/EtOAc). **¹H NMR** (400 MHz, CDCl₃) δ 7.44 – 7.40 (m, 2H), 7.31 (dd, *J* = 8.3, 6.0 Hz, 4H), 7.26 – 7.22 (m, 1H), 6.89 – 6.84 (m, 2H), 6.56 (d, *J* = 15.9 Hz, 1H), 5.99 (dd, *J* = 15.8, 8.2 Hz, 1H), 4.50 (dd, *J* = 8.2, 5.2 Hz, 1H), 4.14 – 4.01 (m, 2H), 3.81 (d, *J* = 0.8 Hz, 3H), 3.67 – 3.59 (m, 1H), 2.57 (t, *J* = 8.4 Hz, 2H), 1.51 (s, 9H). **¹³C NMR** (101 MHz, CDCl₃) δ 137.79, 133.31, 128.98, 128.24, 127.67, 127.12, 124.40, 114.02, 75.64, 68.04, 55.29, 40.66, 28.04.



(T7J) LNT-29

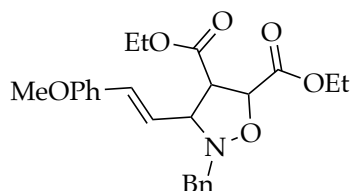
Methyl (E)-2-benzyl-3-(4-methoxystyryl)-4-methylisoxazolidine-4-carboxylate (T7J): Purification by automated silica gel flash chromatography (10 g cartridge, 14 ml/min. 20:1 heptanes/EtOAc to 1:4 heptanes/EtOAc over 12 min) yielded the isoxazolidine **7j** (105 mg, 90%) as a yellow oil. **TLC:** Rf 0.50 (3:1 heptanes/EtOAc). **¹H NMR** (400 MHz, CDCl₃) δ 7.47 – 7.37 (m, 2H), 7.41 – 7.17 (m, 6H), 6.91 – 6.80 (m, 2H), 6.51 (d, *J* = 15.9 Hz, 1H), 5.95 (ddd, *J* = 15.8, 8.7, 1.3 Hz, 1H), 4.24 – 4.05 (m, 1H), 3.89 – 3.71 (m, 8H), 3.44 (q, *J* = 8.4 Hz, 1H), 2.83 (ddd, *J* = 12.8, 8.6, 1.3 Hz, 1H), 2.31 (ddd, *J* = 12.9, 8.0, 1.4 Hz, 1H), 1.57 (s, 1H), 1.50 (d, *J* = 1.3 Hz, 3H). **¹³C NMR** (101 MHz, Chloroform-d) δ 159.46, 137.53, 133.50, 128.19, 128.01, 127.69, 126.77, 124.72, 113.99, 81.10, 69.44, 58.71, 55.29, 52.32, 46.07, 23.71.



(T7K) DJQ-488

dibutyl(E)-2-benzyl-3-(4-methoxystyryl)isoxazolidine-4,5-dicarboxylate (T7K): Purification by automated silica gel flash chromatography (10 g cartridge, 14 ml/min. 20:1 heptanes/EtOAc to 1:4 heptanes/EtOAc over 12 min) yielded the

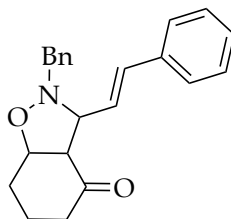
isoxazolidine **7k** (120 mg, 90%) as a white solid. **TLC**: Rf 0.62 (3:1 heptanes/EtOAc). **¹H NMR** (400 MHz, CDCl₃) δ 7.43 – 7.37 (m, 2H), 7.34 – 7.28 (m, 4H), 7.26 – 7.21 (m, 1H), 6.91 – 6.83 (m, 2H), 6.63 (d, *J* = 15.8 Hz, 1H), 5.97 (dd, *J* = 15.8, 8.5 Hz, 1H), 4.21 – 4.14 (m, 2H), 4.12 – 4.02 (m, 4H), 3.91 (t, *J* = 9.0 Hz, 1H), 3.81 (d, *J* = 0.6 Hz, 3H), 3.67 – 3.60 (m, 1H), 1.67 – 1.54 (m, 4H), 1.44 – 1.30 (m, 4H), 0.91 (ddd, *J* = 29.9, 7.6, 7.1 Hz, 6H). **¹³C NMR** (101 MHz, CDCl₃) δ 137.34, 135.24, 128.99, 128.25, 127.87, 127.27, 122.01, 114.01, 72.19, 65.23, 60.25, 56.97, 55.31, 30.45, 19.07, 13.68.



(T7L) DJQ-489

diethyl(E)-2-benzyl-3-(4-methoxystyryl)isoxazolidine-4,5-dicarboxylate (T7L): Purification by automated silica gel flash chromatography (10 g cartridge, 14 ml/min. 20:1 heptanes/EtOAc to 1:4 heptanes/EtOAc over 12 min) yielded the isoxazolidine **7l** (118 mg, 90%) as a white solid. **TLC**: Rf 0.35 (3:1 heptanes/EtOAc). **¹H NMR** (400 MHz, CDCl₃) δ 7.46 – 7.43 (m, 2H), 7.33 (dq, *J* = 8.7, 2.3, 1.5 Hz, 4H), 7.29 (d, *J* = 1.5 Hz, 1H), 6.88 – 6.85 (m, 2H), 6.62 (d, *J* = 15.8 Hz, 1H), 6.02 (dd, *J* = 15.9, 8.6 Hz, 1H), 4.87 (d, *J* = 4.3 Hz, 1H), 4.24 (tdd, *J* = 15.0, 7.5, 3.7 Hz, 5H), 3.86 (d, *J* = 15.2 Hz, 1H), 3.81 (s, 3H), 3.74 (dd, *J* = 8.2, 4.3 Hz, 1H), 3.65 – 3.58 (m, 1H), 1.31 (d, *J* = 7.1 Hz, 3H), 1.25 (d, *J* = 7.1 Hz, 3H). **¹³C NMR** (101 MHz, Chloroform-d) δ 135.12, 128.10, 128.08, 127.87, 126.96, 122.64, 114.02, 73.48, 61.59, 61.50, 58.74, 57.28, 55.30, 14.19, 14.12.

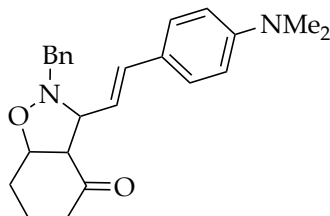
3.5.3. Synthesis of vinyl isoxazolidines from Table 12.



(T8A) DJQ-395

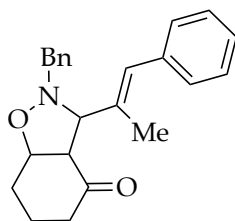
(E)-2-benzyl-3-styrylhexahydrobenzo[d]isoxazol-4(2H)-one (T8A): Purification by automated silica gel flash chromatography (10 g cartridge, 14 ml/min. 20:1 heptanes/EtOAc to 1:4 heptanes/EtOAc over 12 min) yielded the isoxazolidine **8a** (165 mg, 92%) as a white solid. **TLC**: Rf 0.25 (3:1 heptanes/EtOAc). **¹H NMR** (400 MHz, CDCl₃) δ 7.39 (dd, *J* = 8.2, 6.5 Hz, 4H), 7.32 (t, *J* = 7.4 Hz, 4H), 7.28 – 7.23 (m, 2H), 6.67 (d, *J* = 15.9 Hz, 1H), 6.22 (dd, *J* = 15.9, 7.9 Hz, 1H), 4.59 (dt, *J* = 7.8, 4.3 Hz,

1H), 4.10 (d, $J = 14.0$ Hz, 1H), 3.93 (dd, $J = 7.9, 5.9$ Hz, 1H), 3.87 (d, $J = 14.0$ Hz, 1H), 3.01 (t, $J = 6.6$ Hz, 1H), 2.52 (dt, $J = 16.8, 5.0$ Hz, 1H), 2.36 (ddd, $J = 16.5, 10.2, 6.2$ Hz, 1H), 2.09 – 1.99 (m, 1H), 1.93 (dq, $J = 9.8, 4.4$ Hz, 2H), 1.84 (ddd, $J = 14.0, 7.1, 3.7$ Hz, 1H). **¹³C NMR** (101 MHz, CDCl₃) δ 133.49, 128.99, 128.55, 128.23, 127.82, 127.49, 127.25, 126.54, 76.77, 70.16, 60.75, 60.50, 40.02, 26.42, 19.17.



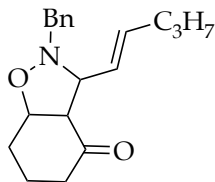
(T8B) DJQ-494

(E)-2-benzyl-3-(4-(dimethylamino)styryl)hexahydrobenzo[d]isoxazol-4(2H)-one (T8B): Purification by automated silica gel flash chromatography (10 g cartridge, 14 ml/min. 20:1 heptanes/EtOAc to 1:4 heptanes/EtOAc over 12 min) yielded the isoxazolidine **8b** (178 mg, 70%) as a red oil. TLC: R_f 0.19 (3:1 heptanes/EtOAc). **¹H NMR** (400 MHz, CDCl₃) δ 7.40 – 7.28 (m, 6H), 7.25 – 7.22 (m, 1H), 6.67 (dd, $J = 8.9, 2.6$ Hz, 2H), 6.56 (d, $J = 15.8$ Hz, 1H), 5.98 (ddd, $J = 15.7, 8.1, 1.0$ Hz, 1H), 4.57 (dt, $J = 7.6, 4.2$ Hz, 1H), 4.12 (d, $J = 14.1$ Hz, 1H), 3.80 (d, $J = 10.6$ Hz, 1H), 3.01 (t, $J = 6.9$ Hz, 1H), 2.96 (d, $J = 1.0$ Hz, 6H), 2.54 – 2.30 (m, 3H), 2.09 – 1.92 (m, 2H), 1.91 – 1.82 (m, 2H). **¹³C NMR** (101 MHz, CDCl₃) δ 128.98, 128.17, 127.56, 127.13, 122.53, 112.32, 70.95, 60.91, 60.13, 40.49, 39.81, 26.54, 18.96.



(T8C) DJQ-492

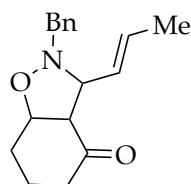
(E)-2-benzyl-3-(1-phenylprop-1-en-2-yl)hexahydrobenzo[d]isoxazol-4(2H)-one (T8C): Purification by automated silica gel flash chromatography (10 g cartridge, 14 ml/min. 20:1 heptanes/EtOAc to 1:4 heptanes/EtOAc over 12 min) yielded the isoxazolidine **8c** (105 mg, 72%) as a pale oil. TLC: R_f 0.33 (3:1 heptanes/EtOAc). **¹H NMR** (400 MHz, CDCl₃) δ 7.42 – 7.20 (m, 10H), 6.94 – 6.53 (m, 1H), 4.57 – 4.47 (m, 1H), 4.25 – 4.02 (m, 1H), 3.93 – 3.63 (m, 2H), 3.48 – 2.92 (m, 1H), 2.53 – 2.02 (m, 3H), 1.89 (s, 3H), 1.89 – 1.78 (m, 2H). **¹³C NMR** (101 MHz, CDCl₃) δ 209.40, 135.35, 132.30, 129.06, 128.99, 128.87, 128.16, 128.01, 127.17, 126.47, 75.19, 60.82, 59.16, 40.29, 26.29, 19.45, 14.86.



(T8D) DJQ-456

(E)-2-benzyl-3-(pent-1-en-1-yl)hexahydrobenzo[d]isoxazol-4(2H)-one (T8D):

Purification by automated silica gel flash chromatography (10 g cartridge, 14 ml/min. 20:1 heptanes/EtOAc to 1:4 heptanes/EtOAc over 12 min) yielded the isoxazolidine **8d** (110 mg, 80%) as a yellow oil. TLC: R_f 0.42 (3:1 heptanes/EtOAc). ¹H NMR (400 MHz, CDCl₃) δ 7.36 (dd, *J* = 5.9, 1.9 Hz, 3H), 7.31 (d, *J* = 7.1 Hz, 2H), 5.70 (dt, *J* = 15.3, 6.8 Hz, 1H), 5.46 – 5.39 (m, 1H), 4.50 (dt, *J* = 8.0, 4.2 Hz, 1H), 4.05 (d, *J* = 14.1 Hz, 1H), 3.75 (d, *J* = 14.1 Hz, 1H), 3.58 (t, *J* = 7.6 Hz, 1H), 2.92 (t, *J* = 7.2 Hz, 1H), 2.50 – 2.45 (m, 1H), 2.31 (ddd, *J* = 16.7, 10.1, 6.2 Hz, 2H), 2.01 (d, *J* = 7.3 Hz, 2H), 1.90 – 1.81 (m, 3H), 1.38 (d, *J* = 7.3 Hz, 2H), 0.87 (d, *J* = 7.3 Hz, 3H). ¹³C NMR (101 MHz, CDCl₃) δ 135.84, 128.92, 128.16, 127.12, 70.71, 60.66, 39.64, 34.39, 26.56, 22.13, 18.77, 13.59.

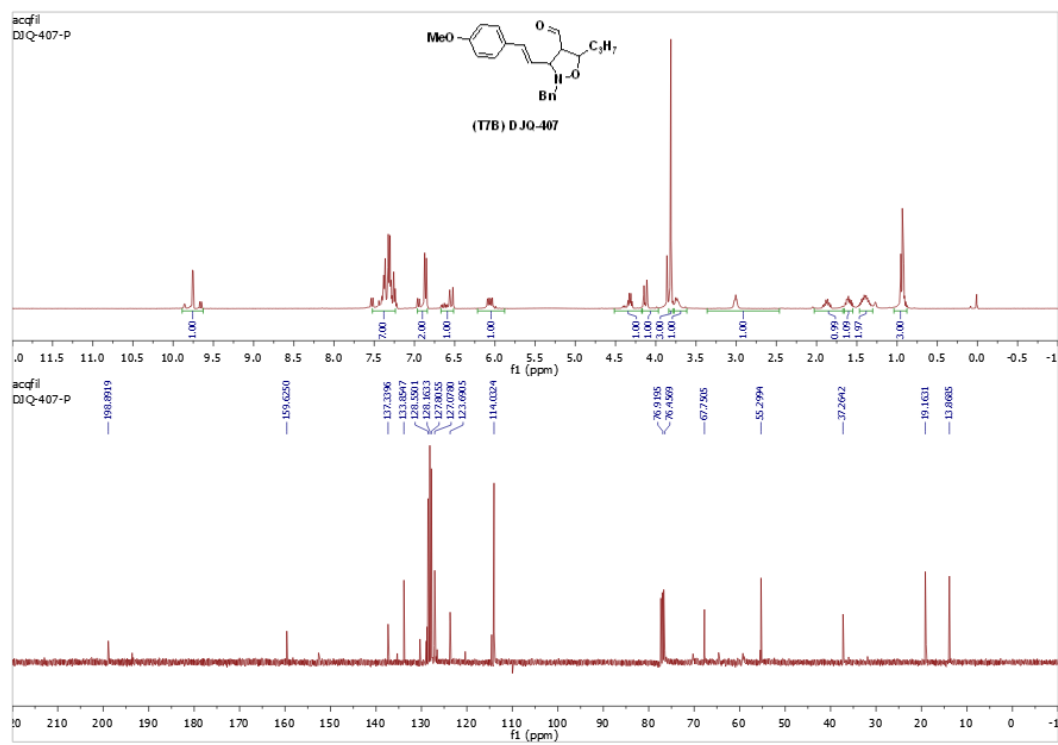
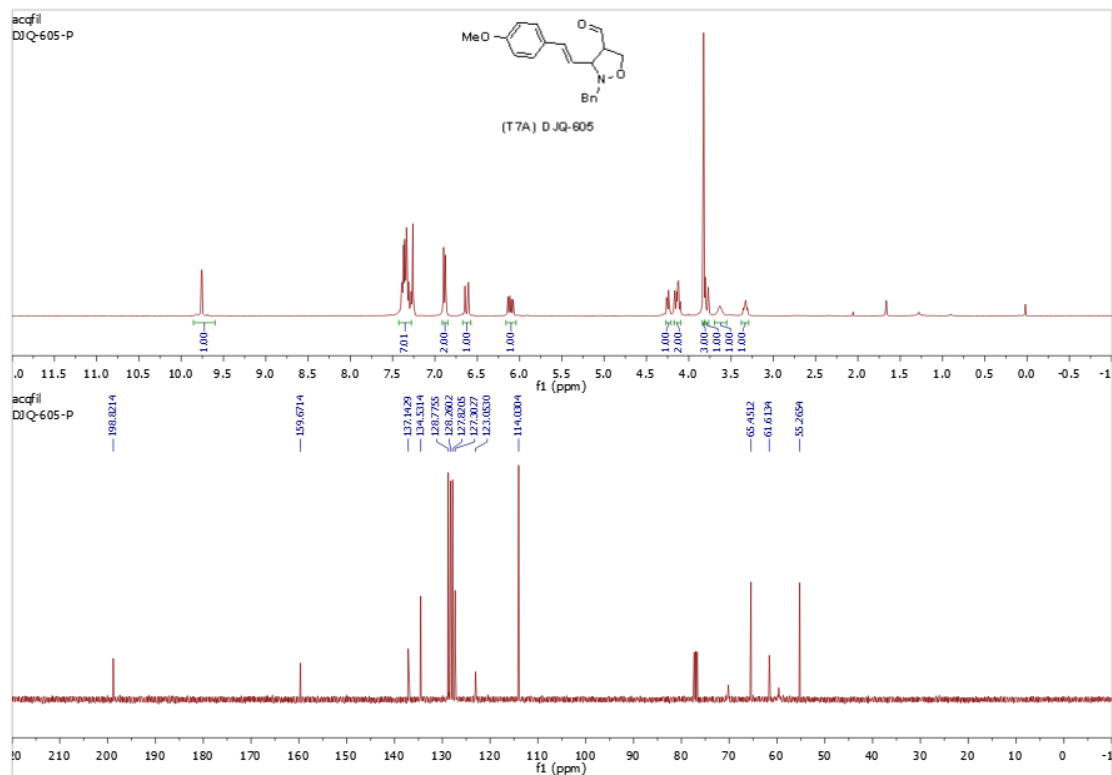


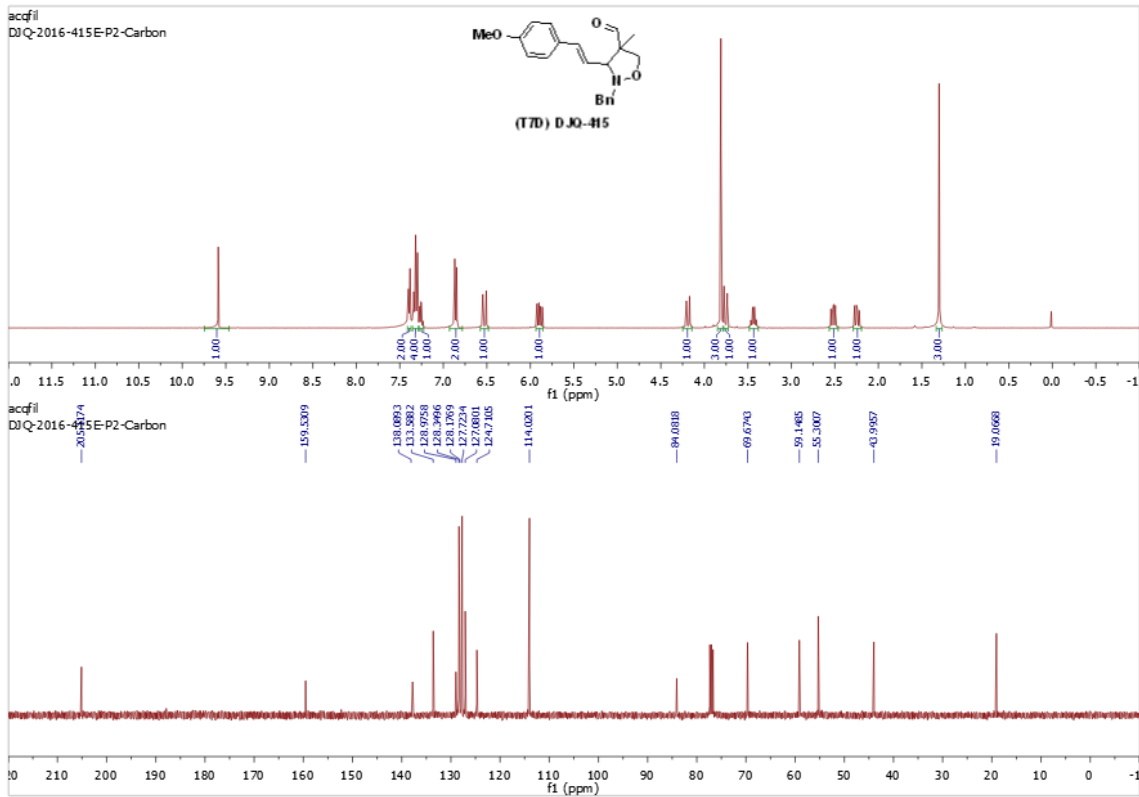
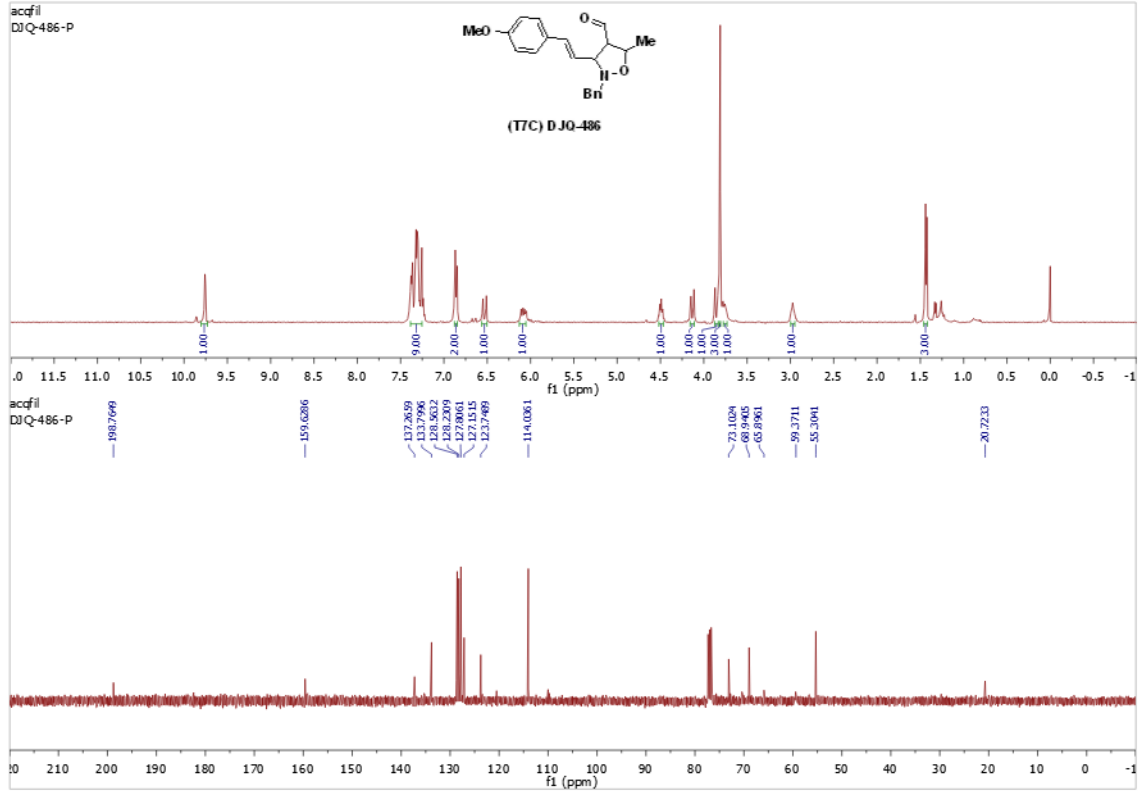
(T8E) DJQ-497

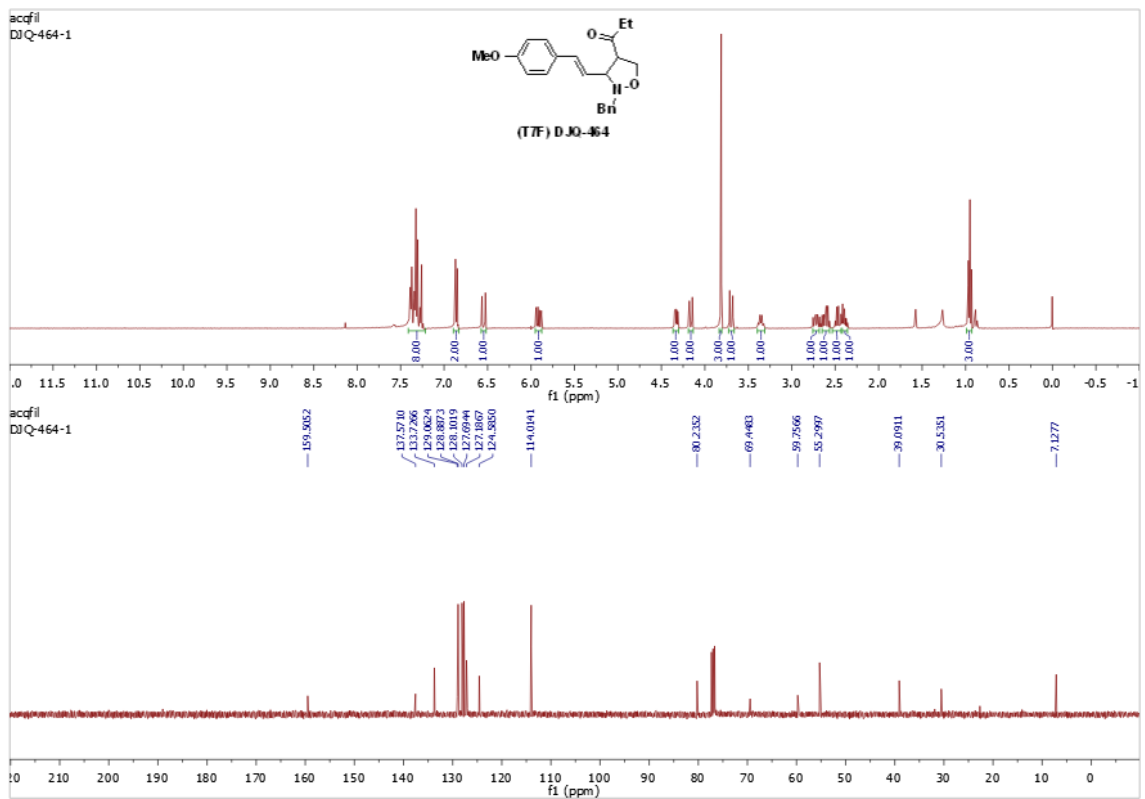
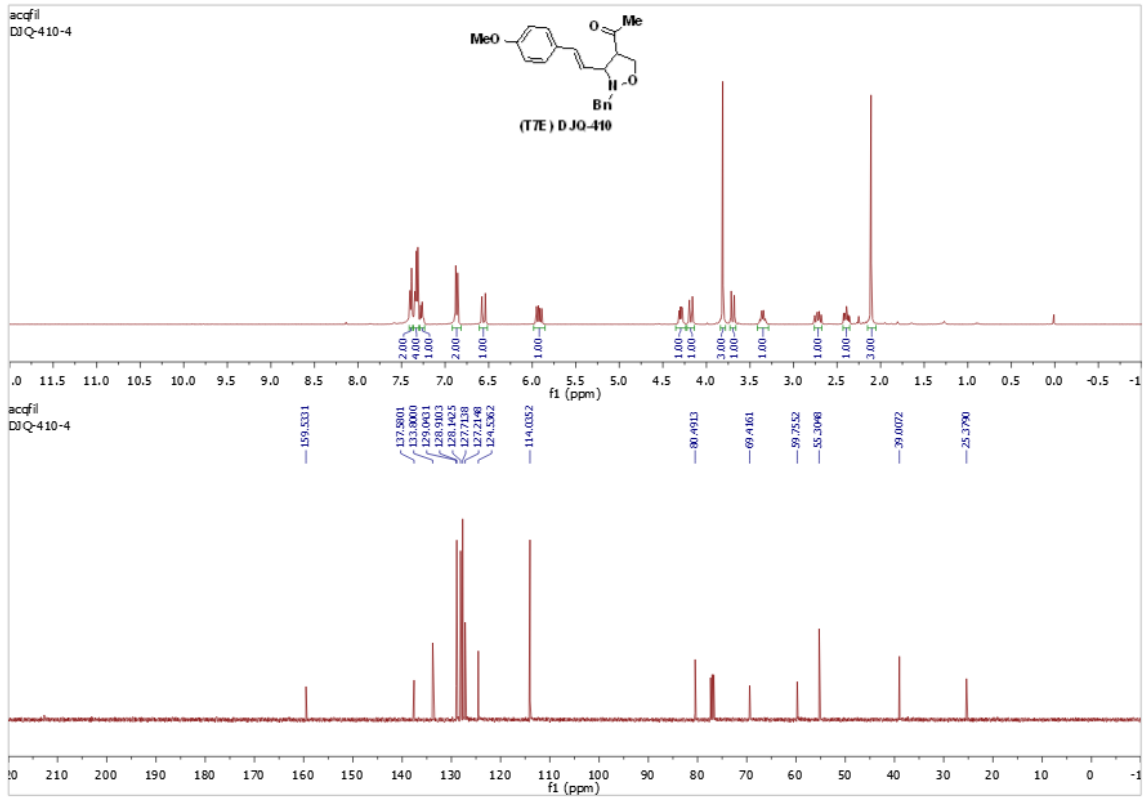
(E)-2-benzyl-3-(prop-1-en-1-yl)hexahydrobenzo[d]isoxazol-4(2H)-one (T8E):

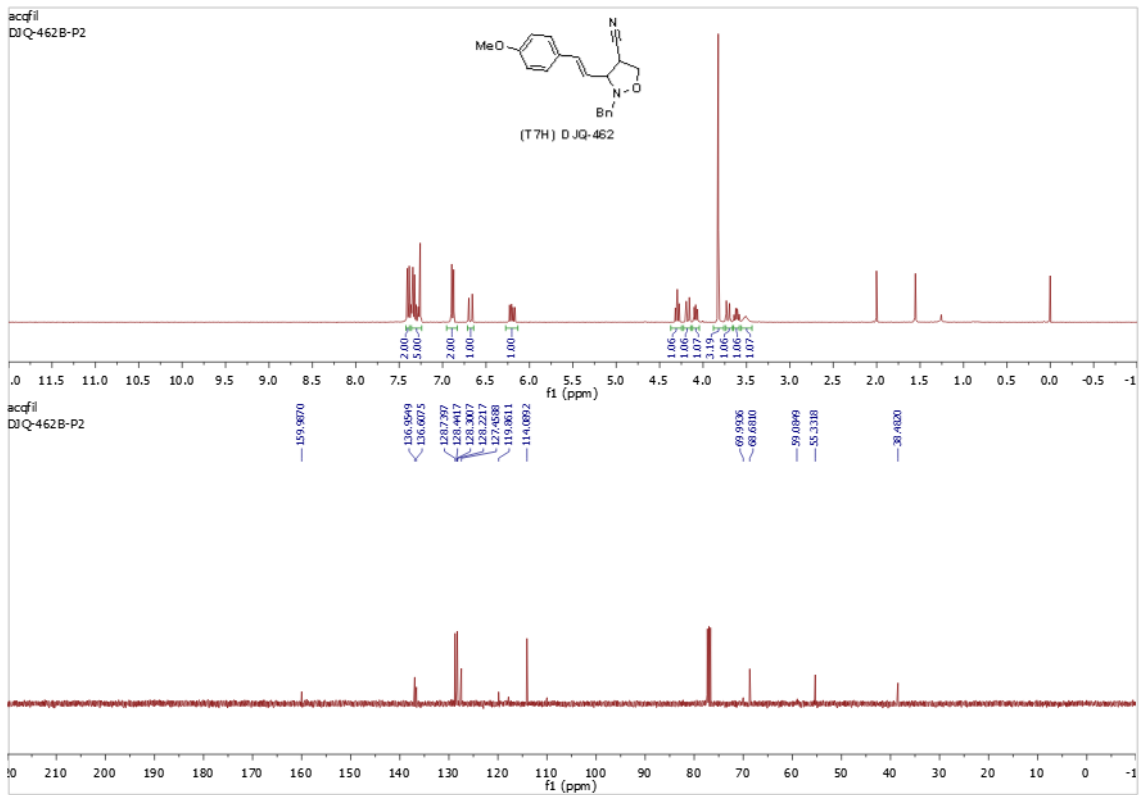
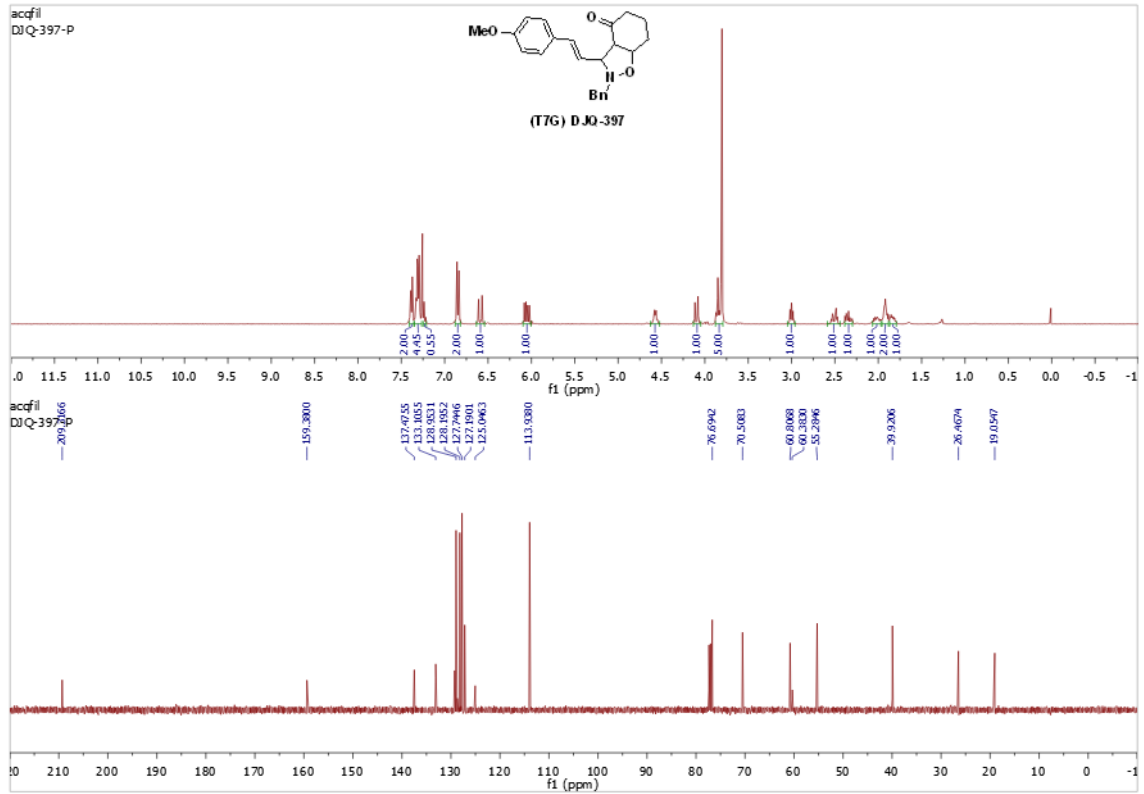
Purification by automated silica gel flash chromatography (10 g cartridge, 14 ml/min. 20:1 heptanes/EtOAc to 1:4 heptanes/EtOAc over 12 min) yielded the isoxazolidine **8e** (209 mg, 70%) as a yellow oil. TLC: R_f 0.38 (3:1 heptanes/EtOAc). ¹H NMR (400 MHz, CDCl₃) δ 7.38 – 7.24 (m, 5H), 5.80 – 5.66 (m, 1H), 5.46 (ddq, *J* = 15.2, 8.2, 1.5 Hz, 1H), 4.51 (ddt, *J* = 11.9, 8.1, 4.4 Hz, 1H), 4.08 – 4.00 (m, 1H), 3.77 (dd, *J* = 19.9, 14.0 Hz, 1H), 3.63 – 3.41 (m, 1H), 2.90 (q, *J* = 8.8, 8.0 Hz, 1H), 2.47 (dt, *J* = 16.4, 5.0 Hz, 1H), 2.35 – 2.26 (m, 1H), 2.00 (dddd, *J* = 15.7, 7.7, 3.6, 1.8 Hz, 1H), 1.89 – 1.75 (m, 3H), 1.70 (ddd, *J* = 6.3, 4.3, 1.6 Hz, 3H). ¹³C NMR (101 MHz, CDCl₃) δ 130.57, 128.91, 128.86, 128.15, 127.10, 76.35, 70.76, 60.52, 59.90, 39.63, 26.54, 18.73, 17.95.

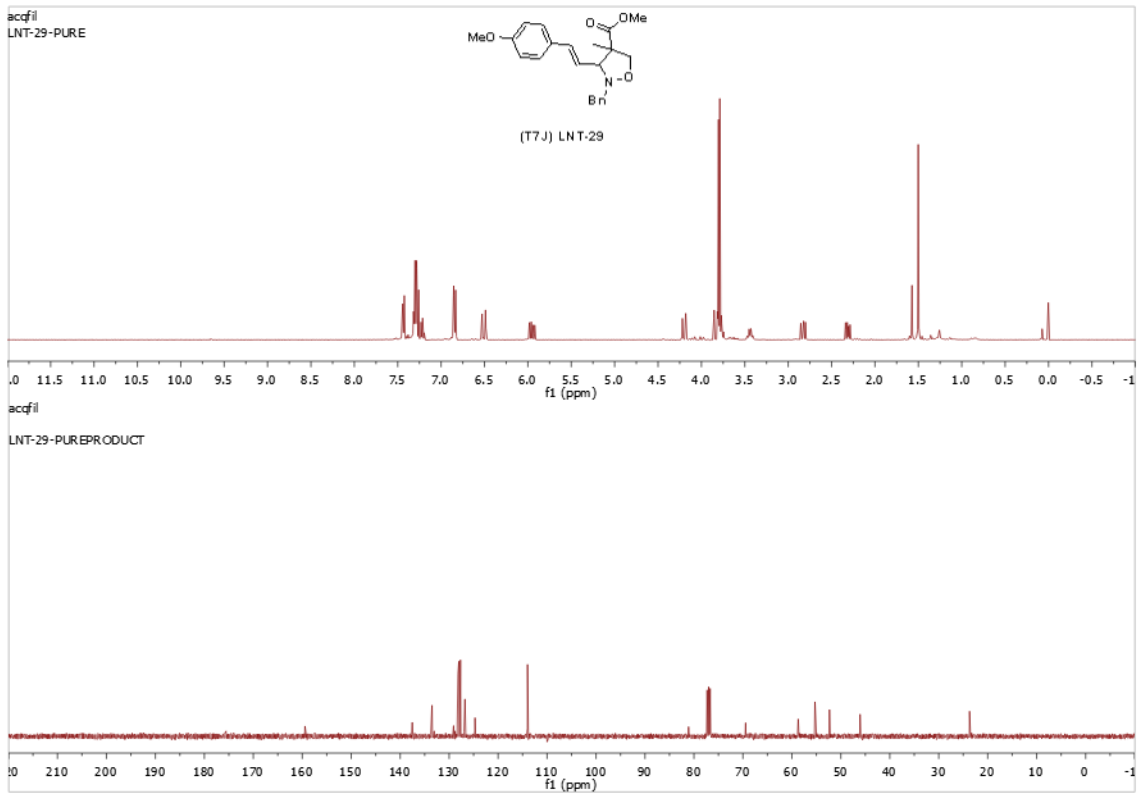
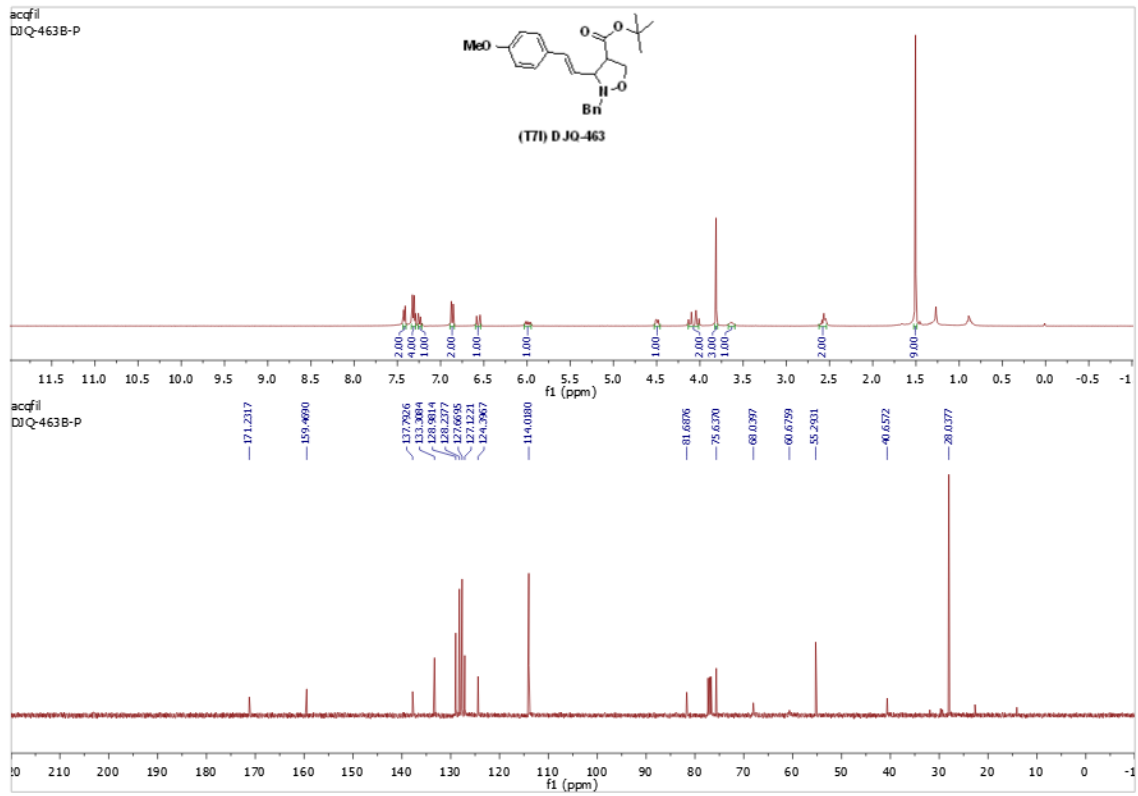
3.5.4. ^1H NMR and ^{13}C NMR of vinyl isoxazolidines

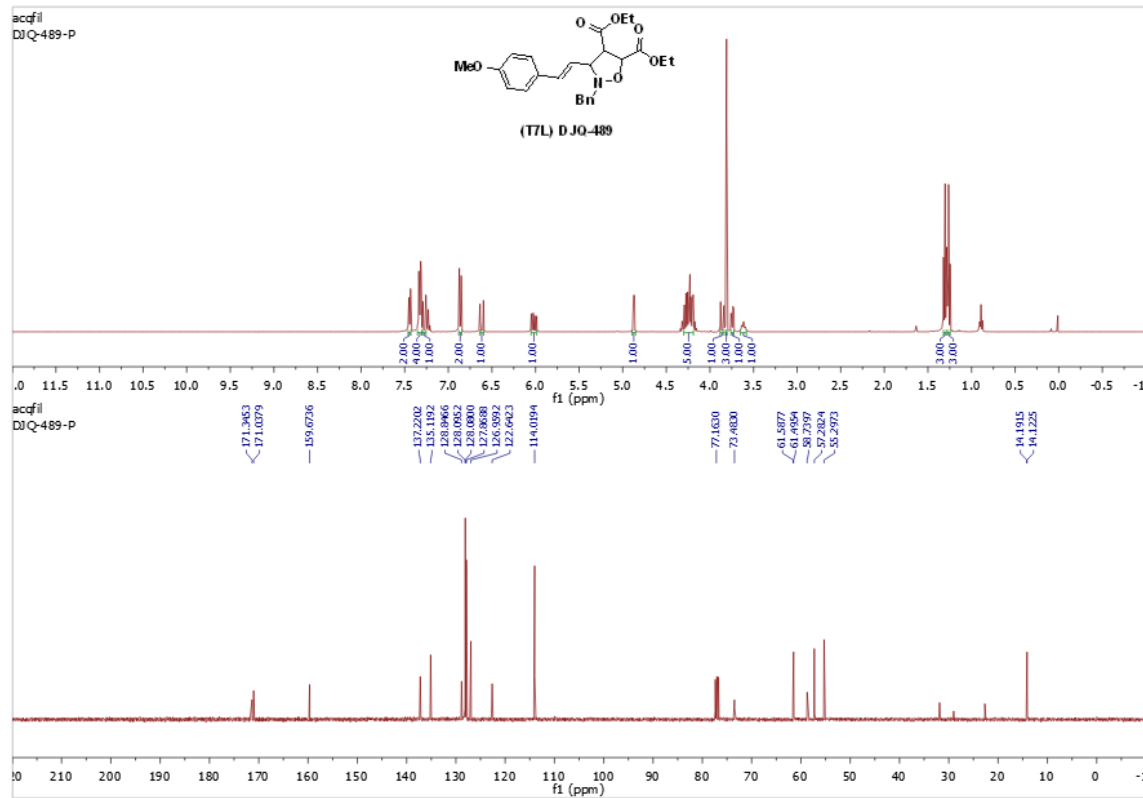
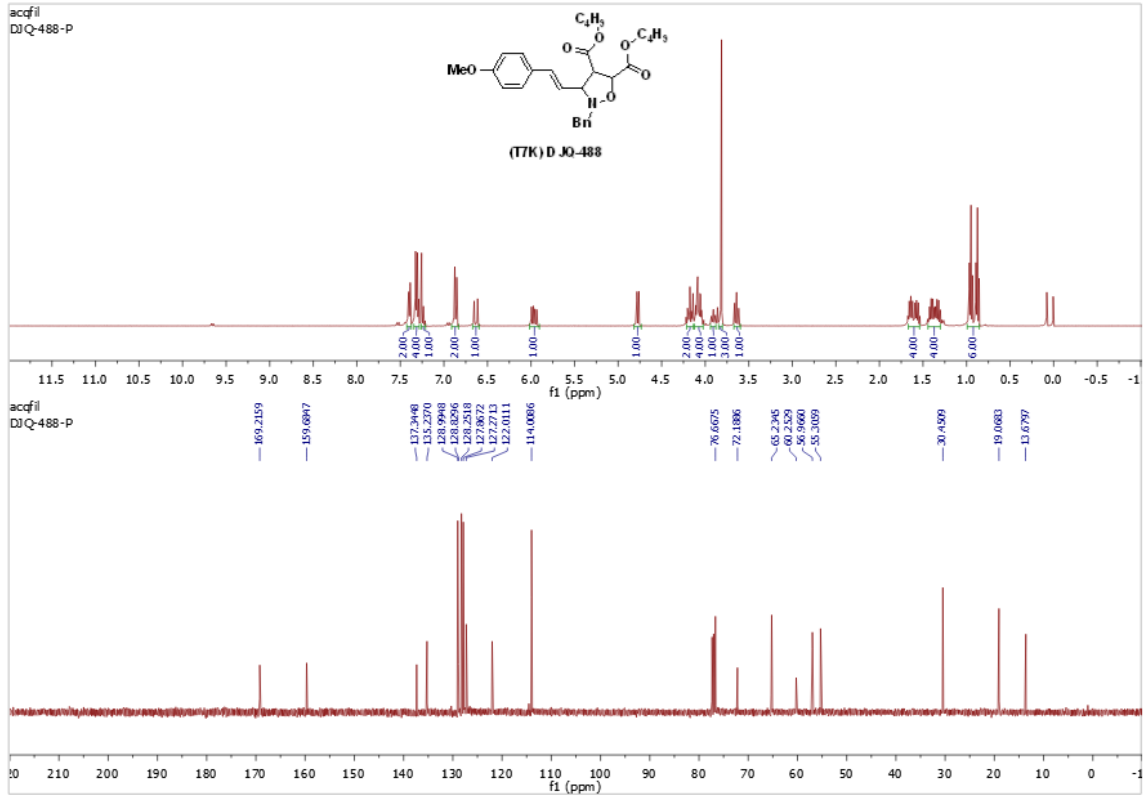


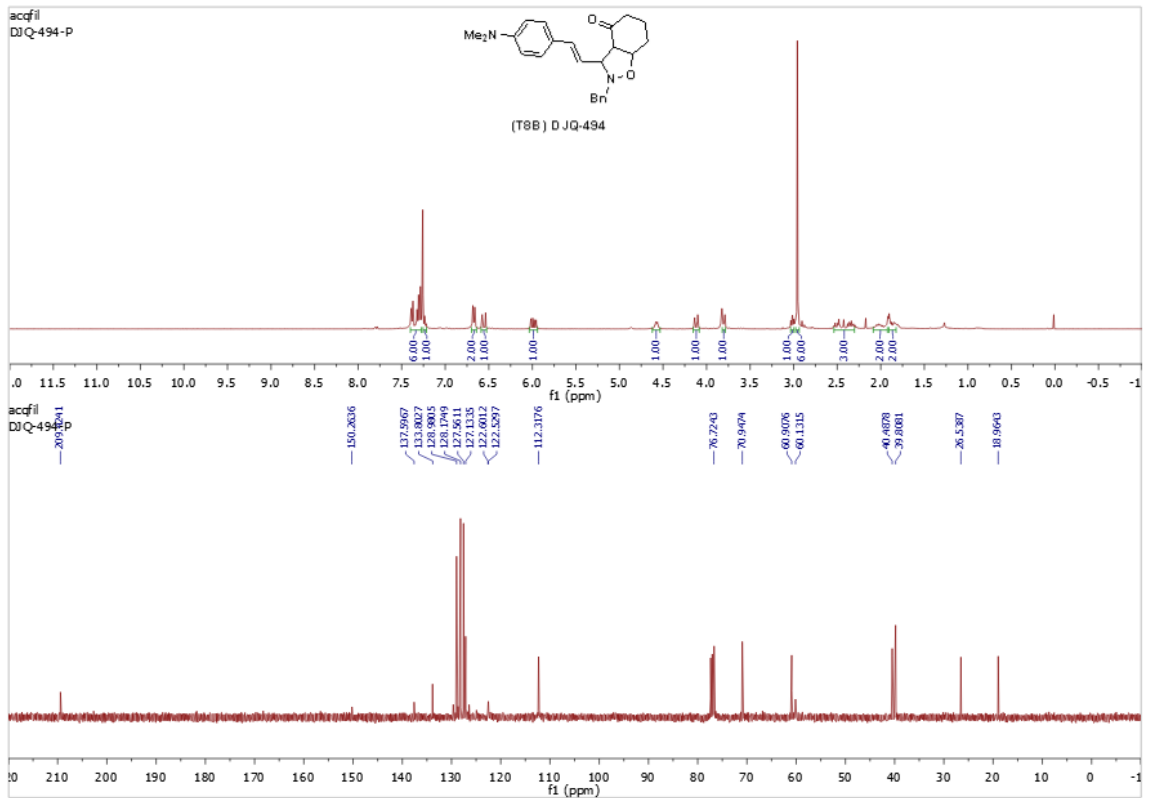
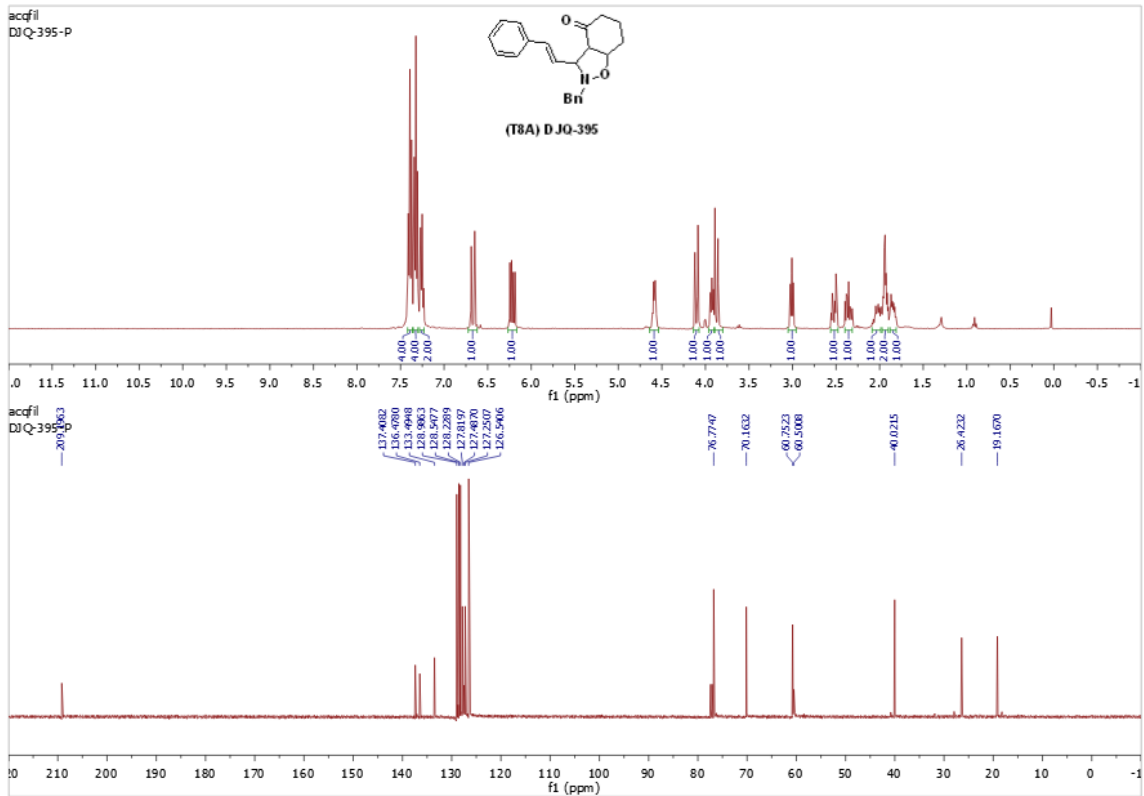


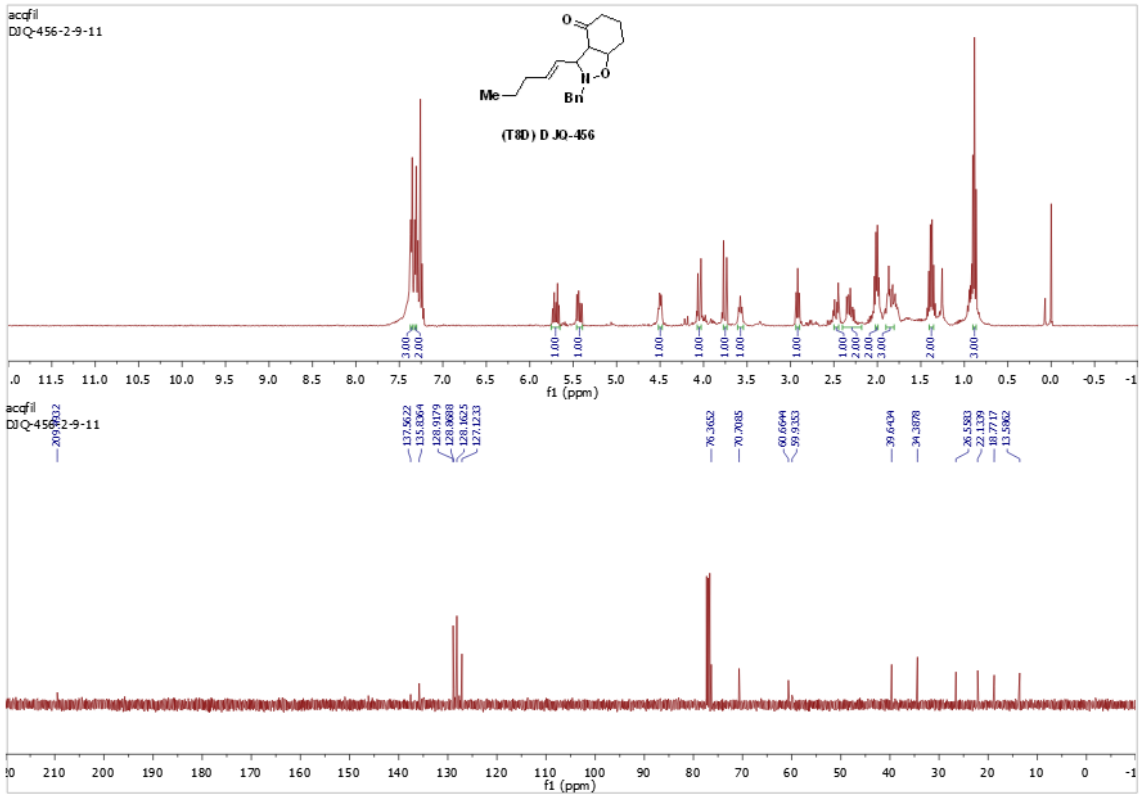
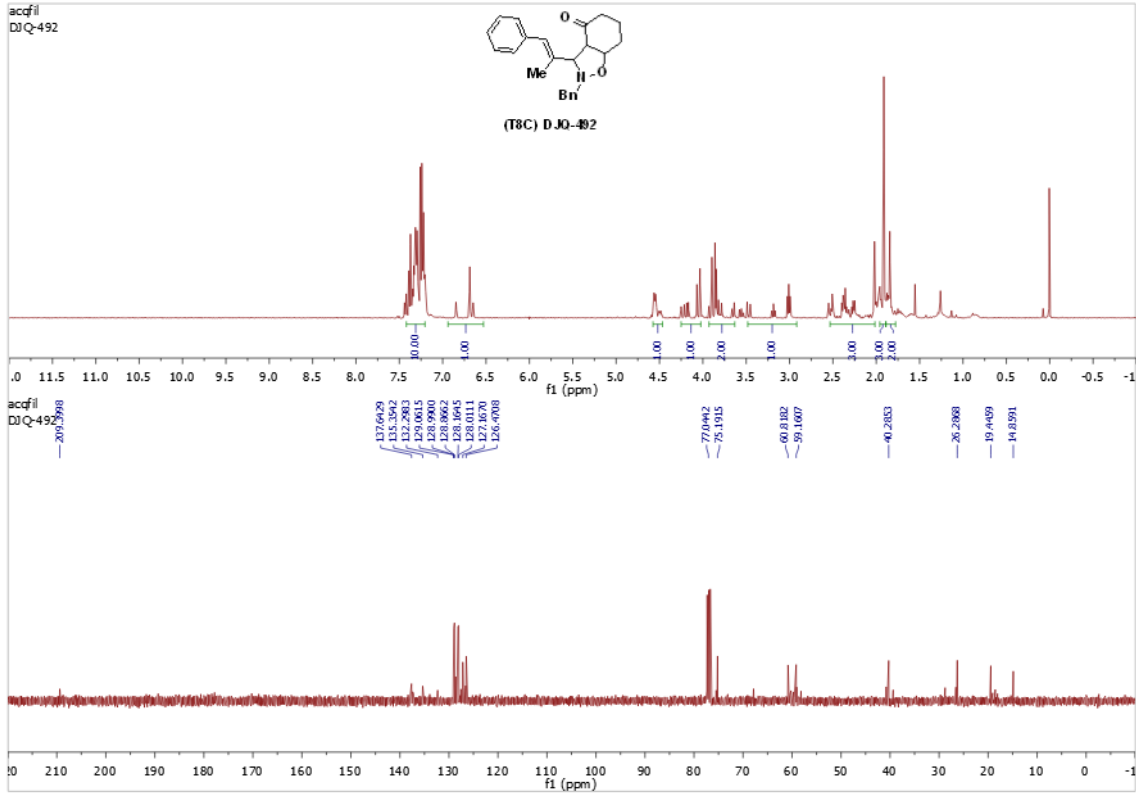


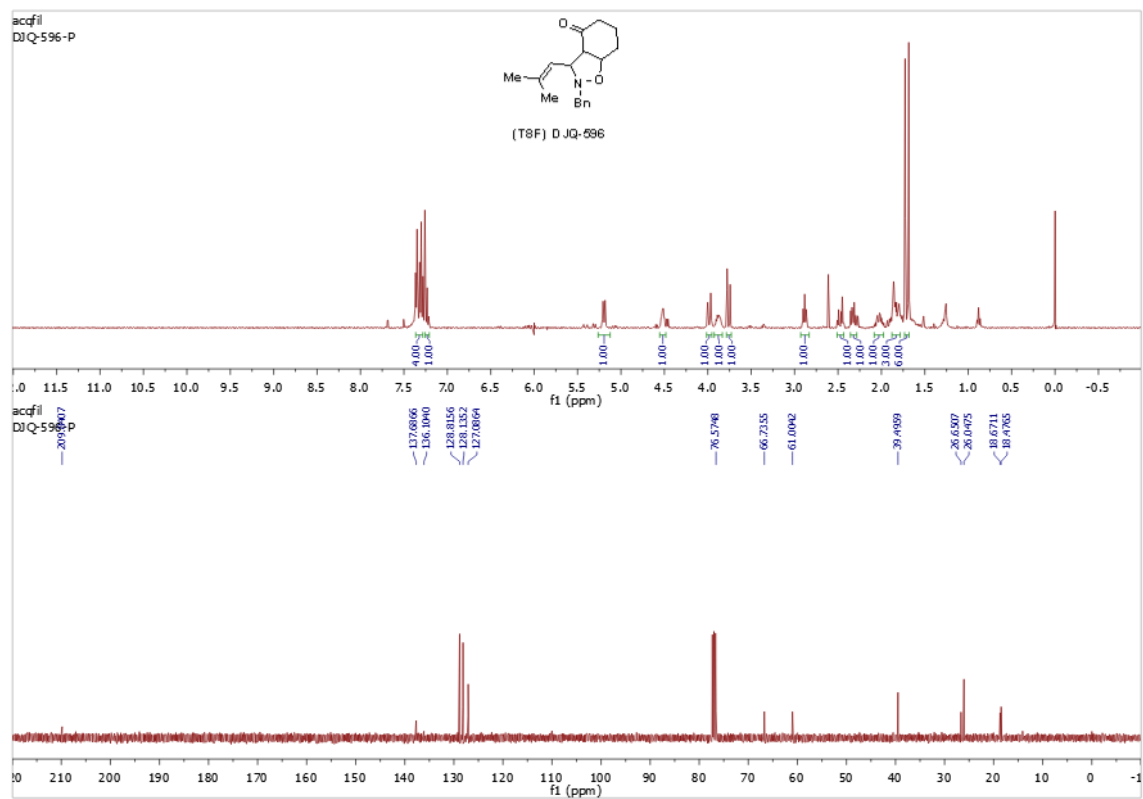
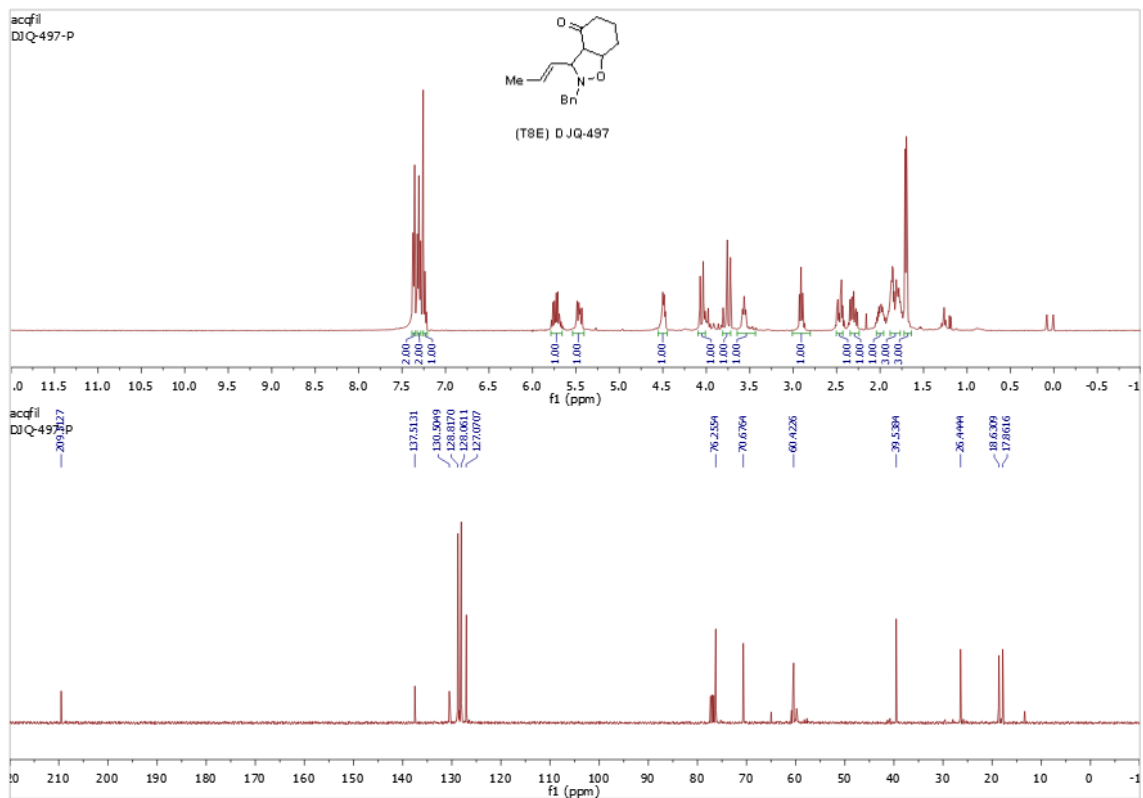


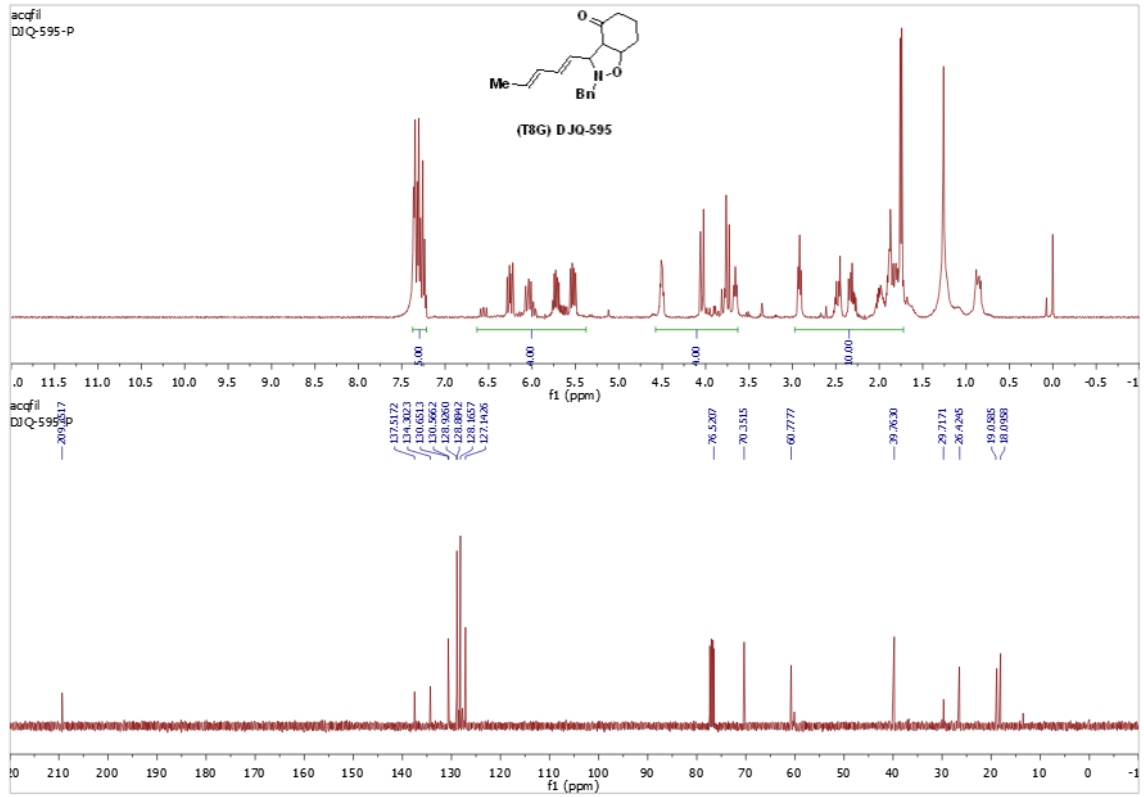












Chapter 4

Nitrone Photoisomerization

In Chapter 2, the thermal isomerization of an Oxaziridine was highlighted as a possible synthetic route to the Nitrone moiety. Interestingly, the reverse reaction is also possible via a photochemical isomerization from the nitrone to the isoelectronic oxaziridine isomer (Spence, Taylor, & Buchardt, 1970). Though this method (Figure 19) was developed as early as the 1950s, it has been largely overshadowed throughout the years by a much more favorable reaction pathway.

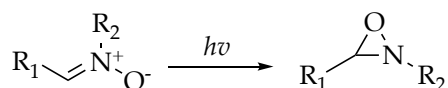


Figure 19. Nitrone Photoisomerization to Oxaziridine

4.1 A Method Overlooked

Imine oxidation is a preferred pathway to the oxaziridine moiety because of the superior heteroatom transfer of the afforded electron-deficient oxaziridines. This class of oxaziridine is not readily accessible through the condensation-photoisomerization pathway by means of a nitrone. In chapter 2, N-Electron deficient nitrones were described as too unstable to isolate and only formed in-situ (Ricci, Gioia, Fini, Mazzanti, & Bernardi, 2009). This implies that the photorearrangement of nitrones to oxaziridines is unfortunately limited to N-alkyl oxaziridines because the respective N-alkyl nitrones are readily accessible.

Davis oxaziridine, obtained through the imine oxidation of a camphor-derived carbonyl has been applied to novel chemical transformations. The Holton-Taxol Total Synthesis utilizes this oxaziridine (Figure 20) for selective hydroxylation onto a highly functionalized taxane framework (Holton, et al., 1994). The N-Sulfonyl Oxaziridine moiety is found throughout the literature time and time again being utilized in similarly powerful transformations.

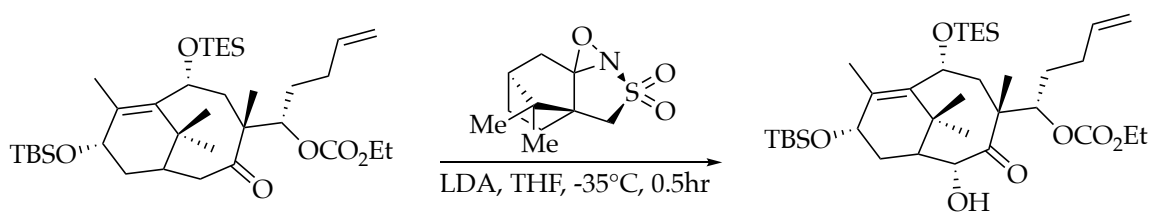


Figure 20. Hydroxylation at C2 in the Holton-Taxol Synthesis

Unfortunately, the respective N-Sulfonyl Nitron has not been isolated and therefore photochemical isomerization from this vantage point would be inaccessible. Despite the clear synthetic utility of N-Sulfonyl oxaziridines the recent literature, highlighted in the next section, demonstrates a growing demand for the synthesis of novel, N-alkyl oxaziridines.

4.2 Heteroatom Transfer

Researchers from Rice University have recently discovered that camphor-derived, N-alkyl oxaziridines rapidly oxidize aryl metals to the respective phenol (Figure 21). This method is drastically more efficient than previous methods for aryl oxidation which often requires harsh reaction conditions (Kurti, et al., 2016).

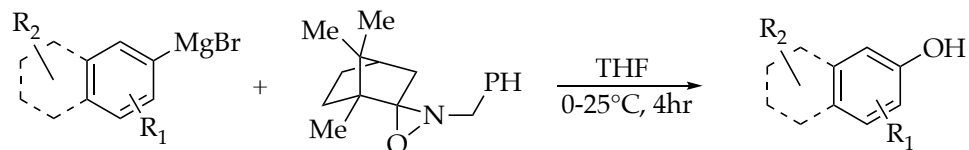


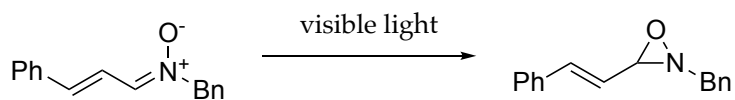
Figure 21. A Mild Aryl Metal Oxidation by N-Alkyl Oxaziridine

These results indicate a new demand for N-alkyl oxaziridines to be employed as valuable heteroatom transfer reagents. To meet these demands the GML group sought to revisit the classical photoisomerization of nitrones to oxaziridines and determine both optimal and practical reaction conditions that would afford novel oxaziridines for further investigation of their heteroatom transfer capabilities.

4.3 Results and Discussion

With a structurally rich library of nitrones, the GML Group sought out to begin photoisomerization to form the respective N-alkyl oxaziridines. Cinnamaldehyde derived nitron was used for these optimization studies and provided the respective oxaziridine in good to excellent yields under visible light (Table 13). These results were surprising because previous reports of nitron photoisomerization required UV irradiation to promote similar reactions. (Spence, Taylor, & Buchardt, 1970). The continued development of a more practical reaction methodology was pursued to arrive at optimal conditions readily available to any common synthetic organic research lab. Optimization studies began with a quartz reaction vessel possessing a UV cutoff of 160 nm, allowing for sufficient light to reach the target reagent.

Table 13

Photorearrangement Optimization

Entry	Solvent (UV Cutoff)	Concentration	Vessel (UV Cutoff)	Time	% Yield
574-1	Acetone (340 nM)	0.01 M	quartz (160 nM)	2hr	35
574-2	Benzene (295 nM)	0.01 M	quartz (160 nM)	2hr	40
574-3	Ethyl Ether (255 nM)	0.01 M	quartz (160 nM)	2hr	31
574-4	Heptanes (230 nM)	0.01 M	quartz (160 nM)	2hr	10
574-5	Benzene (295 nM)	0.05 M	quartz (160 nM)	2hr	20
574-6	Benzene (295 nM)	0.10 M	quartz (160 nM)	2hr	22
574-7	Benzene (295 nM)	0.50 M	quartz (160 nM)	2hr	28
574-8	Benzene (295 nM)	1.00 M	quartz (160 nM)	2hr	25
574-9	Benzene (295 nM)	0.01 M	borosilicate (275 nm)	18hr	66
574-10	Benzene (295 nM)	0.03 M	borosilicate (275 nm)	18hr	98
574-11	Benzene (295 nM)	0.05 M	borosilicate (275 nm)	18hr	72

Various organic solvents were screened to determine the appropriate media for this reaction, Benzene afforded a significant 40% yield of the desired oxaziridine product (Table-13, Entry 574-2).

As the Beer-Lambert law suggests that concentration plays a pivotal role in the absorption of light, different concentrations of the starting reagent in Benzene were tested. In agreement with this law, the results for these tests indicated a significant effect on the yield at differing concentrations (Table 13, Entry 574-9 - 574-11). 0.03 M, a relatively dilute concentration, provided the most desirable conversion to the oxaziridine product. At 0.01 M and 0.05 M, slightly less and slightly more concentrated, the reaction conversion was decreased. These results indicated that optimal absorbance for the cinnamaldehyde derived nitron under the specified reaction conditions were obtained nearing 0.03 M.

Some organic chemists shy away from photochemical reactions because of the intricate reaction set up. As the quartz reaction vessel employed in these experiments would only hold about 4 mL of solution, the GML Lab sought to obtain similar results with a more common type of lab glassware. A simple borosilicate, Pyrex round bottom (250 mL), common to all organic research labs, was employed to allow for the scale-up of this reaction. Satisfyingly, similar results were obtained, albeit with longer reaction times (18 hr.), at a 1 mmol scale. These results indicated that after optimization, the photoisomerization could proceed with a simple reaction set up that was much more familiar in comparison to more intricate photochemical reaction set ups.

With optimal reaction conditions in hand, the GML group sought to develop a library of structurally diverse vinyl oxaziridines. Aromatic nitrones exhibited modest conversions to the desired oxaziridine whereas aliphatic nitrones showed significantly diminished yields (Table 14, Entry T10F).

Table 14

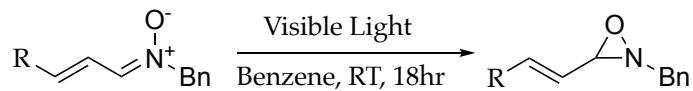
Oxaziridine Scope

Entry	Nitrone	Oxaziridine	% Yield
T14A			44
T14B			44
T14C			64
T14D			40
T14E			35
T14F			14

Per the Woodward-Fieser Rules, compounds with increasing conjugation allow for a greater wavelength of maximum absorption. In agreement with these rules, the results for increasingly conjugated nitrones showed a drastic increase in conversion to the respective oxaziridine products.

Cinnamaldehyde-derived nitrones exhibited a remarkable conversion of greater than 95% to the desired oxaziridine. These reactions allowed for direct conversion with no need for work-up, purification or the addition of any additives (Table 15). Aliphatic-unsaturated compounds such as hexenal and dodecadienal also exhibited good to excellent yields indicating that aliphatic oxaziridines could be obtained if the conjugation for absorption was available.

Table 15

Alpha-Beta Unsaturated Oxaziridine Scope

Entry	Nitron	Oxaziridine	% Yield
T15A			95
T15B			95
T15C			92
T15D			40
T15E			98
T15F			78

4.4 Conclusion

These results indicate a simple method for the direct conversion of nitrones to oxaziridine, under simple visible light irradiation and the use of common lab glassware. Cinnamaldehyde derived nitron allowed for many functional group modifications and proceeded to the respective vinyl oxaziridines in excellent yields. Current research in the GML lab is exploring the use of photocatalysis to improve the yields for aromatic and saturated oxaziridines which previously showed diminished yields. This method avoids the use of harmful UV radiation by applying substrates with applicable absorption, the use of photocatalysis can further broaden the scope of this reaction to arrive at valuable synthetic intermediates.

Each method developed herein has utilized substituted hydroxylamines to successfully obtain heteroatomic scaffolds and build structural complexity. Hydroxylamines remain a powerful tool in the synthetic toolbox of organic chemists allowing for a convenient route for the introduction of nitrogen into heteroatomic organic frameworks.

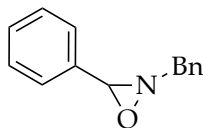
4.5 Experimental

Reagents were obtained from Aldrich Chemical, Acros Organics or Alfa Aesar and used without further purification. Solvents were obtained from EMD Milipore DrySol and degassed with nitrogen. Reactions were performed in 4-mL glass vials. TLC was performed on 0.25 mm E. Merck silica gel 60 F254 plates and visualized under UV light (254 nm) or by staining with potassium permanganate (KMnO₄). Silica flash chromatography was performed on E. Merck

230–400 mesh silica gel 60. Automated chromatography was performed on a ISOLERA Prime instrument with 10 g. SNAP silica gel normal phase cartridges using a flow rate of 12.0 mL/min and a gradient of 0–30% EtOAc in Heptanes over 12 column volumes with UV detection at 254 nm. NMR spectra were recorded on Varian Mercury II 400 MHz Spectrometer at 24 °C in CDCl₃ unless otherwise indicated. Chemical shifts are expressed in ppm relative to solvent signals: CDCl₃ (¹H, 7.23 ppm; ¹³C, 77.0 ppm); coupling constants are expressed in Hz.

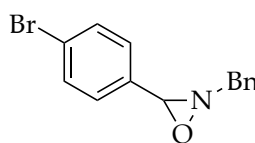
4.5.1. General method for the synthesis of vinyl oxaziridines. 1mMol of nitron is dissolved in 30mL of de-gassed Benzene to a 0.03M solution. Solution delivered to a 50mL round bottom flask (borosilicate) UV cutoff approximately 300nm. Nitron solution is irradiated under a 105 Watt Compact Fluorescent Lamp (Limo Studio Full Spectrum Light) for 6 hours. After irradiation, the solvent is reduced by rotary evaporation to afford the respective oxaziridine. Filtration by silica gel with 20% EtOAc in Heptanes over 12 column volumes provided the desired oxaziridine in good to excellent yields.

4.5.2. Synthesis of vinyl oxaziridines from Table 10.



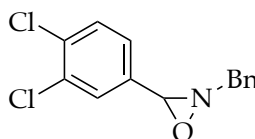
(T10A) DJQ-534-2

2-benzyl-3-phenyl-1,2-oxaziridine (T10A): After irradiation, reducing the solvent afforded the oxaziridine **10a** ^1H NMR (400 MHz, Chloroform-*d*) δ 7.54 – 7.27 (m, 10H), 4.70 (s, 1H), 4.11 (d, $J = 13.5$ Hz, 1H), 3.99 (d, $J = 13.5$ Hz, 1H). ^{13}C NMR (101 MHz, Chloroform-*d*) δ 130.09, 128.85, 128.63, 128.47, 127.90, 127.65, 80.29, 65.84.



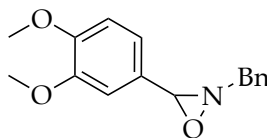
(T10B) DJQ-538

2-benzyl-3-(4-bromophenyl)-1,2-oxaziridine (T10B): After irradiation, reducing the solvent afforded the oxaziridine **10b** ^1H NMR (400 MHz, Chloroform-*d*) δ 7.53 – 7.47 (m, 2H), 7.42 – 7.32 (m, 5H), 7.31 – 7.28 (m, 2H), 4.65 (s, 1H), 4.09 (d, $J = 13.5$ Hz, 1H), 3.97 (d, $J = 13.5$ Hz, 1H). ^{13}C NMR (101 MHz, Chloroform-*d*) δ 131.70, 129.31, 128.82, 128.68, 128.00, 124.37, 79.53, 65.76.



(T10C) DJQ-535

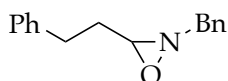
2-benzyl-3-(3,4-dichlorophenyl)-1,2-oxaziridine (T10C): After irradiation, reducing the solvent afforded the oxaziridine **10c** ^1H NMR (400 MHz, Chloroform-*d*) δ 7.45 – 7.27 (m, 7H), 7.26 – 7.22 (m, 1H), 5.13 (s, 1H), 4.14 (d, $J = 13.4$ Hz, 1H), 4.02 (d, $J = 13.4$ Hz, 1H). ^{13}C NMR (101 MHz, Chloroform-*d*) δ 134.85, 129.35, 129.08, 128.67, 128.11, 127.59, 65.87.



(T10D) DJQ-534

2-benzyl-3-(3,4-dimethoxyphenyl)-1,2-oxaziridine (T10D): After irradiation, reducing the solvent afforded the oxaziridine **10d** ^1H NMR (400 MHz, Chloroform-

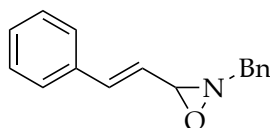
d) δ 7.43 – 7.29 (m, 5H), 7.06 (ddd, $J = 8.1, 1.9, 0.7$ Hz, 1H), 6.91 – 6.81 (m, 2H), 4.65 (s, 1H), 4.11 (d, $J = 13.5$ Hz, 1H), 3.98 – 3.93 (m, 2H), 3.87 (dd, $J = 5.8, 0.7$ Hz, 6H). ^{13}C NMR (101 MHz, Chloroform-*d*) δ 149.35, 135.46, 128.86, 127.88, 126.92, 121.13, 110.53, 109.34, 80.43, 65.78, 55.91.



(T10F) DJQ-539

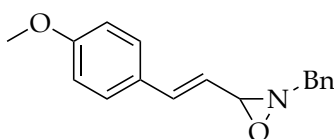
2-benzyl-3-phenethyl-1,2-oxaziridine (T10F): After irradiation, reducing the solvent afforded the oxaziridine **10f** ^1H NMR (400 MHz, Chloroform-*d*) δ 7.46 – 7.01 (m, 10H), 4.81 – 3.34 (m, 3H), 3.38 – 1.62 (m, 4H). ^{13}C NMR (101 MHz, Chloroform-*d*) δ 129.50, 129.02, 128.64, 128.53, 128.46, 128.36, 128.35, 128.29, 127.34, 127.27, 126.20, 125.80, 99.41, 65.50, 62.27, 60.72, 45.91, 33.07, 32.85, 30.03.

4.5.3. Synthesis of vinyl oxaziridines from Table 11.



(T11A) DJQ-515E

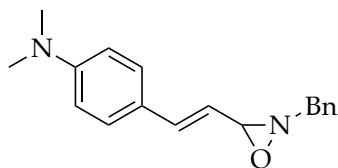
(E)-2-benzyl-3-styryl-1,2-oxaziridine (T11A): After irradiation, reducing the solvent afforded the oxaziridine **11a** ^1H NMR (400 MHz, CDCl₃) δ 7.43 – 7.30 (m, 10H), 6.98 (d, $J = 16.2$ Hz, 1H), 5.96 (ddd, $J = 16.2, 7.7, 1.0$ Hz, 1H), 4.39 (d, $J = 7.7$ Hz, 1H), 4.03 (d, $J = 13.4$ Hz, 1H), 3.89 (d, $J = 13.5$ Hz, 1H). ^{13}C NMR (101 MHz, Chloroform-*d*) δ 138.57, 128.87, 128.80, 128.71, 128.65, 127.92, 126.93, 124.29, 81.01, 65.54.



(T11B) DJQ-520

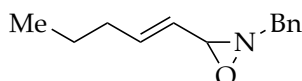
(E)-2-benzyl-3-(4-methoxystyryl)-1,2-oxaziridine (T11B): After irradiation, reducing the solvent afforded the oxaziridine **11b** ^1H NMR (400 MHz, Chloroform-*d*) δ 7.53 – 7.39 (m, 4H), 7.37 – 7.33 (m, 3H), 6.93 (d, $J = 16.1$ Hz, 1H), 6.90 – 6.84 (m, 2H), 5.84 (ddd, $J = 16.1, 7.8, 0.8$ Hz, 1H), 4.38 (d, $J = 7.8$ Hz, 1H), 4.03 (d, $J = 13.5$ Hz,

1H), 3.89 (d, $J = 13.5$ Hz, 1H), 3.83 – 3.80 (m, 3H). ^{13}C NMR (101 MHz, CDCl_3) δ 138.12, 128.82, 128.65, 128.33, 128.11, 127.89, 121.87, 114.12, 81.36, 65.54, 55.30



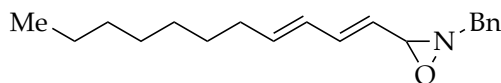
(T11C) DJQ-528

(E)-4-(2-(2-benzyl-1,2-oxaziridin-3-yl)vinyl)-N,N-dimethylaniline (T11C): After irradiation, reducing the solvent afforded the oxaziridine **11c**. ^1H NMR (400 MHz, Chloroform- d) δ 7.42 – 7.36 (m, 5H), 7.31 – 7.29 (m, 2H), 6.89 (d, $J = 16.1$ Hz, 1H), 6.67 – 6.64 (m, 2H), 5.73 (ddd, $J = 16.3, 7.9, 1.4$ Hz, 1H), 4.36 (dd, $J = 7.9, 1.0$ Hz, 1H), 4.02 (d, $J = 13.5$ Hz, 1H), 3.86 (d, $J = 13.5$ Hz, 1H), 2.97 (d, $J = 0.8$ Hz, 6H). ^{13}C NMR (101 MHz, cdcl_3) δ 150.79, 138.80, 135.62, 128.78, 128.60, 128.32, 128.14, 127.79, 119.15, 112.01, 81.94, 65.54, 40.27.



(T11D) DJQ-518-3

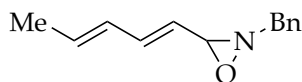
(E)-2-benzyl-3-(pent-1-en-1-yl)-1,2-oxaziridine (T11D) After irradiation, reducing the solvent afforded the oxaziridine **11d**. ^1H NMR (400 MHz, Chloroform- d) δ 7.39 – 7.31 (m, 5H), 6.18 (dtd, $J = 15.7, 6.7, 0.9$ Hz, 1H), 5.28 (ddq, $J = 15.7, 7.8, 1.4$ Hz, 1H), 4.19 (dd, $J = 7.8, 0.9$ Hz, 1H), 3.98 (dd, $J = 13.5, 0.9$ Hz, 1H), 3.79 (dd, $J = 13.5, 0.8$ Hz, 1H), 2.09 (tdd, $J = 6.5, 5.5, 1.3$ Hz, 2H), 1.44 (qd, $J = 7.4, 0.9$ Hz, 2H), 0.94 – 0.89 (m, 3H). ^{13}C NMR (101 MHz, Chloroform- d) δ 141.52, 128.76, 128.58, 127.79, 125.84, 81.09, 65.47, 34.32, 21.65, 13.62.



(T11E) DJQ-571-2

2-benzyl-3-((1E,3E)-undeca-1,3-dien-1-yl)-1,2-oxaziridine (T11E) After irradiation, reducing the solvent afforded the oxaziridine, **11e**. ^1H NMR (400 MHz, Chloroform- d) δ 7.41 – 7.31 (m, 5H), 6.58 (dd, $J = 15.5, 10.5$ Hz, 1H), 6.13 – 6.05 (m, 1H), 5.86 (dt, $J = 14.7, 7.0$ Hz, 1H), 5.32 (dd, $J = 15.5, 7.8$ Hz, 1H), 4.22 (d, $J = 7.9$ Hz, 1H), 3.96 (d, $J = 13.4$ Hz, 1H), 3.83 (d, $J = 13.5$ Hz, 1H), 2.11 (qd, $J = 7.1, 1.4$ Hz, 2H), 1.44 – 1.38 (m, 2H), 1.30 (s, 8H), 0.90 (td, $J = 6.7, 4.1$ Hz, 3H). ^{13}C NMR (101 MHz,

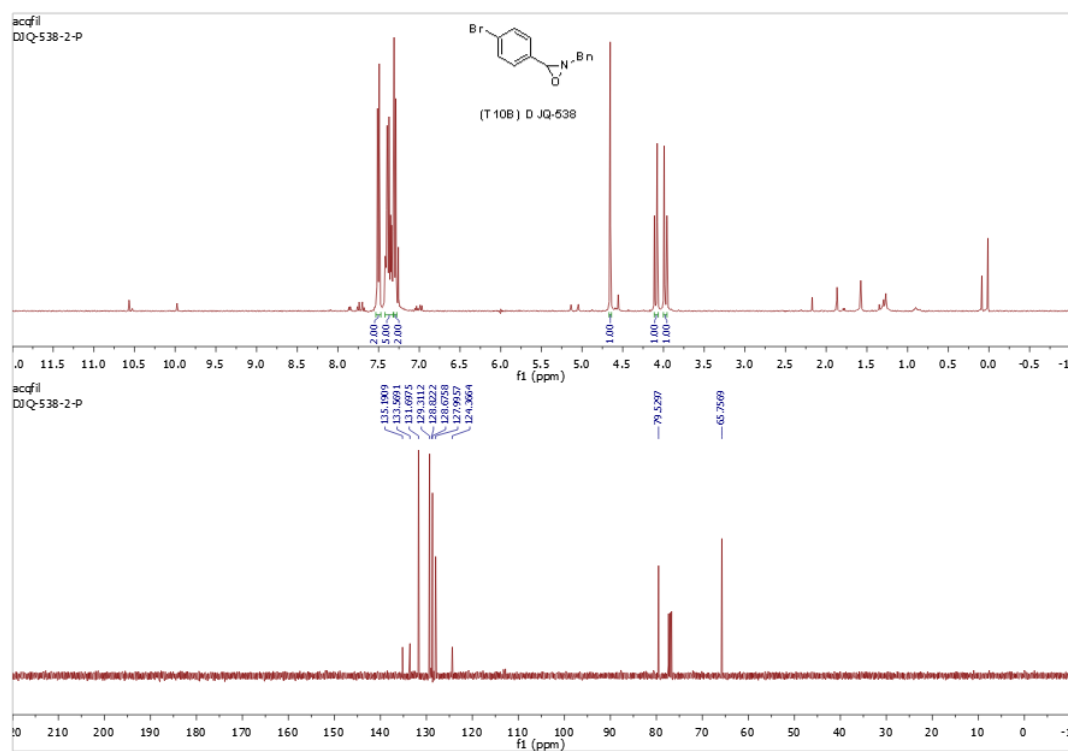
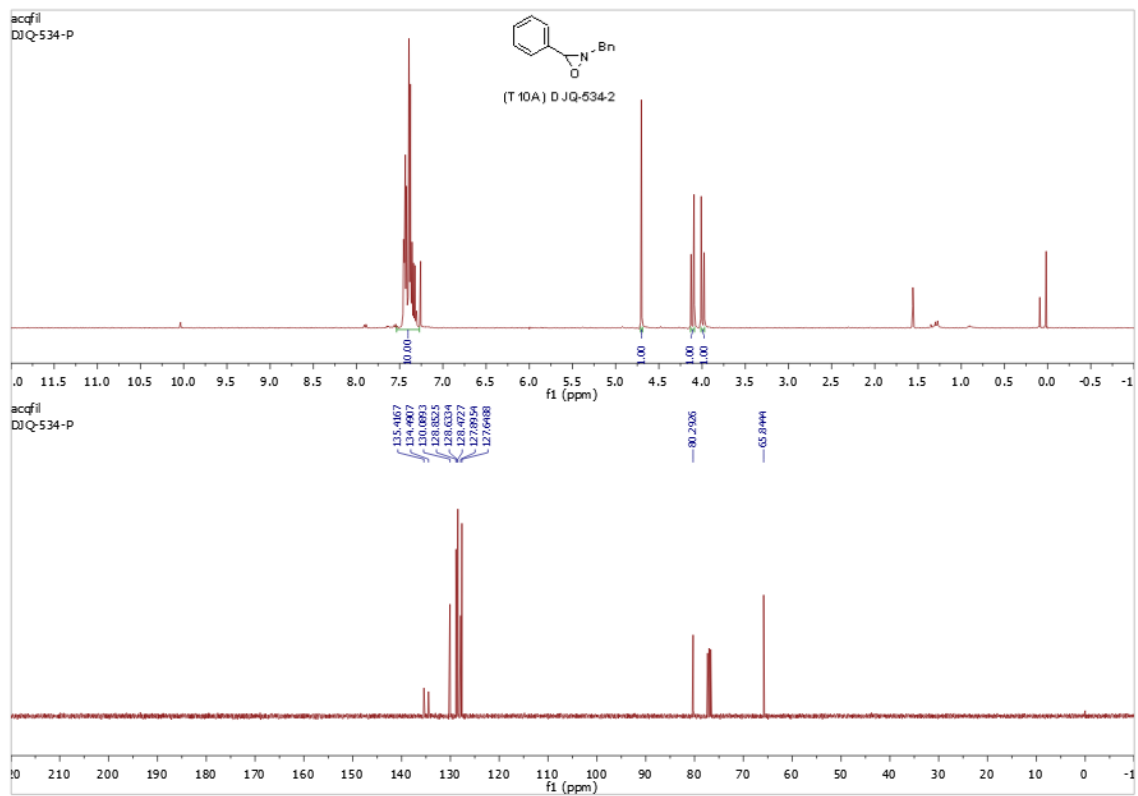
Chloroform-*d*) δ 139.16 , 139.08 , 128.79 , 128.60 , 127.83 , 124.83 , 80.96 , 65.53 , 32.64 , 31.79 , 29.12 , 28.97 , 22.64 , 14.09 .

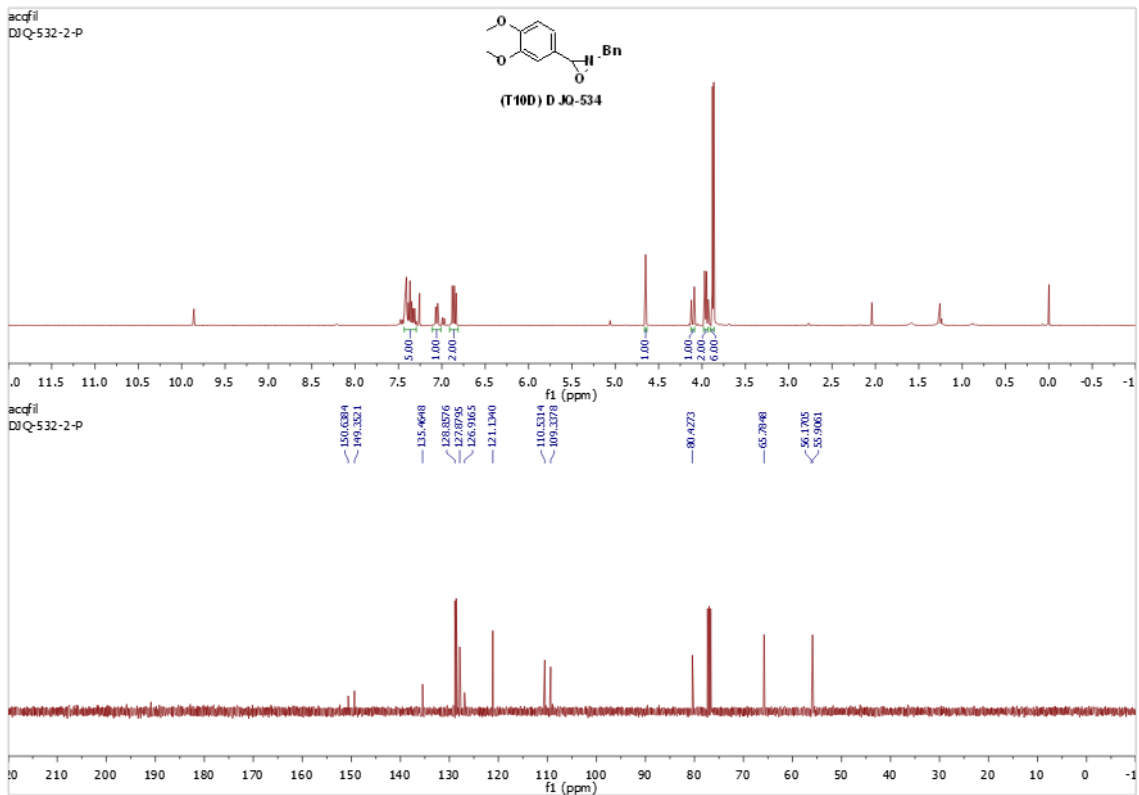
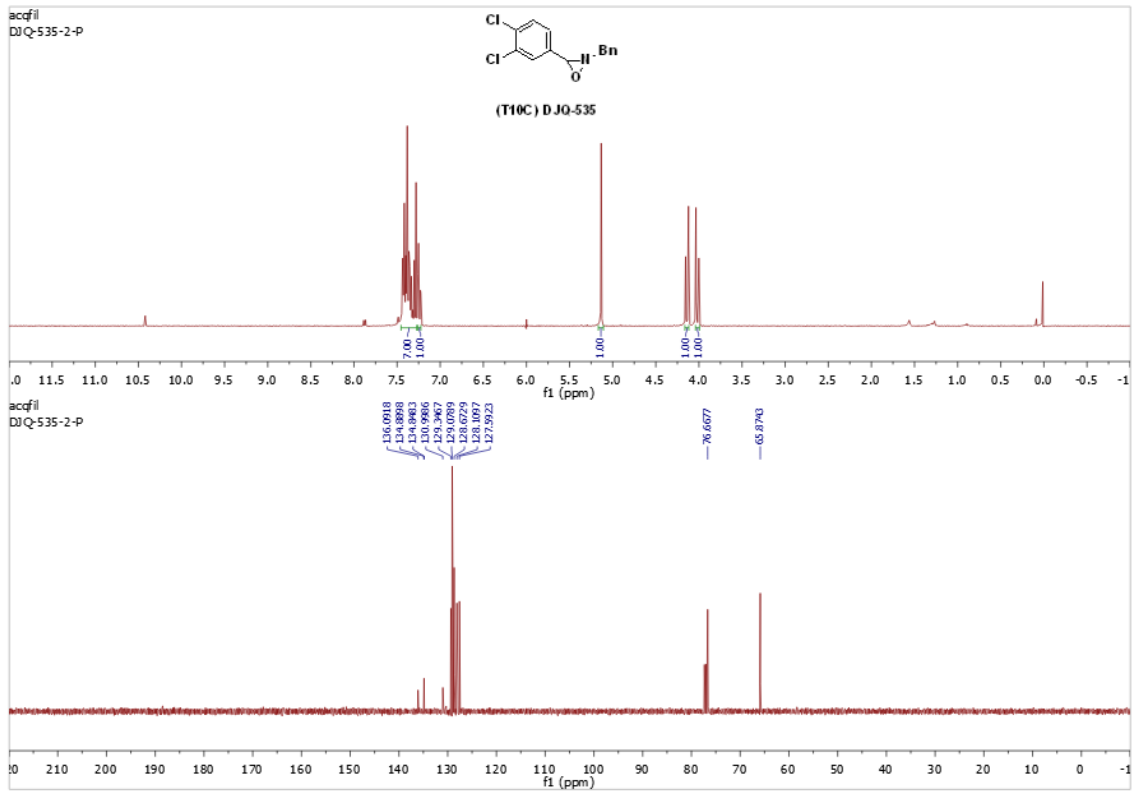


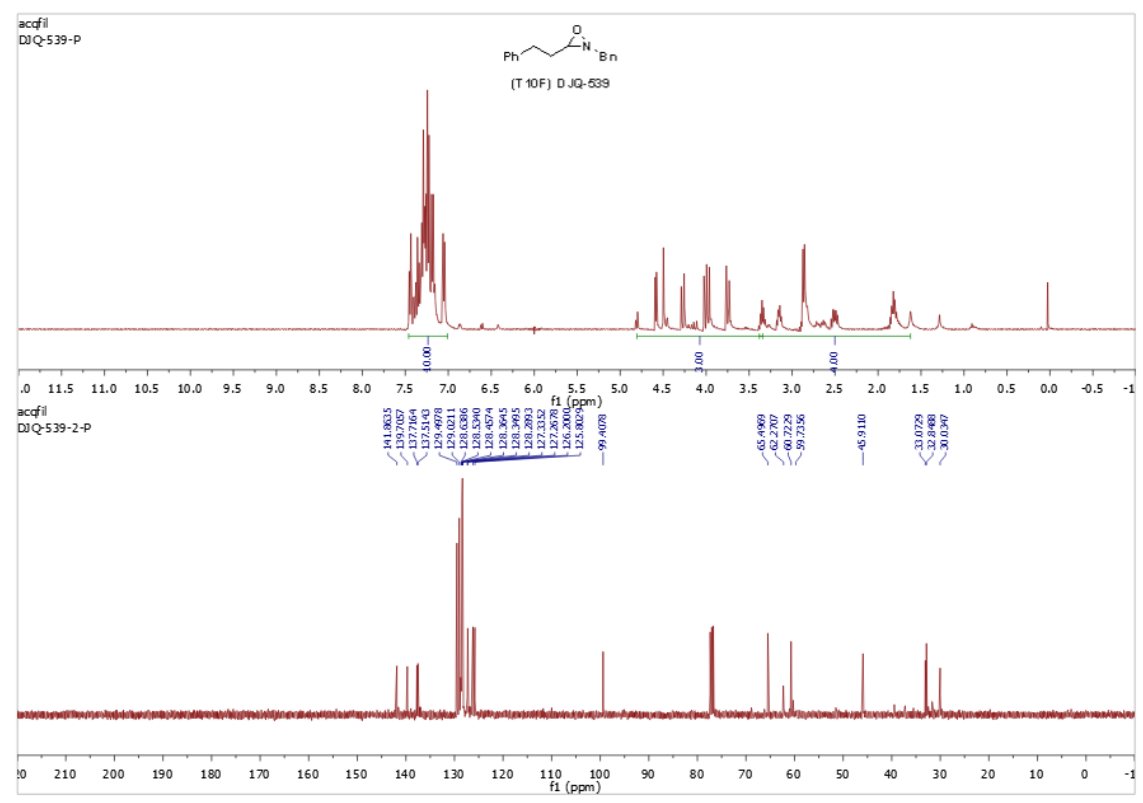
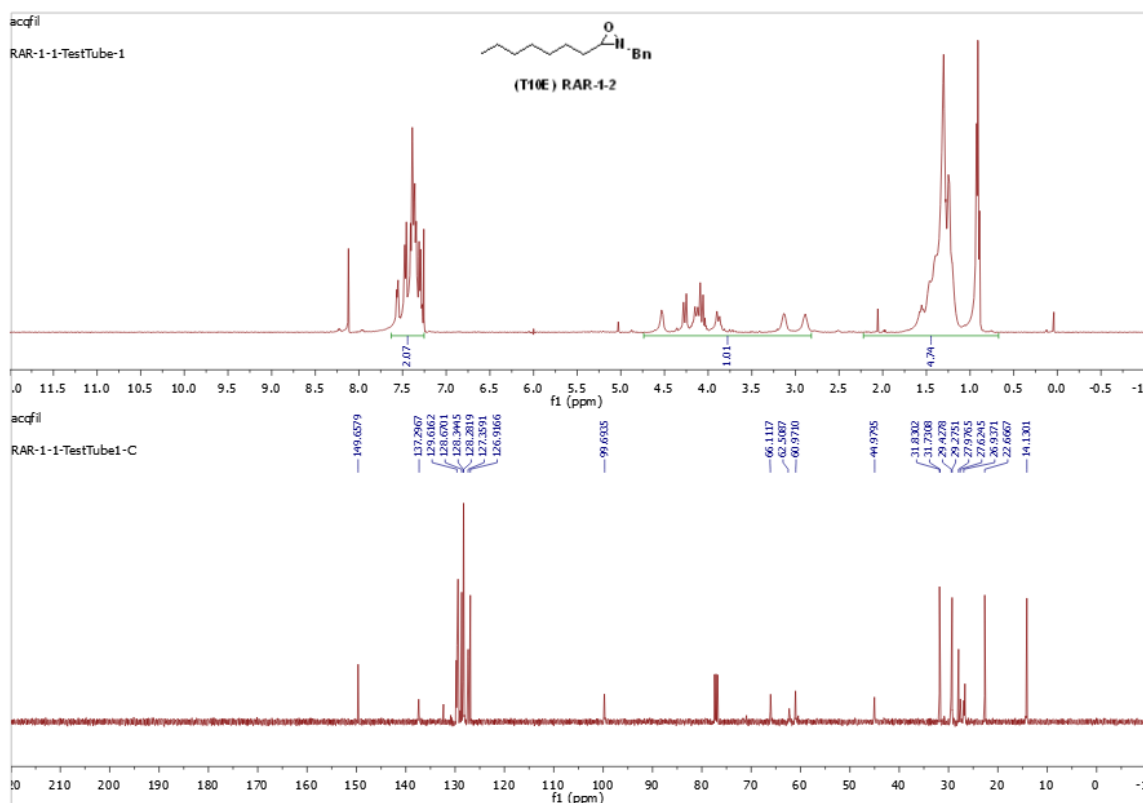
(T11F) DJQ-585-2

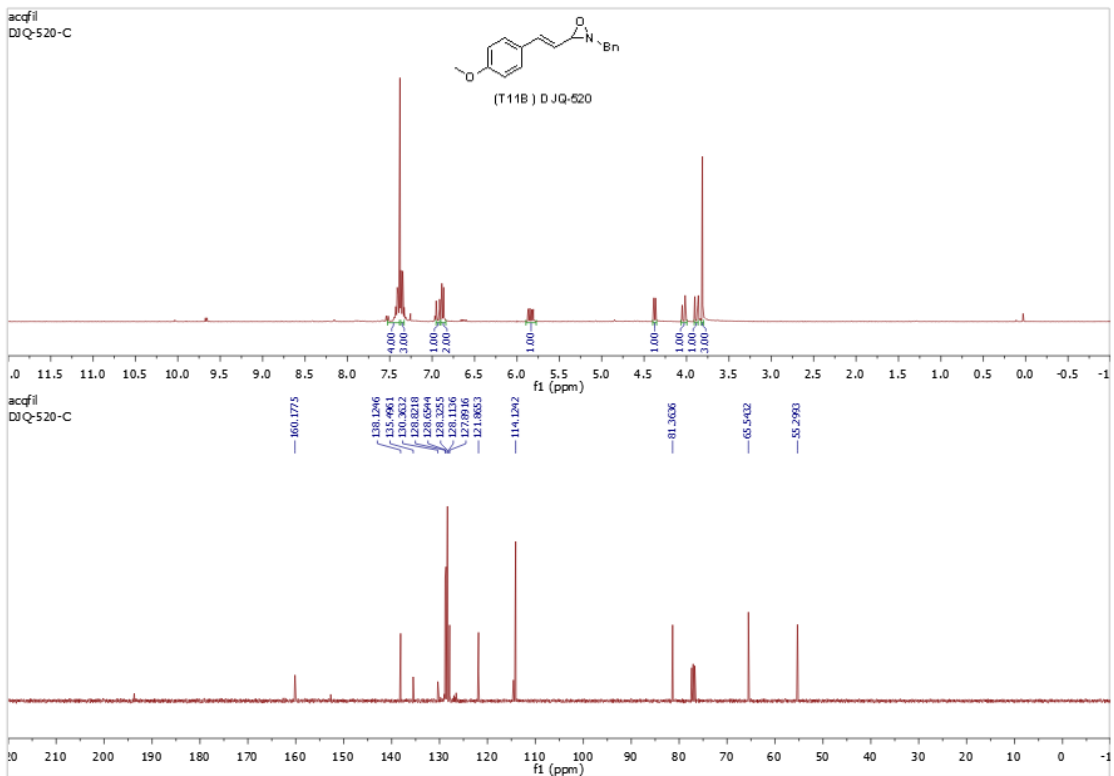
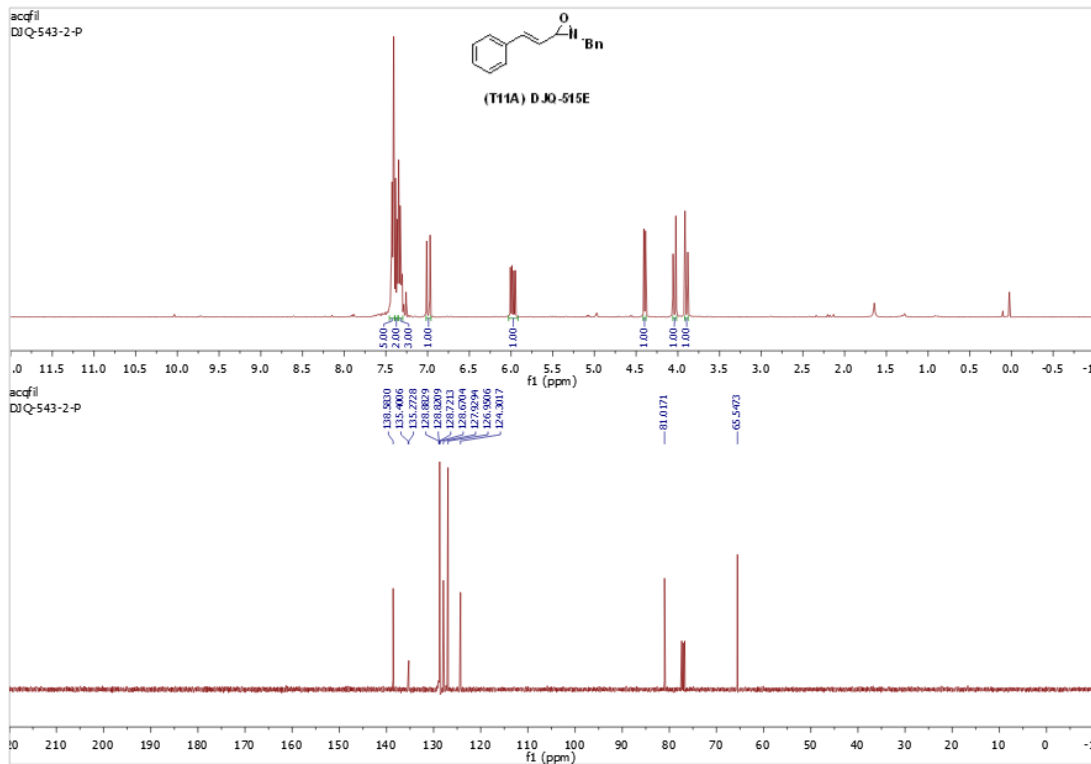
(E)-2-benzyl-3-(prop-1-en-1-yl)-1,2-oxaziridine (T11F) After irradiation, reducing the solvent afforded the oxaziridine, **11F** $^1\text{H NMR}$ (400 MHz, Chloroform-*d*) δ 7.42 – 7.28 (m, 5H), 6.58 (dd, $J = 15.6, 10.5$ Hz, 1H), 6.11 (ddq, $J = 15.6, 10.6, 1.7$ Hz, 1H), 5.87 (dq, $J = 15.2, 6.7$ Hz, 1H), 5.45 – 5.25 (m, 1H), 4.22 (d, $J = 7.9$ Hz, 1H), 3.97 (d, $J = 13.5$ Hz, 1H), 3.82 (d, $J = 13.5$ Hz, 1H), 1.83 – 1.78 (m, 3H). $^{13}\text{C NMR}$ (101 MHz, Chloroform-*d*) δ 138.92 , 133.56 , 130.02 , 128.78 , 128.60 , 127.83 , 124.70 , 80.93 , 65.51 , 18.21 .

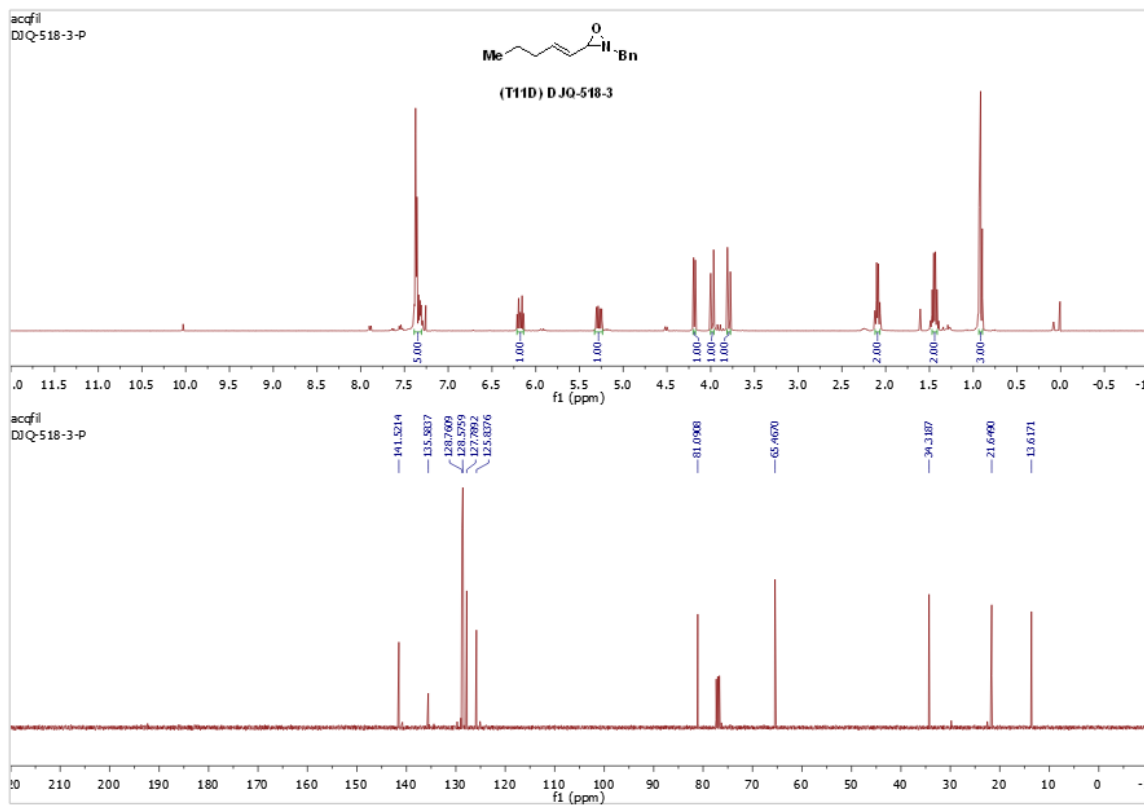
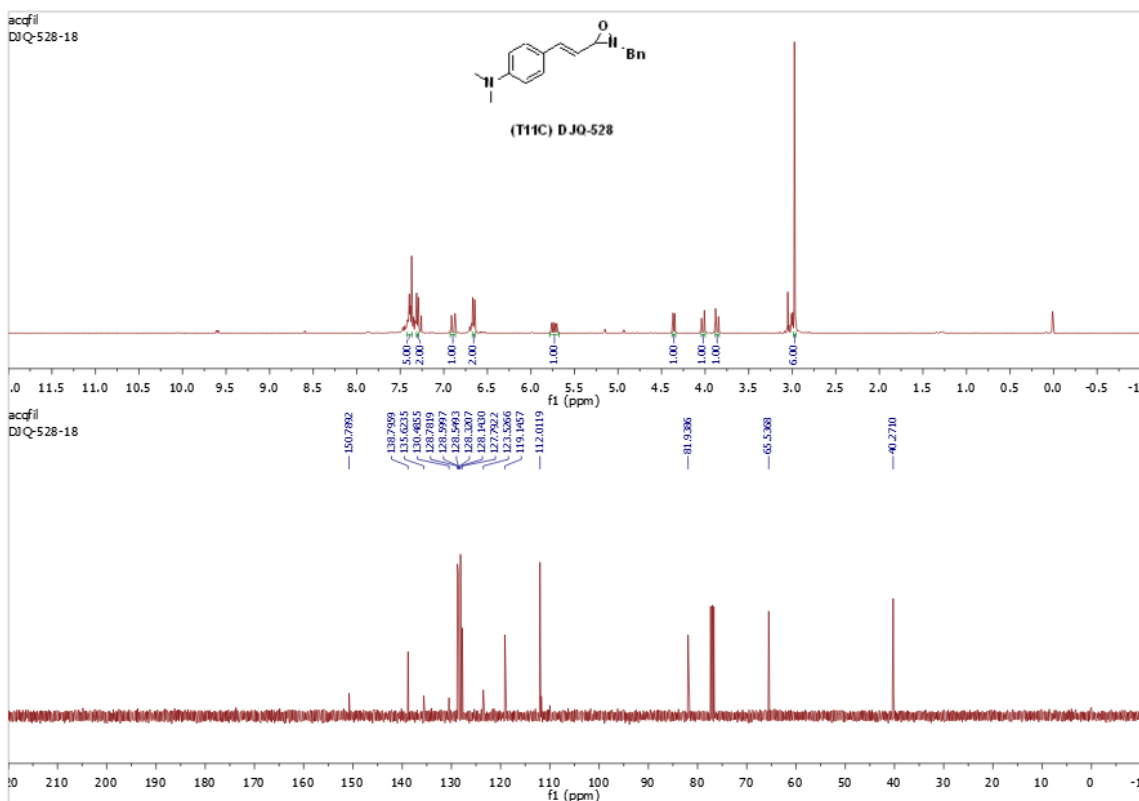
4.5.4. ^1H NMR and ^{13}C NMR of vinyl oxaziridines.

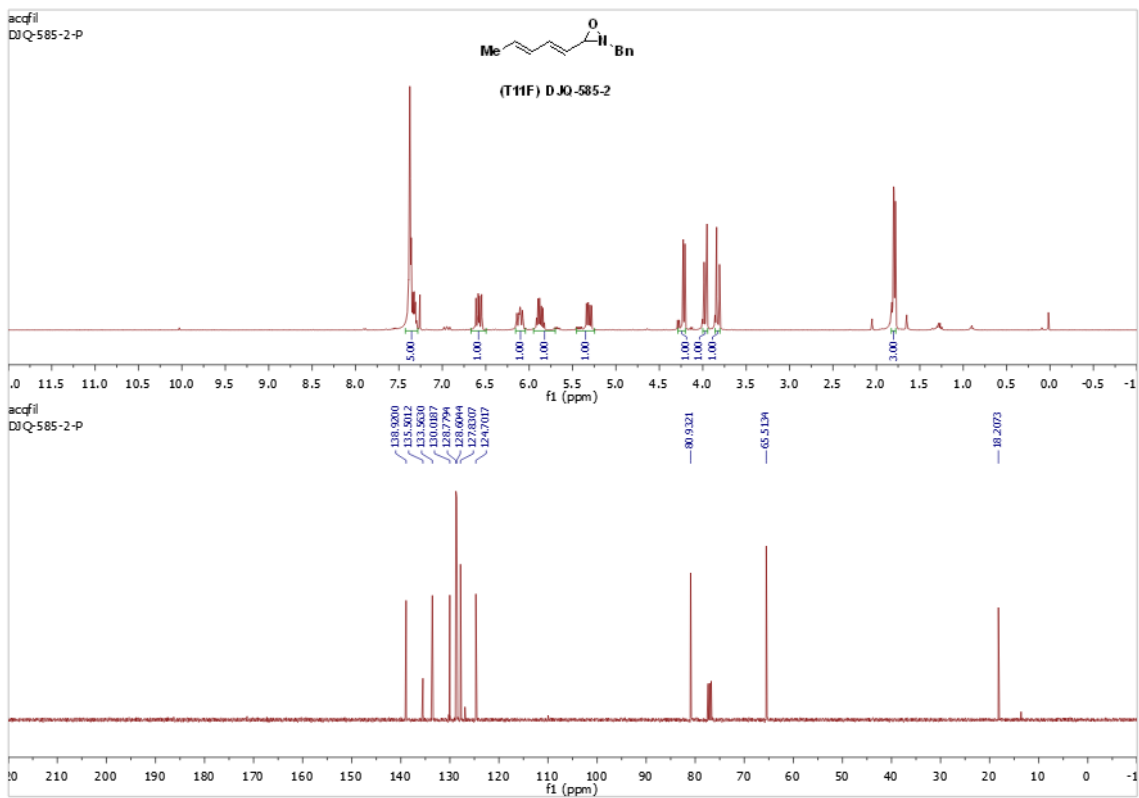
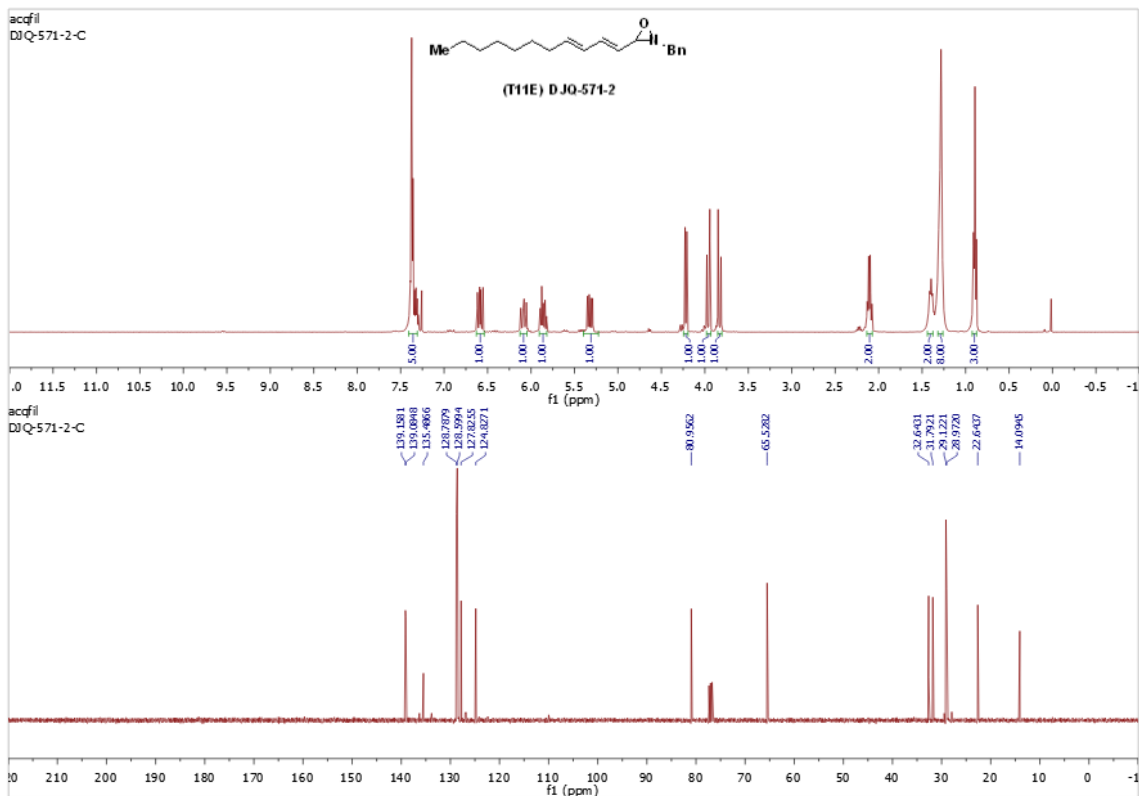












References

- Bates, R. W., Khanizeman, R. N., Hirao, H., Tay, Y. S., & Sae-Lao, P. (2014). A Total Synthesis of (+)-Negamycin through Isoxazolidine Allylation. *Organic and Biomolecular Chemistry*, 4879-4884.
- Beebe, A. W., Dohmeier, E. F., & Moura-Letts, G. (2015). Diastereoselective Synthesis of Substituted Diaziridines from Simple Ketones and Aldehydes. *Chemical Communications*, 13511-13514.
- Beziere, N., Hardy, M., Poulhes, F., Karoui, H., Tordo, P., Ouari, O., . . . Peyrot, F. (2014). Metabolic Stability of Superoxide Adducts Derived from Newly Developed Cyclic Nitron Spin Traps. *Free Radical Biology and Medicine*, 150-158.
- Chang, H.-R., Lau, W., Parker, H.-Y., & Westmoreland, D. G. (1996). Applications of ESR Techniques to the Study of Free Radical Processes and Kinetics in Acrylic Polymerizations. *Macromolecular Symposia*, 253-263.
- Colladon, M., Scarso, A., & Strukul, G. (2008). Mild Catalytic Oxidation of Secondary and Tertiary Amines to Nitrones and N-Oxides with H₂O₂ Mediated by Pt(II) Catalysts. *Green Chemistry*, 793-798.
- Evans, D. A., Miller, S. J., Lectka, T., & Matt, P. v. (1999). Chiral Bis(oxazoline)Copper(II) Complexes as Lewis Acid Catalysts for the Enantioselective Diels-Alder Reaction. *Journal of the American Chemical Society*, 7559-7573.
- Gothelf, K. V., & Jorgensen, K. A. (2000). Catalytic Enantioselective 1,3-Dipolar Cycloaddition Reaction of Nitrones. *Chemical Communications*, 1449-1458.
- Halpern, H. J., Pou, S., Peric, M., Yu, C., Barth, E., & Rosen, G. M. (1993). Detection and Imaging of Oxygen-Centered Free Radicals with Low-Frequency Electron Paramagnetic Resonance and Signal-Enhancing Deuterium-Containing Spin Traps. *Journal of the American Chemical Society*, 218-223.
- Hashimoto, T., & Maruoka, K. (2015). Recent Advances of Catalytic Asymmetric 1,3-Dipolar Cycloadditions. *Chemical Reviews*, 5366-5412.
- Holton, R. A., Kim, H.-B., Somoza, C., Liang, F., Biediger, R. J., Boatman, D. P., . . . Liu, J. H. (1994). First Total Synthesis of Taxol. 2. Completion of the C and D Rings. *Journal of the American Chemical Society*, 1599-1600.

- Kano, T., Hashimoto, T., & Maruoka, K. (2005). Asymmetric 1,3-Dipolar Cycloaddition Reaction of Nitrones and Acrolein with a Bis-Titanium Catalyst as Chiral Lewis Acid. *Journal of the American Chemical Society*, 11926-11927.
- Kurti, L., Gao, H., Zhou, Z., Kwon, D.-H., Coombs, J., Jones, S., . . . Ess, D. H. (2016). Rapid Heteroatom Transfer to Arylmetals Utilizing Multifunctional Reagent Scaffolds. *Nature Chemistry*, 681-688.
- Lobo, V., Phatak, A., & Chandra, N. (2010). Free Radicals, Antioxidants and Functional Foods: Impact on Human Health. *Pharmacognosy Review*, 118-126.
- Macaluso, A., & Hamer, J. (1964). Nitrones. *Chemical Reviews*, 473-495.
- Morales, S., Guijarro, F. G., Alonso, I., Ruano, J. L., & Cid, B. M. (2016). Dual Role of Pyrrolidine and Cooperative Pyrrolidine / Pyrrolidinium Effect in Nitron Formation. *ACS Catalysis*, 84-91.
- Partridge, K. M., Anzovino, M. E., & Yoon, T. P. (2008). Cycloadditions of N-Sulfonyl Nitrones Generated by Lewis Acid Catalyzed Rearrangement of Oxaziridines. *Journal of the American Chemical Society*, 2920-2921.
- Quinn, D. J., Haun, G. J., & Moura-Letts, G. (2016). Direct Synthesis of Nitriles from Aldehydes with Hydroxylamine O-Sulfonic Acid in Acidic Water. *Tetrahedron Letters*, 3844-3847.
- Ricci, A., Gioia, C., Fini, F., Mazzanti, A., & Bernardi, L. (2009). Organocatalytic Asymmetric Formal [3+2] Cycloaddition with in Situ-Generated N-Carbamoyl Nitrones. *Journal of the American Chemical Society*, 9614-9615.
- Seerden, J.-P. G., Boeren, M. M., & Scheeren, H. W. (1997). 1,3-Dipolar Cycloaddition Reactions of Nitrones with Alkyl Vinyl Ethers Catalyzed by Chiral Oxazaborolidines. *Tetrahedron*, 11843-11852.
- Spence, G. G., Taylor, E. C., & Buchardt, O. (1970). Photochemical Reactions of Azoxy Compounds, Nitrones, and Aromatic Amine N-Oxides. *Chemical Reviews*, 231-265.
- Yoon, T. P., Williamson, K. S., & Michaelis, D. J. (2014). Advances in the Chemistry of Oxaziridines. *ACS Chemical Reviews*, 16.
- Zhao, J., Song, X., Qian, Y., Ben, R., Lu, X., Zhu, H.-L., & Chao, H. (2013). Activation of C-H Bonds in Nitrones Leads to Iridium Hydrides with Antitumor Activity. *Journal of Medicinal Chemistry*, 6531-6535.